National Library of Canada
Acquisitions and Bibliographic Services Branch
395 Wellington Street
Ottawa, Ontario
K1A 0N4

Bibliothèque nationale du Canada
Direction des acquisitions et des services bibliographiques
395, rue Wellington
Ottawa (Ontario)
K1A 0N4

Your file Votre référence

Our file Notre référence

NOTICE

The quality of this microform is heavily dependent upon the quality of the original thesis submitted for microfilming. Every effort has been made to ensure the highest quality of reproduction possible.

If pages are missing, contact the university which granted the degree.

Some pages may have indistinct print especially if the original pages were typed with a poor typewriter ribbon or if the university sent us an inferior photocopy.

Reproduction in full or in part of this microform is governed by the Canadian Copyright Act, R.S.C. 1970, c. C-30, and subsequent amendments.

AVIS

La qualité de cette microforme dépend grandement de la qualité de la thèse soumise au microfilmage. Nous avons tout fait pour assurer une qualité supérieure de reproduction.

S'il manque des pages, veuillez communiquer avec l'université qui a conféré le grade.

La qualité d'impression de certaines pages peut laisser à désirer, surtout si les pages originales ont été dactylographiées à l'aide d'un ruban usé ou si l'université nous a fait parvenir une photocopie de qualité inférieure.

La reproduction, même partielle, de cette microforme est soumise à la Loi canadienne sur le droit d'auteur, SRC 1970, c. C-30, et ses amendements subséquents.

Canada

MEDIATED AND DIRECT ELECTROCHEMICAL STUDIES ON GLUCOSE OXIDASE

Arthur Fernandez

A Thesis

in

The Department

of

Chemistry and Biochemistry

Presented in Partial Fulfilment of the Requirements

for the Degree of Master of Science at

Concordia University

Montreal, Quebec, Canada

September, 1994

ISBN 0-315-97617-9

ABSTRACT

Mediated and Direct Electrochemical Studies
on Glucose Oxidase

Arthur Fernandez

Glucose oxidase (GOx) was covalently modified with ferrocenecarboxylic acid (FCA) using 1-ethyl-3-(3-dimethylamino)propyl)-carbodiimide hydrochloride and N-hydroxysulfosuccinimide to promote selective coupling to surface lysines. Derivatives with 5-12 covalently-bound ferrocene groups per GOx dimer were obtained, yielding ≥ 58% activity. k_{obs} for intramolecular electron transfer was 1.6 s^{-1} for GOx-$(FCA)_{12}$. Increasing the FCA:GOx ratio for bimolecular, FCA-mediated GOx electrochemistry, gave a corresponding decrease in the bimolecular rate constant, k_{12}. The limiting k_{12} value at FCA:GOx ≈ 0 was found to be $1.2 \pm 0.2 \times 10^5$ M^{-1} s^{-1}. Gold electrode modification with the thiol-containing electrochemical promoters; L-cysteine, 3-mercaptopropionic acid and 2-aminoethanethiol, yielded varying degrees of cytochrome c electrochemical reversibility. The L-cysteine-modified gold electrode gave quasi-reversible cytochrome c electrochemistry and resisted electrode fouling better than 4,4'-bipyridyl. Voltammetric signals persisted > 27 hours for repurified and unpurified commercial cytochrome c using L-cysteine modification, whereas with bipyridyl modification the signal fell to zero in < 22 and < 4 hours for repurified and unpurified commercial cytochrome c, respectively. Direct electrochemistry of twice gel-filtered GOx was promoted using aminoethanethiol, and GOx-bound FAD exhibited $E^{0'}$ = -0.250 V vs Ag/AgCl. Two redox couples appeared

in the voltammogram of GOx in 0.4-0.8 M urea with $E^{0'}$ = -0.410 and -0.205 V (vs Ag/AgCl), and the couple at -0.205 V was found to increase with urea concentration. An N-mercaptopropionyl-dopamine-modified gold electrode yielded catalytic currents for native GOx; thus, an immobilized mediator (dopamine) can shuttle electrons from the buried $FADH_2$ redox center of GOx to the electrode.

"True science is a loving science. The man who pursues such science is confronted by the secret life of things which has confronted none before him; this life places itself in his hands, and he experiences it, and is filled with its happening to the rim of his existence. Then he interprets what he has experienced in simple and fruitful concepts, and celebrates the unique and incomparable that happened to him with reverent honesty."

Martin Buber

ACKNOWLEDGEMENTS

I, her first (graduating) graduate student, would like to thank my co-supervisor, Susan Mikkelsen, for her clarity, encouragement, and the confidence she has placed in me (and for getting most of my jokes).

I would like to thank my other co-supervisor, Ann English, for her guidance in the preparation of this thesis, her constructive criticisms during my research and her interest in my professional development.

Thanks also to my friend and colleague, Fernando Battaglini, whose passion for his subject is so inspiring, for helping me to understand more fully what I was doing. Gracias por todo.

Thanks to my colleagues and friends: Kelly Millan for her hilarious "Kelly stories", Beata Kolakowski for keeping up morale, and Steve Marmor for assuring me that one can indeed finish a thesis.

Thanks to Line, Craig, George, Yazhen and Raj for helping out whenever I needed them and for their encouragement during my program.

Finally, to my wife Stefani, who knew I was a graduate student and married me anyway; thanks for her love, support and patience when I couldn't spend enough time with her.

TABLE OF CONTENTS

List of Figures and Schemes

List of Tables

Abbreviations

A	Ampere
AMP	adenosine monophosphate
CM	carboxymethyl
CV	Cyclic Voltammogram
cyt c	cytochrome c
D-GOx	deglycosylated GOx
EDC	1-ethyl-3-(3-dimethylaminopropyl)carbodiimide hydrochloride
eqn.	equation
FAD	flavin adenine dinucleotide
FC	ferrocene
FCA	ferrocenemonocarboxylic Acid
FDA	ferrocenedicarboxylic acid
FPLC	fast protein liquid chromatography
GCE	Glassy Carbon Electrode
GOx	glucose oxidase
LSV	linear sweep voltammetry
NHS	*N*-hydroxysulfosuccinimide
PAGE	polyacrylamide gel electrophoresis
Pi	phosphate

1.0 INTRODUCTION

Studies of the electron-transfer reactions of redox proteins and enzymes have drawn considerable interest in recent years for the insights they have afforded concerning many of the most fundamental processes in nature.[1] For example, cellular respiration and photosynthesis are two of the most fundamental applications of electron-transfer using biomolecules. Topics that have received much attention include mechanisms of intermolecular electron transfer between redox proteins and the role of the protein itself in facilitating and/or controlling electron transfer.[2] Another extensive branch of these studies includes the investigation of electron-transfer reactions and mechanisms of redox proteins and enzymes at electrodes using established electrochemical techniques.[3,4]

An important practical application of electron-transfer reactions of redox proteins and enzymes at an electrode is in the development of biosensors. These are discrete bioanalytical devices that are based on the coupling of biological components with a measurement device such as an electrode or optical fiber.[5] The development of biosensors has great potential for a variety of novel applications such as *in vivo*, real-time determinations of particular species that are important diagnostics. Over thirty years ago, Clark and Lyons[6] achieved a breakthrough with the development of a glucose biosensor using glucose oxidase (GOx) immobilized on an electrode surface.

The original Clark and Lyons biosensor was based on the amperometric detection of hydrogen peroxide, which is one of the products of GOx-catalyzed glucose oxidation. GOx has also been used in thermometric biosensors that are based on the measurable enthalpy change associated with glucose oxidation.[7] A commercially available

amperometric blood-glucose measuring device, based on a ferrocene-derivative as mediator, has already found widespread use.[8] This biosensor uses the ferrocene to shuttle electrons from the reduced $FADH_2$ prosthetic groups of GOx, which are formed after glucose oxidation, to the electrode surface creating a current that is proportional to glucose concentration.

GOx (β-D-glucose:O_2 oxidoreductase, EC 1.1.3.4) is considered an ideal enzyme for biosensor applications because it is highly stable, has high turnover and is highly specific for glucose, a commercially and diagnostically important substrate.[9] The structure of GOx has recently been elucidated[10] and this enzyme is the focus of continuing intensive biosensor research. It is a flavoenzyme that catalyzes the reaction between β-D-glucose and O_2 to yield H_2O_2 and δ-gluconolactone.[11] It is isolated from cultures of the mold *Aspergillus niger*,[12] and its structure is that of a glycoprotein dimer whose total molecular weight is approximately 160 kDa.[13,14] Each monomer has an active site containing a flavin adenine dinucleotide (FAD) prosthetic group that is tightly but non-covalently bound to the polypeptide.[10] The reaction of GOx with glucose in the presence of O_2 proceeds as follows:

β-D-glucose + FAD-GOx -----> D-glucono-δ-lactone + $FADH_2$-GOx (1.1)

$FADH_2$-GOx + O_2 -----> FAD-GOx + H_2O_2 (1.2)

An one-electron mediator, such as a ferricinium derivative, can also oxidize $FADH_2$-GOx:

$$FADH_2\text{-GOx} + 2FC^+ \text{ -----> } FAD\text{-GOx} + 2FC + 2H^+ \quad (1.3)$$

where FC^+ is the oxidized ferricinium form of the ferrocene and FC is the reduced form. At an electrode surface the FC^+ species can be regenerated, which causes a current to be detected that is proportional to the rate of formation of FC, and hence the glucose concentration. A mediator such as O_2 or ferricinium is required because the reduced form of the enzyme, $FADH_2$-GOx, shows no electrochemical activity at a bare electrode.[8] Degani and Heller[15,16] first reported the modification of GOx in such a way that the modified enzyme can transfer electrons directly to an electrode surface. This modification is based on the covalent incorporation of ferrocenes into the protein, and they proposed that *intramolecular* electron transfer occurred between GOx-bound $FADH_2$ and ferricinium "relays" inside the enzyme, followed by reoxidation of these covalently-attached ferrocenes at the electrode surface. A previous study[17] done in our laboratory showed that the modification procedure used by Heller et al. causes a sizable loss of activity. In addition, the rate of intramolecular electron transfer in modified GOx was found to be too slow by about three orders of magnitude to compete with freely-diffusing O_2. The research described here in Section 2.0, is a continuation of this work, using a different modification procedure, which was aimed at selectively modifying the lysine residues of GOx for possible applications in a glucose biosensor.

An entirely different approach to the problem of direct electron transfer between redox proteins and electrodes is in the modification of the electrode surface itself. In a major breakthrough, Hill and coworkers[18] showed that 4,4'-bipyridyl, which is postulated to form a monolayer at a gold electrode surface, promotes the direct reversible

electrochemistry of cytochrome c (cyt c). Concurrently, Yeh and Kuwana[19] showed that cyt c displays reversible electron transfer at a Sn-doped indium-oxide electrode. Direct, reversible electrochemistry of cyt c was also observed by Taniguchi et al.[20] using a gold electrode that was modified with bis(4-pyridyl) disulfide; by Digleria et al.[21] using amino-acid modified electrodes; and by Hill et al.[22] using oligopeptides as promoters. The monolayer that forms as a result of electrode modification with the above promoters alters the surface charge and properties of the electrode. The work reported here includes an investigation of simple sulfur-containing molecules and their ability to promote the electrochemistry of cyt c. This small (MW = 12.4 kDa) redox protein was chosen since it has been widely used in previous studies of modified electrodes, it is structurally well-characterized, and is well-behaved electrochemically.[3] An investigation of the promoters' ability to yield a persistent electrochemical signal from cyt c was also undertaken. Initially 4,4'-bipyridyl promotes quasi-reversible cyclic voltammetry for cyt c at a gold electrode; however, it quickly loses this capability, resulting in a time-dependent attenuation of the CV signal. In this study, a comparison of the persistence of CV signals for cyt c at a gold electrode modified with 4,4'-bipyridyl and the amino-acid L-cysteine as promoters was made.

The cyt c studies prepared the groundwork for the use of sulfur-containing compounds as promoters of GOx electrochemistry. The electrochemistry of native, deglycosylated[23], and urea-denatured forms of GOx was investigated in conjunction with aminoethanethiol (AET) as promoter at a gold electrode surface and the results are reported here. Deglycosylation was done in order to remove the carbohydrate layer

surrounding GOx, which was thought to increase the distance between the $FADH_2$ prosthetic groups and the electrode. Urea denaturation was also done in order to shorten this distance. Finally, the ability of an immobilized mediator, dopamine, on a gold electrode to shuttle electrons from $FADH_2$-GOx to the electrode surface was investigated.

The results in this thesis are presented in two parts. The first (Section 2.0) describes the modification of GOx with ferrocenemonocarboxylic acid (FCA), the quantitation of iron incorporated into the enzyme, and the characterization of the modified enzyme using fluorescence. Also included is the measurement of inter- and intramolecular electron-transfer rates using cyclic voltammetry. The second part (Section 3.0) presents results of the voltammetry of cyt c, and native and deglycosylated GOx at gold electrodes modified with sulfur-containing promoters, and with the immobilized dopamine mediator. Heterogeneous electron-transfer rate constants were evaluated and are compared for the promoter-modified electrodes.

Reagentless, selective *in situ* analyte quantitation is the key aim of biosensor research. This work presents part of ongoing research directed towards developing technology for the design of reliable electrochemical biosensors that use enzymes as chemical recognition elements.

1.1 References

1. Marcus, R. A.; Sutin, N., *Biochim. Biophys. Acta* **1985**, 811, 265-322.
2. Beratan, D. N.; Betts, J. N.; Onuchic, J. N. *Science* **1991**, 252, 1285-1288.

3. Armstrong, F. A.; Hill, H. A. O.; Walton, N. J. *Quart. Rev. Biophys.* **1985**, 18, 261-322.

4. Sigel, H.; Sigel A., *Metal Ions in Biological Systems*, 27, ed. Marcel Dekker, N. Y., **1991**, p. 431.

5. Rechnitz, G. A. *J. Clin. Lab. Anal.* **1987**, 1, 308-312.

6. Clark, L. C.; Lyons, C. *Ann. N. Y. Acad. Sci.* **1962**, 102, 29.

7. Muehlbauer, M. J.; Guilbeau, E. J.; Towe, B. C. *Anal. Chem.* **1989**, 61, 77-83.

8. Hill, H. A. O.; Sanghera, G. S., *Biosensors: A Practical Approach*, IRL Press, Oxford, **1990**, pp. 113-118.

9. Wilson, R.; Turner, A. P. F. *Biosens. Bioelectron.* **1992**, 7, 165-185.

10. Hecht, H. J.; Kalisz, H. M.; Hendle, J.; Schmid, R. D.; Schomburg, D. *J. Mol. Biol.* **1993**, 229, 153-172.

11. Duke, F. R.; Weibel, M.; Page, D. S.; Bulgrin, V. G.; Luthy, J. *J. Am. Chem. Soc.* **1969**, 91:14, 3904.

12. Swoboda, B. E. P.; Massey, V. *J. Biol. Chem.* **1965**, 240, 2209-2215.

13. O'Malley, J. J.; Weaver, J. L. *Biochemistry* **1972**, 11, 3527-3532.

14. Frederick, K. R.; tung, J.; Emerick, R. S.; Masiarz, F. R.; Chamberlin, S. H; Vasavada, A.; Rosenberg, S.; Chakraborty, S.; Schopter, L. M.; Massey, V. *J. Biol. Chem.* **1990**, 265, 3793.

15. Degani, Y.; Heller, A. *J. Phys. Chem.* **1987**, 92, 1285.

16. Degani, Y.; Heller, A. *J. Am. Chem. Soc.* **1988**, 110, 2615.

17. Badia, A.; Carlini, R.; Fernandez, A.; Battaglini, F.; Mikkelsen, S. R.; English, A. M. *J. Am. Chem. Soc.* **1993**, 115, 7053.

18. Eddowes, M. J.; Hill, H. A. O. *J. Chem Soc., Chem. Commun.* **1977**, 771-772.

19. Yeh, P.; Kuwana, T. *Chem. Lett.* **1977**, 1145-1148.

20. Taniguchi, I.; Toyosawa, K.; Yamaguchi, H.; Yasukouchi, K. *J. Chem. Soc., Chem. Commun.* **1982**, 1032-1033.

21. Di Gleria, K.; Hill, H. A. O.; Lowe, V. J.; Page, D. J. *J. Electroanal. Chem.* **1986**, 213, 333-338.

22. Barker, P. D.; Di Gleria, K.; Hill, H. A. O.; Lowe, V. J. *Eur. J. Biochem* **1990**, 190, 171-175.

23. Kalisz, H. M.; Hecht, H. J.; Schomburg, D.; Schmidt, R. D. *Biochim. Biophys. Acta* **1991**, 1080, 138.

2. FCA-MEDIATED ELECTROCHEMISTRY OF GLUCOSE OXIDASE

2.0 Introduction

The GOx-catalyzed oxidation of glucose leads to the reduction of the enzyme's active site groups to $FADH_2$ (eqn. 1.1), which are then reoxidized by freely diffusing O_2 (eqn. 1.2).[1,2] The catalytic cycle can also proceed in an oxygen-free environment in the presence of glucose with other freely diffusing electron-transfer mediators such as ferricinium derivatives (FC^+),[3] quinones[4], phenothiazines[5], and ruthenium and osmium complexes.[6,7] A pH value of 7.5 was found to be optimal for GOx catalytic activity when used with a group of mediators that include ferrocenes and tetracyanoquinodimethane (TCNQ).[1] This is useful in that the pH of human blood is 7.4. In the case of a one-electron mediator such as FC^+, the following reactions occur where eqn. 2.1 is generally believed to be the rate-limiting step:[34]

$$FADH_2\text{-GOx} + FC^+ \xrightarrow{k_1} FADH^{\cdot}\text{-GOx} + H^+ + FC \qquad (2.1)$$

$$FADH^{\cdot}\text{-GOx} + FC^+ \xrightarrow[\text{(fast)}]{k_2} FAD\text{-GOx} + H^+ + FC \qquad (2.2)$$

Direct transfer of electrons from $FADH_2$-GOx to electrode surfaces such as gold or glassy carbon is not observed since the $FAD/FADH_2$ redox centers are buried > 13 Å

below the enzyme surface.[2,8] In contrast, the free FAD/$FADH_2$ couple in solution easily transfers electrons to a variety of electrode surfaces.[3]

To mediate electron transfer from the redox centers of the enzyme to the surface of an electrode, a low molecular-weight redox couple is added to an oxygen-free GOx solution. In this case, the mediator can gain access to the enzyme's active site and shuttle electrons from $FADH_2$ to the electrode surface.[3] The ferrocene/ferricinium (FC/FC^+) couple is one of several that can be used for the mediation of electron transfer between reduced GOx and electrodes:[9]

$$\beta\text{-D-glucose} + \text{FAD-GOx} \text{ -----> } \text{D-glucono-}\delta\text{-lactone} + FADH_2\text{-GOx} \quad (1.1)$$

$$FC \overset{\text{electrode}}{\rightleftharpoons} FC^+ + e^- \quad (2.3)$$

$$FADH_2\text{-GOx} + 2FC^+ \text{ -----> } \text{FAD-GOx} + 2FC + 2H^+ \quad (1.3)$$

In the above scheme, a current is generated by the electrochemical oxidation of free FC to FC^+ (eqn. 2.3), with the subsequent bimolecular reduction of freely diffusing FC^+ by the reduced form of GOx (eqn. 1.3).

Electrical communication between the buried FAD redox centers of GOx and an amperometric electrode has also been achieved through the use of enzyme-bound mediators.[3] The covalent derivatization of GOx with low molecular-weight electron-transfer mediators, such as ferrocene derivatives and pentaammineruthenium(III) has been of considerable recent interest in the ongoing development of a glucose

biosensor.[10,3,11,12,15,13] Heller and coworkers, and others have shown[3,15] that GOx can be made electroactive by the covalent binding of ferrocenemonocarboxylic acid (FCA) to lysine residues in GOx.[3,15] According to their scheme, an electrocatalytic current that varies with the concentration of glucose appears as a result of the oxidation of FCA at the electrode surface with its concomitant reduction by $FADH_2$ through *intramolecular* electron-transfer:[14]

$$FADH_2\text{-}GOx\text{-}(FCA)_n \overset{\text{electrode}}{\rightleftharpoons} FADH_2\text{-}GOx\text{-}(FCA^+)_n + ne^- \qquad (2.4)$$

$$FADH_2\text{-}GOx\text{-}(FCA^+)_n \text{ -----> } FAD\text{-}GOx\text{-}(FCA)_2(FCA^+)_{n-2} + 2H^+ \qquad (2.5)$$

Two methods for the covalent derivatization of GOx have been used to selectively bind ferrocenes to primary amino groups of lysine residues (Lys) in GOx.[14] The first is based on the use of 1-ethyl-3-(3-dimethylaminopropyl) carbodiimide hydrochloride, (EDC), to promote amide bond formation. Using this method, Degani and Heller reported that reproducible derivatization of GOx with ~40% loss of activity with FCA was achieved if the enzyme was incubated in 3 M urea. It was concluded that unfolding of the protein with urea was required to increase exposure of the primary amino groups during the reaction with EDC while still retaining the two non-covalently bound FAD prosthetic groups within the enzyme.[3] With this procedure, an average of 12 ± 1 molecules of FCA were bound to each molecule of GOx.[15]

One drawback with the EDC-Urea procedure, however, is that the *o*-acylisourea intermediate, formed in the reaction of EDC with the carboxyl group of FCA, is expected to show reactivity with nucleophiles other than the targeted Lys residues (Scheme 2.1a). *o*-acylisoureas are susceptible to hydrolysis and are known to react with alcohols and thiols to form esters and thioesters.[16,17] *o*-acylisourea can also rearrange to form stable *N*-acylureas.[18] An alternative method involves the formation of an N-hydroxysuccinimide ester by reacting the *o*-acylisourea intermediate with *N*-hydroxysulfosuccinimide (NHS) (Scheme 2.1b). The resulting NHS ester is resistant to hydrolysis[19] and requires a stronger nucleophile for acylation than the parent species. NHS-esters have also demonstrated high selectivity for Lys residues.[20]

In this work, different EDC, NHS and FCA ratios were used to optimize the covalent modification of GOx. The goal is to retain high activity while maximizing the rate of intramolecular electron transfer from $FADH_2$ to covalently-bound ferricinium.

Evidence for the covalent modification of GOx was sought by the analysis of protein tryptophan (Trp) fluorescence. Covalently-bound FCA is expected to quench Trp emission of the native enzyme and after it nas been denatured in 8 M urea. Adsorbed or associated FCA, on the other hand, would be released in urea and quenching would be relieved. Heterogeneous (electrochemical) activities were measured by voltammetry to obtain kinetic parameters for the modified enzymes, including bimolecular and intramolecular electron-transfer rate constants.

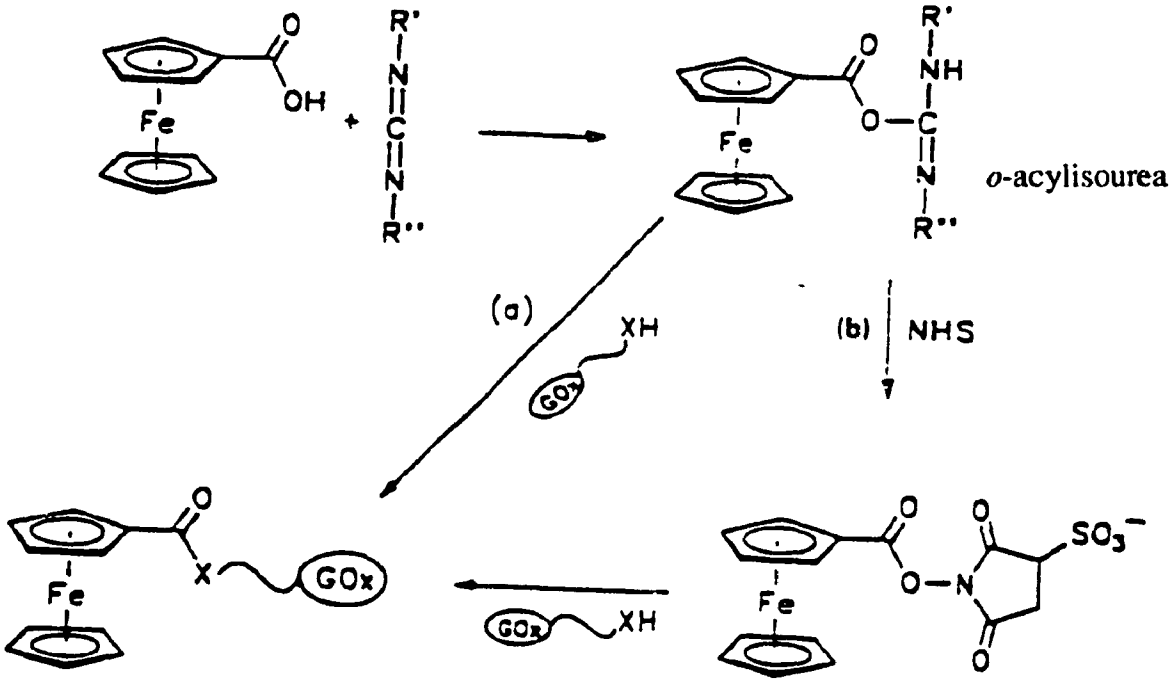

Scheme 2.1 Amide bond formation between FCA and GOx using EDC in the absence (pathway a) and presence (pathway b) of NHS. XH is any nucleophilic species, such as tyrosine-OH, cysteine-SH, or lysine or N-terminal-NH_2 groups.

Further work reported here involved studies on homogeneous, bimolecular electron transfer between freely-diffusing FCA^+ and $FADH_2$-GOx in a voltammetric system. This can be described with the following equations:

$$FCA \underset{\text{(fast)}}{\overset{\text{electrode}}{\rightleftharpoons}} FCA^+ + e^- \qquad (2.3)$$

$$2FCA^+ + FADH_2\text{-GOx} \xrightarrow{k_{obs}} 2FCA + FAD\text{-GOx} + 2H^+ \qquad (1.3)$$

$$\beta\text{-D-glucose} + FAD\text{-GOx} \longrightarrow D\text{-glucono-}\delta\text{-lactone} + FADH_2\text{-GOx} \qquad (1.1)$$

In saturating glucose, under anaerobic conditions, the concentration of $FADH_2$-GOx (eqn. 1.1) is assumed to be constant and equal to the total enzyme concentration. This would allow the evaluation of k_{obs}, the bimolecular rate constant, for reaction 1.3 under pseudo-first order conditions. However, as the concentration of free FCA is increased in relation to GOx, a corresponding depletion of $FADH_2$-GOx near the electrode *surface* is expected since, at higher FCA concentrations, the rate of $FADH_2$-GOx regeneration (eqn. 1.1) may be comparable to the rate of FCA regeneration (eqn. 1.3).[21] Therefore, the assigment of the rate determining step to eqn. 1.3 alone becomes uncertain, and k_{obs} depends on the FCA:GOx ratio. Extrapolation to zero FCA concentration yields the true value of k_{obs} for reaction 1.3.

Linear sweep voltammetry (LSV)[22] was used for all kinetic experiments involving FCA-modified GOx and the bimolecular reactions between free FCA and GOx. However,

an electrochemical method was sought that would reduce the contribution of the residual electrode charging current that is intrinsic to charged surfaces undergoing a continuous change in potential. Chronoamperometry (CA)[22] was used for comparison with LSV since this method relies on an instantaneous potential change at the electrode surface (a potential-step technique) and the results are discussed in Section 2.2.6 and 2.3.

The work described in this chapter is part of an ongoing project in our laboratory aimed at facilitating electron transfer from GOx to amperometric electrodes for applications in a glucose biosensor. Concurrent with the experiments described here, various GOx-$(FC)_n$ derivatives were prepared by both EDC-Urea and EDC-NHS methods, and were characterized by similar procedures.[14] This chapter details the preparation and characterization of three GOx-$(FCA)_n$ derivatives from the EDC-NHS reaction only.

2.1 Experimental Section

2.1.1 Materials. Glucose oxidase (GOx, E.C. 1.1.3.4) from *Aspergillus niger* was purchased from Boehringer Mannheim; Grade II lot number 11158832-20 was used for all FCA mediation experiments and lot number 12635524-33 was used for all other experiments. Horseradish peroxidase (HRP, E.C. 1.11.1.7, 10 mg/mL suspension in 3.2 M ammonium sulfate, ~ 250 units/mg), *o*-dianisidine dihydrochloride, 4-(2-hydroxylethyl)-1-piperazineethanesulfonic acid (HEPES) and 1-ethyl-3-(3-dimethylaminopropyl)carbodiimide hydrochloride (EDC) were all purchased from Sigma. Ferrocenemonocarboxylic acid (FCA) and α-D-glucose were obtained from Aldrich; N-hydroxysulfosuccinimide (NHS) was purchased from Pierce; 3-(2-pyridyl)-5,6-bis(4-

phenylsulfonic acid)-1,2,4-triazine (ferrozine) was obtained from ICN Biochemicals. Coomassie Brilliant Blue G-250 protein assay dye reagent and electrophoresis grade urea were from Bio-Rad. Mono- and dibasic sodium phosphate, and mono- and dibasic potassium phosphate were from Fisher. All other chemicals were of the best available quality and were used as received.

Non-reagent materials and equipment used included: Sephadex G-15 (≤ 1,500 MW fractionation range) gel filtration resin from Pharmacia; YM 30 (30,000 MW cutoff) ultrafiltration membranes and ultrafiltration cells from Amicon; Acrodisc syringe filters (0.2 and 1.2 μm-pore) from Gelman Sciences; glassy carbon (GCE) working and Ag/AgCl reference electrodes from Bioanalytical Systems (BAS) and Pt wire from Fisher. Distilled water that was further purified by passage through a Sybron-Barnstead Nanopure ion-exchange system was used in the preparation of all solutions. Absorption and fluorescence spectra were recorded using Varian (Cary 1), Hewlett-Packard (model 8451A) and Shimadzu (model RF-5000) instruments. Electrochemical measurements were recorded on a BAS-100A Electrochemical Analyzer.

2.1.2 Methods

2.1.2.1 GOx-$(FCA)_n$ derivatization procedure. The reagent concentrations and ratios used for covalent modification of GOx using the EDC-NHS procedure are summarized in Table 2.1. FCA was dissolved with sonication in 0.15 M Na-HEPES at pH 9.6. Following this, the pH was adjusted to 7.3 ± 0.1 with 1 N HCl and the solution was cooled to 0 °C. EDC and NHS were then added, and after 30 min activation, the pH was readjusted to 7.3 and GOx (15 mg/ml) was added. This reaction mixture was left at 4 °C

for 15 h. The resulting turbid orange solution was centrifuged, filtered and concentrated to ~2 mL by ultrafiltration. GOx-$(FCA)_n$ was separated from excess reagents by gel filtration on a 1.5- x 54-cm G-15 column and stored at 4 °C for ~24 h. A second gel filtration was performed and the sample was sterilized by filtration through a 0.2 μm filter and stored in 0.085 M NaPi buffer, pH 7.0, in sterile glass vials at 4 °C.

2.1.2.2 GOx Activity Assay. The activities of GOx-$(FCA)_n$ and native GOX were measured using a coupled peroxidase-*o*-dianisidine assay procedure[23,24] as follows:

$$\beta\text{-D-glucose} + H_2O + O_2 \xrightarrow{GOx} \text{D-glucono-}\delta\text{-lactone} + H_2O_2 \qquad (1.1)$$

$$H_2O_2 + 2\ DH_2 \xrightarrow{HRP} 2\ H_2O + D_2 \qquad (2.6)$$

where HRP is horseradish peroxidase, DH_2 is the colorless reduced form of the *o*-dianisidine dye, and D_2 the oxidized form (Scheme 2.2) with $\varepsilon_{436} = 8.3 \times 10^3\ M^{-1}\ cm^{-1}$. The change in absorbance over time was measured for this coupled-enzyme system in 0.1 M KPi buffer (pH 7.0) at 23 °C. The assay solution was prepared from the following stock solutions: ~0.1 U mL^{-1} GOx, 2.4×10^{-7} M *o*-dianisidine, and 0.56 M mutarotated glucose, all in 0.1 M KPi buffer, pH 7.0; horseradish peroxidase (HRP) stock was 2 mg/mL in 2.56 M $(NH_4)_2SO_4$. An assay solution was prepared from the above stocks on adding 50 μL of the GOx solution, 2500 μL of air-saturated *o*-dianisidine solution, 500 μL of the mutarotated glucose solution, and 10 μL of the HRP solution (total volume: 3.06 mL) to a cuvette immediately prior to spectrophotometric measurement. The concentration of the species in the assay solution was 0.002 U mL^{-1} GOx, 1.96×10^{-7} M

o-dianisidine, 0.092 M mutarotated glucose and 6.5 x 10^{-3} mg/mL HRP.[24] Activities for modified GOx are reported relative to the activity of native GOx.

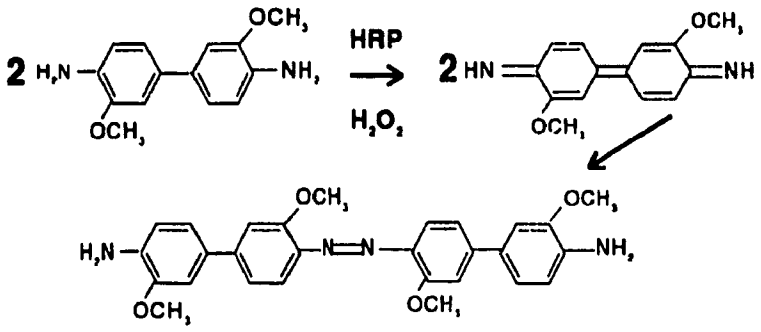

Scheme 2.2 HRP-Catalyzed Oxidation of *o*-Dianisidine by H_2O_2

2.1.2.3 Total Protein and Iron Quantitation. The standard Coomassie Blue procedure from Bio-Rad[25] was used to determine total protein concentrations spectrophotometrically at 594 nm. A calibration curve with native GOx concentrations ranging from 5 to 25 µg/mL was prepared, and GOx samples requiring protein quantitation were diluted so that their absorption, following reaction with Coomassie Blue, fell within the range of the calibration curve.

The iron content (and hence the GOx:FCA ratios) of the GOx-$(FCA)_n$ samples were determined using a previouly described procedure[26] involving ferrocene demetallation with concurrent protein precipitation by trichloroacetic acid. Subsequent reaction of the free iron(II) with ferrozine forms a 3:1 magenta complex with reported molar absorptivities greater than 2 x 10^4 M^{-1} cm^{-1} [27,28] at 562 nm. A linear calibration

curve for FCA solutions ranging in concentration from 1 to 4 mg/mL was prepared. The detection limit for iron using this procedure is 0.01 mg/L, corresponding to ~0.2 μM ferrocene.[26]

2.1.2.4 Protein Fluorescence Studies. Excitation of 0.35-μM native GOx and GOx-$(FCA)_n$ solutions was performed at 280 nm, and emission spectra were recorded between 290 and 500 nm. Slit widths of 5.0 nm were used for both excitation and emission, and the sample temperature was maintained at 22 ± 1 °C. Corrections to all spectra for inner filter effects[29a] were done using:

$$F_c = F_o \cdot \text{antilog}[(A_{ex} + A_{em})/2] \tag{2.7}$$

where F_c and F_o are the corrected and observed emission intensities, and A_{ex} and A_{em} are the absorbances at the excitation and emission wavelengths, respectively. Native GOx and GOx-$(FCA)_n$ samples were denatured by incubation overnight at 4 °C in 8 M urea before recording their emission spectra. Covalent modification of GOx with FCA was verified by comparing the emission spectra of the denatured GOx-$(FCA)_n$ samples with those of noncovalent mixtures containing equivalent FCA:GOx ratios.

Average distances between the bound FCA groups and Trp residues of GOx were calculated assuming Förster resonance energy transfer.[30] The efficiency of energy transfer (E) between the donor (Trp) and acceptor (FCA) is related to their separation (r) by:

$$E = r^6/(r^{-6} + R_o^{-6}) \tag{2.8}$$

where R_o is the distance at which donor fluorescence is quenched by 50%. R_o is defined by:

$$R_o = 9.79 \times 10^3 (\kappa^2 n^{-4} Q_a J)^{1/6} \quad (2.9)$$

where κ^2, the orientation factor, is 0.67 for random orientation between donor and acceptor;[31] n, the refractive index, is generally given a value of 1.33 for proteins;[32] Q_a, the quantum yield for Trp, is 0.2 in the absence of acceptor;[33] and J is the spectral overlap integral. The J value for Trp ---> FCA energy transfer was determined graphically[30] over the spectral region from 290 tc 450 nm.

2.1.2.5 Voltammetry. A standard three-electrode cell configuration consisting of a glassy carbon working electrode, Ag/AgCl reference and Pt auxiliary electrodes was used. The glassy carbon electrode (GCE) had a surface area of 0.071 cm^2 and was polished with 0.05 μm alumina and sonicated prior to each run. Immediately following gel filtration(s) and protein quantitation, 1 mL of native GOx or GOx-$(FCA)_n$ solution was added to the cell and deoxygenated through N_2 purging. All electrochemical measurements were performed under a continuous stream of wet high purity grade N_2. Mutarotated 1 M glucose solutions in 0.1 M NaPi buffer were deoxygenated and transferred by gas-tight syringe to the cell. Voltammograms using linear sweep voltammetry (LSV) were recorded from 0.0 to 0.5 V (vs. Ag/AgCl) at a scan rate of 2 mV s^{-1}, unless otherwise noted. Chronoamperometry was performed under cell and electrode conditions that were identical to LSV. The applied potential at the GCE was stepped to 0.550 V from a resting value of 0.000 V for various time intervals and brought back to 0.000 V for an

equivalent time interval. The resulting current was plotted against time.

2.2 Results

2.2.1 Protein and Iron assays. Typical calibration curves for total protein and FCA iron assays are shown in Figures 2.1 and 2.2. Both curves have correlation coefficients exceeding 0.99. All samples to be assayed were diluted to fall within the concentration range of these curves and triplicate analyses were carried out. The ratio of covalently-bound FCA to GOx obtained from coupling reactions using various EDC, NHS and FCA ratios are summarized in Table 2.1.

2.2.2 Activity of GOx-$(FCA)_n$ Derivatives. Enzyme activities are also shown in Table 2.1. The results show that activities of GOx-$(FCA)_n$ are not significantly sensitive to EDC concentration. Furthermore, the presence of EDC and NHS, in the absence of FCA, yielded only a small activity loss of 8%. These results also show that a fourfold increase in EDC concentration, from 50 to 200 mM, yielded a twofold increase in covalently-bound FCA.

2.2.3 Protein Fluorescence of GOx-$(FCA)_n$. Figure 2.3 shows the dependence of native GOx fluorescence on urea concentration. The increase in fluorescence intensity observed upon unfolding is typical of proteins containing chromophores such as FAD that can quench fluorescence through resonance energy transfer. From this figure, it can be seen that > 5 M urea is required for complete unfolding of GOx.

Table 2.2 summarizes the fluorescence maxima and the calculated (eqn. 2.9) FCA-Trp distance for GOx-$(FCA)_{12}$ samples. Figure 2.4 shows the emission spectra of GOx-

$(FCA)_{12}$ and GOx control samples in 8 M urea. Unmodified GOx and a non-covalent mixture of 12:1 FCA/GOx have both red-shifted fluorescence (λ_{max} ~350 nm), whereas for derivatized GOx-$(FCA)_{12}$ λ_{max} has only shifted to 344 nm. Red-shifted λ_{max} values are expected, due to the exposure of Trp residues to an aqueous environment upon unfolding at high urea concentrations.[14,29b] Comparing the fluorescence of GOx-$(FCA)_{12}$ with a noncovalent mixture of 12:1 FCA:GOx shows extensive quenching of Trp fluorescence in GOx-$(FCA)_{12}$ alone. Therefore, Trp quenching must be due to covalently-bound FCA in the unfolded state of GOx-$(FCA)_{12}$ and not to entrapped FCA in the protein matrix, since this should diffuse away upon unfolding. Quenching was not significant for the FCA:GOx noncovalent mixture, and it has been found that noncovalent FC:GOx ratios up to 40 do not show diffusional quenching at the concentrations (0.35 μM GOx) used in these analyses.[14]

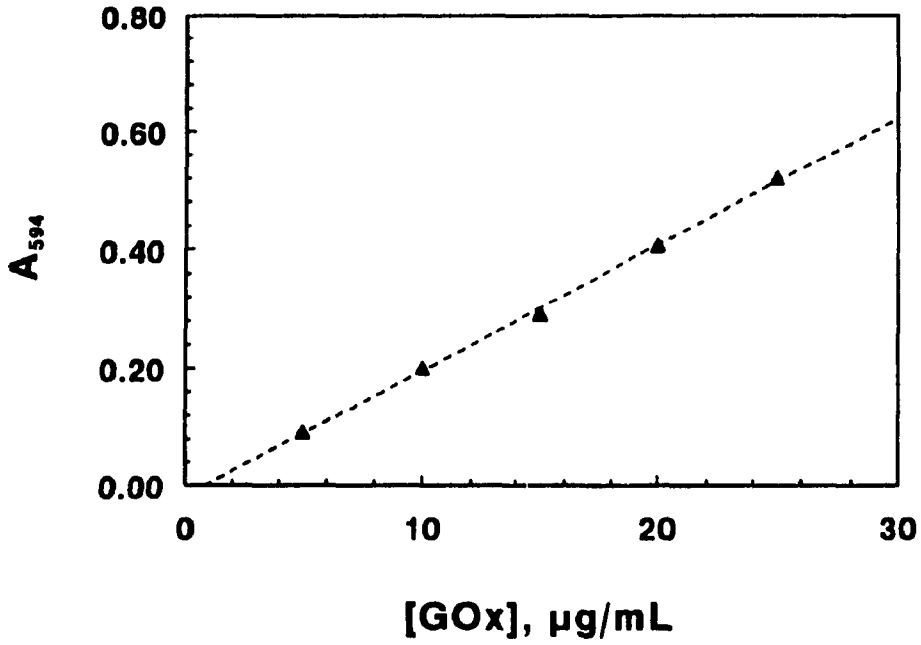

Figure 2.1 Coomassie blue total protein assay. The calibration curve was prepared using native GOx solutions in 0.085 M NaPi buffer, pH 7.2, having concentrations ranging from 5 to 25 µg/mL. The absorbance of these solutions was measured at 594 nm.

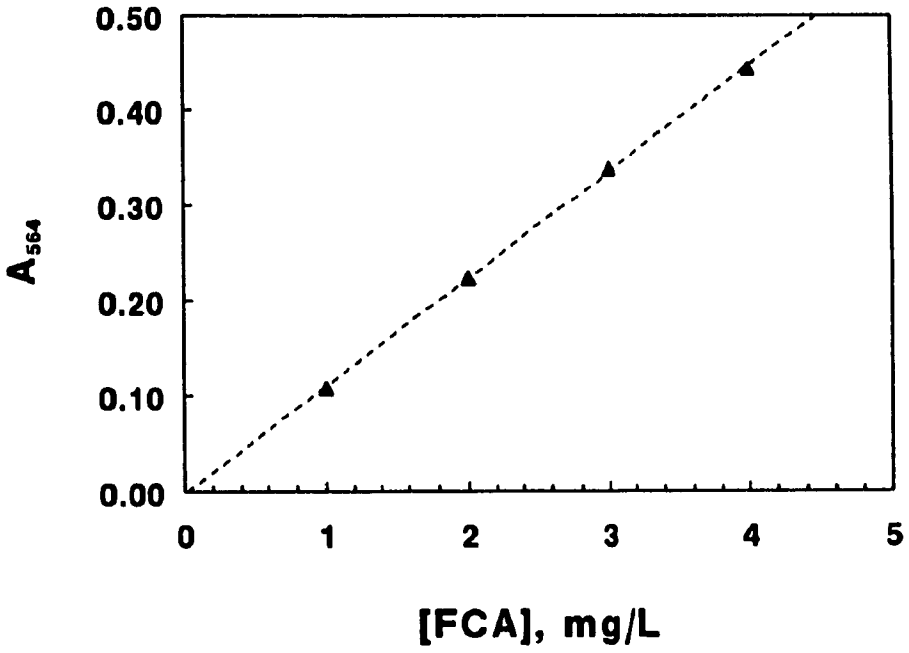

Figure 2.2 Analysis of FCA Fe in modified GOx using ferrozine. The calibration curve was prepared using FCA standard solutions containing 1 to 4 mg/L in 0.085M NaPi buffer, pH 7.2. Absorbance of Fe-(ferrozine)$_3$ complex was measured at 564 nm.

Table 2.1 Glucose Oxidase FCA-Modification Reactions[a]

Reagent Ratios (mol)			Product Characterization	
FCA mM	EDC mM	NHS mM	FC:GOx	% Activity
0	0	0	0	100
0	50	75	0	92
50	100	75	5 ± 1	61
100	50	75	6 ± 1	58
100	200	75	12	64

[a] Solutions contained 100 μM GOx with the given concentrations of EDC and NHS in 0.15 M Na-HEPES (pH 7.2) and were left standing at 4 °C for 15 h before gel filtration to remove excess reagents.

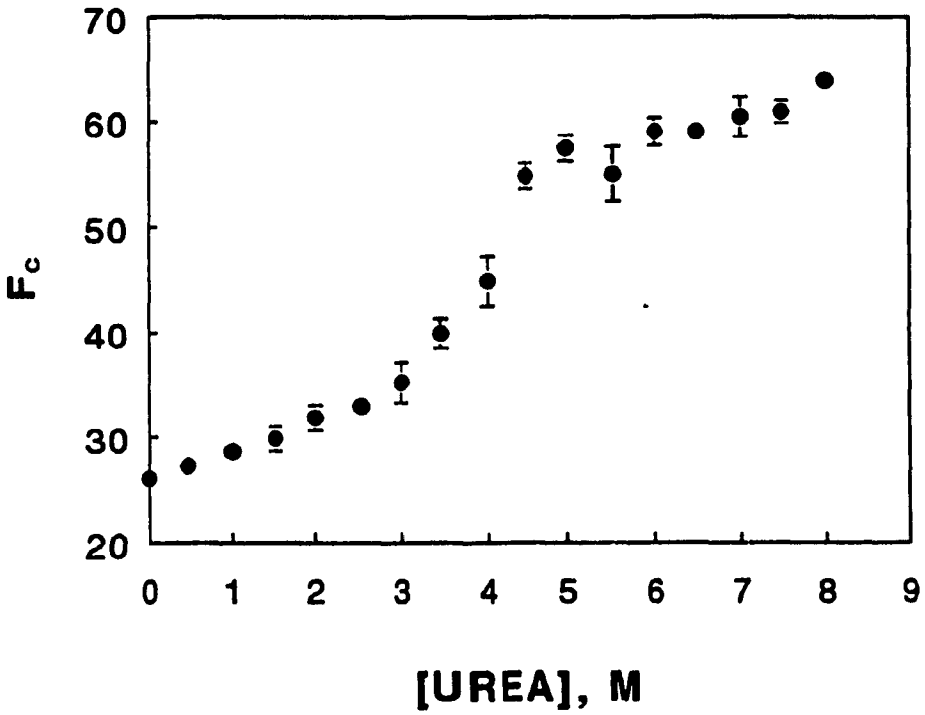

Figure 2.3 Fluorescence intensity (F_c) of GOx vs urea concentration. Fluorescence was measured at 350 nm for 0.36 μM GOx that was incubated with various urea concentrations overnight at 4 °C. F_c was corrected for inner filter effects (eqn. 2.7); λ_{ex} = 280 nm; slit widths = 5 nm.

Table 2.2 Fluorescence Maxima (λ_{max}) and Relative Fluorescence Intensities (%F) for GOx and GOx-$(FCA)_{12}$ in Phosphate Buffer and in 8 M urea[a]

	Buffer			8 M Urea[b]	
Protein	λ_{max} (nm)	%F	r(FCA-Trp)[c] Å	λ_{max} (nm)	%F
GOx + 12 FCA	334	100	-	350	100
GOx[c]	336	101	-	350	104
GOx-$(FCA)_{12}$[d]	336	65	18	344	86

[a] All samples contained 0.35 μM GOx in 0.085 M NaPi buffer at pH 7.0; λ_{ex} = 280 nm.

[b] Samples were left standing overnight in 8 M urea at 4 °C to ensure protein unfolding.

[c] Sample incubated in EDC and NHS in the absence of FCA.

[d] GOx-$(FCA)_{12}$ represents GOx derivatized with 12 FCA groups using the EDC-NHS procedure.

[e] FCA-(Trp) distances were calculated using eqn. 17 with R_o = 16.2 Å.[14]

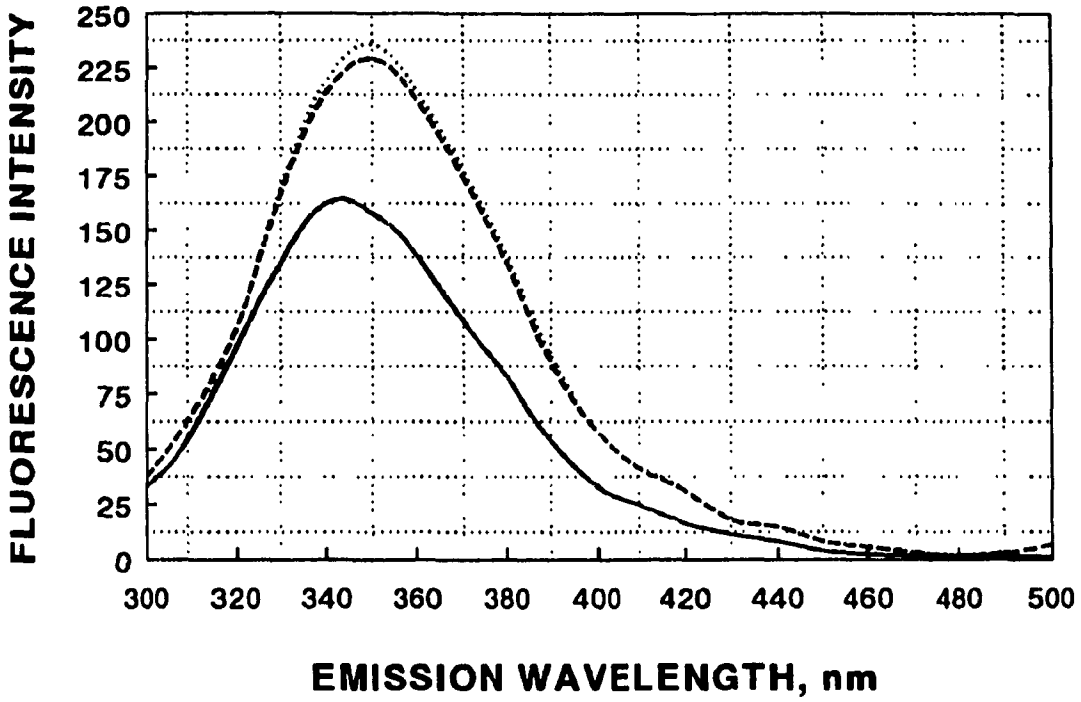

Figure 2.4 Emission spectra for 0.35 μM GOx and GOx-$(FCA)_{12}$ in 85 mM phosphate buffer (pH 7.0, 22.5 °C) containing 8 M urea. Excitation wavelength was at 280 nm and slit widths of 5.0 nm were used for both excitation and emission over a range of 290 to 500 nm. SOLID LINE, GOx-$(FCA)_{12}$; DASHED LINE, 12:1 noncovalent mixture of FCA:GOx; DOTTED LINE, GOx only. Samples were incubated in 8 M urea, overnight at 4 °C, before spectra were recorded.

2.2.4 Voltammetric Measurement of Intramolecular Electron-Transfer Rates in GOx-(FCA)$_n$. *Intramolecular* electron-transfer from $FADH_2$ to FC^+ groups covalently bound to the GOx molecule has been described as an electron-proton-electron-proton type of mechanism:[14]

$$FADH_2\text{-GOx-(FC)}_n \overset{\text{electrode}}{\rightleftharpoons} FADH_2\text{-GOx-(FC)}_{n-1}(FC^+) + e^- \quad (2.10)$$

$$FADH_2\text{-GOx-(FC)}_{n-1}(FC^+) \overset{k_1}{\text{------>}} FADH^{\bullet}\text{-GOx-(FC)}_n + H^+ \quad (2.11)$$

$$FADH^{\bullet}\text{-GOx-(FC)}_n \overset{\text{electrode}}{\rightleftharpoons} FADH^{\bullet}\text{-GOx-(FC)}_{n-1}(FC^+) + e^- \quad (2.12)$$

$$FADH^{\bullet}\text{-GOx-(FC)}_{n-1}(FC^+) \overset{k_2}{\text{------>}} FAD\text{-GOx-(FC)}_n + H^+ \quad (2.13)$$

$$\beta\text{-D-glucose} + FAD\text{-GOx-(FC)}_n \overset{k_3}{\text{----->}} \text{D-glucono-}\delta\text{-lactone} + FADH_2\text{-GOx-(FC)}_n \quad (1.1)$$

where k_3 is equal to $k_{cat}/\{1+K_m/[\text{glucose}]\}$.[14] FAD in GOx is instantaneously reduced by saturating glucose (10 mM glucose for modified enzyme, K_m = 0.3mM[14]) to $FADH_2$, therefore the limiting anodic current, i_{max}, arising from the electrochemical oxidation of reduced GOx-$(FC)_n$ is independent of voltage scan rate and is given by the following expression derived in the concurrent study:[14,34]

$$i_{max} = 2FA\,(D_{GOx}\,k_{obs})^{1/2}\,[GOx\text{-(FC)}_n] \quad (2.14)$$

where F is the Faraday constant (96,487 coulombs/mol), A is the geometric electrode area (0.071 cm^2), D_{GOx} is the diffusion coefficient of GOx (4.1 x 10^{-7} cm^2 s^{-1}),[15] [GOx-$(FC)_n$] is the active site concentration, and k_{obs} is equal to $k_1k_2/(k_1^{1/2}+k_2^{1/2})^2$.[14] For the scheme given by eqns. 1.1 and 2.10 - 2.13, the normalized limiting anodic current (i_{max}/[GOx-$(FC)_n$] is *independent* of protein concentration, and k_{obs} can be obtained from the plot of i_{max}/[GOx-$(FC)_n$] vs [GOx-$(FC)_n$]$^{1/2}$, since the limiting y-intercept value at high enzyme dilution is $2FA(D_{GOx}\ k_{obs})^{1/2}$.

Voltammetric dilution experiments were performed to determine i_{max} and hence, k_{obs}. Figure 2.5A shows a plot of i_{max}/[GOx-$(FC)_n$] vs [GOx-$(FC)_n$]$^{1/2}$ for active GOx-$(FCA)_{12}$, obtained by successive dilutions with a deaerated 10 mM glucose solution. Each point is the average i_{max} /[GOx-FCA_{12}] value, corrected for activity loss (Table 2.1), for three successive runs. The y-intercept value of 11.2 mA/M gave a k_{obs} value of 1.6 s^{-1} (eqn. 2.14).

Figure 2.5B shows the result of similar experiments using GOx-$(FCA)_6$ and GOx-$(FCA)_4$, which did not yield normalized currents independent of protein concentration. The k_{obs} values from these experiments were not evaluated since cyclic voltammograms of these derivatives in the absence of glucose showed the presence of free FCA in solution.

For bimolecular electron transfer, a plot of i_{max}/[GOx-$(FC)_n$] vs [GOx-$(FC)_n$]$^{1/2}$ is expected to be linear, with a positive slope proportional to the square root of the bimolecular rate constant.[14] The positive slopes in Figure 2.5B are thus also indicative of free FCA in solution. At higher concentrations of protein ([GOx-$(FCA)_n$]$^{1/2}$ $\geq$ 7.6), a

decrease in the normalized current is attributed to the aggregation of modified GOx.[14]

2.2.5 Voltammetric Measurement of Bimolecular Electron-Transfer Rates Between GOx and Free FCA. The bimolecular rate constant, k_{12}, for electron transfer from reduced native GOx to free FCA^+ in solution, can be evaluated from the diffusion-limited catalytic current, i_{max}, that is obtained through linear sweep voltammetry (LSV). The electrochemical oxidation of FCA followed by its homogeneous reduction with $FADH_2$-GOx can be described by the catalytic reaction scheme, $E_RC_I^{\bullet}$.[34,35] In this scheme, the reversible electrochemical reaction (E_R) of a reactant (eqn. 2.3) is followed by the rate-limiting, irreversible, bimolecular chemical reactions (C_I) that regenerate the redox species (eqns. 2.1 and 2.2). The catalytic reaction scheme, $E_RC_I^{\bullet}$ is described by the following equations:

$$\text{FCA} \overset{\text{electrode}}{\rightleftharpoons} \text{FCA}^+ + e^- \qquad (2.3)$$

$$\text{FCA}^+ + \text{FADH}_2\text{-GOx} \xrightarrow{k_1} \text{FCA} + \text{FADH}^{\bullet}\text{-GOx} + \text{H}^+ \qquad (2.1)$$

$$\text{FCA}^+ + \text{FADH}^{\bullet}\text{-GOx} \xrightarrow{k_2} \text{FCA} + \text{FAD-GOx} + \text{H}^+ \qquad (2.2)$$

$$\beta\text{-D-glucose} + \text{FAD-GOx-(FC)}_n \xrightarrow[\text{(fast)}]{k_3} \text{D-glucono-}\delta\text{-lactone} + \text{FADH}_2\text{-GOx-(FC)}_n \qquad (1.1)$$

where $k_3 = k_{cat}/\{1+K_m/[\text{glucose}]\}$. As glucose concentration is increased, k_3 ceases to be rate-limiting.

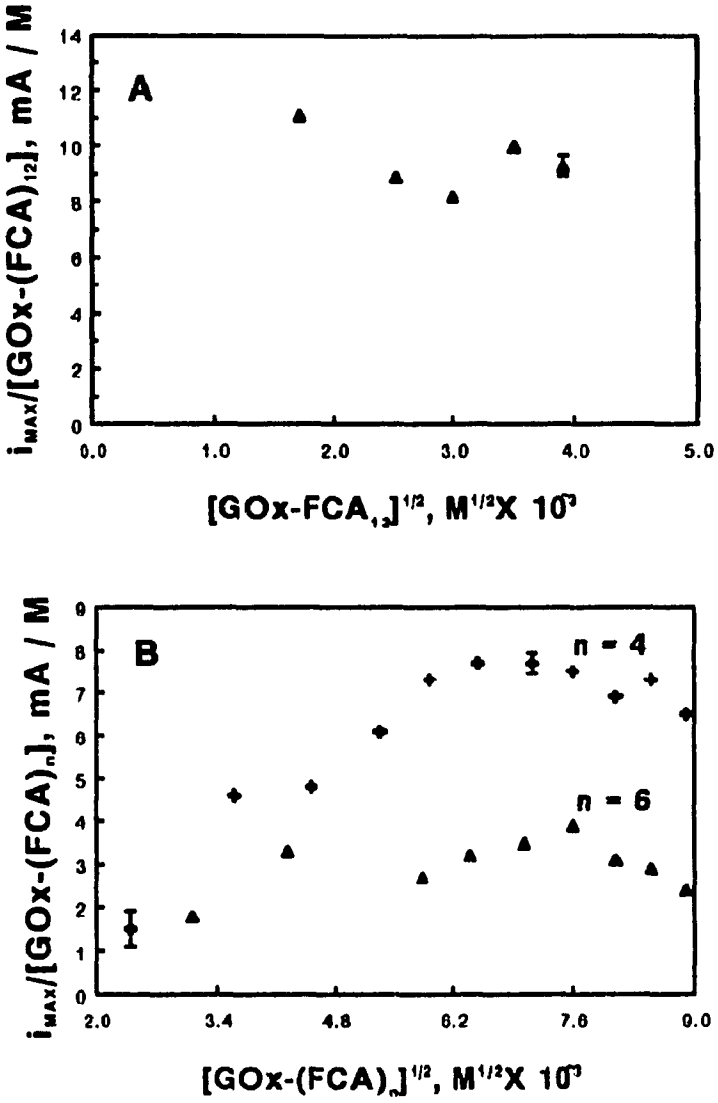

Figure 2.5 Average normalized limiting anodic currents, $i_{max}/[GOx\text{-}(FCA)_n]$, from triplicate voltammograms vs square root of GOx-$(FCA)_n$ concentration. Conditions: 0.085 M NaPi buffer, pH 7.2, scan rate 0.002 V s^{-1}. Plots for [A] GOx-$(FCA)_{12}$ which was subjected to three gel filtrations prior to voltammetry and [B] GOx-$(FCA)_n$ which was subjected to two gel filtrations.

As shown in Figure 2.6, for fixed GOx and FCA concentrations, i_{max} reaches a plateau at high glucose concentration. With a saturating glucose concentration of 100 mM, FAD in GOx is rapidly reduced by glucose to $FADH_2$. Under these conditions, the limiting anodic current, i_{max}, is independent of voltage scan rate and is given by the following expression derived in the concurrent study:[14,34]

$$i_{max} = FA\ (2D_{FCA}\ k_{12}\ [FADH_2\text{-}GOx])^{1/2}\ [FCA] \qquad (2.15)$$

where F and A are defined in eqn. 2.14, D_{FCA} is the diffusion coefficient of FCA (3×10^{-6} $cm^2\ s^{-1}$ at 25°C)[15], $[FADH_2\text{-}GOx]$ is the concentration of active sites, and $k_{12} = k_1k_2/(k_1+k_2)$ $M^{-1}\ s^{-1}$.[14]

In the presence of saturating glucose, it is generally assumed that all GOx is present in the reduced form, $FADH_2$-GOx, such that enzyme concentration in eqn. 2.15 is equal to the total GOx concentration. However, as the concentration of free FCA is increased relative to GOx, the rate of $FADH_2$ oxidation (eqns. 2.1 and 2.2) will also increase, and approach the rate of $FADH_2$-GOx regeneration (eqn. 1.1). Consequently, depletion of $FADH_2$-GOx may occur at the electrode *surface* (as opposed to the bulk solution) if the rate of $FADH_2$-GOx oxidation becomes comparable with the rate of its production. For different GOx:FCA ratios, Figure 2.7 shows plots of i_{max} vs $[FCA]^{3/2}$ according to the following eqn:

$$i_{max} = FA\ (2D_{FCA}\ k_{12}\ [FADH_2\text{-}GOx]/[FCA]\ )^{1/2}\ \ [FCA]^{3/2} \qquad (2.16)$$

where F, A, and D are as defined for eqn. 2.14 and the [GOx]:[FCA] ratio is held constant throughout each experiment. The corresponding k_{12} values, given in Table 2.3, indicate that as the GOx:FCA ratio decreases, there is an decrease in k_{12}.

Figure 2.8 shows a plot of k_{12} vs [FCA]:[GOx]. It is clear that at higher ratios the calculated k_{12} values significantly underestimate the true value obtained at low [FCA]:[GOx] ratios, where the assumption that the *reduced* GOx concentration is equal to the *total* GOx concentration holds. The estimated value at the intercept is $5.9 \pm 2 \times 10^4$ M^{-1} s^{-1}, and is the true value of k_{12} when [GOx] >> [FCA]. Therefore, at high FCA:GOx ratios the concentration of $FADH_2$-GOx does not remain constant at the initial GOx concentration, and the bimolecular electron-transfer steps in eqns. 2.1 and 2.2 ($FADH_2$/$FADH^{\bullet}$ oxidation) are not the only rate-limiting steps.[5]

2.2.6 Comparison of Linear Sweep Voltammetry and Chronoamperometry. In the electrochemical system described in Section 2.2.5, the measurement of the faradaic current due to the oxidation of free FCA is subject to the degree of uncertainty which is inherent in linear sweep voltammetry (LSV). The current plotted as a function of applied potential in a typical voltammogram for the $E_RC_I^{\bullet}$ catalytic current scheme (given in Section 2.2.5) has two components: The first consists of a background or residual current which depends on the capacitance of the electrode-solution interface (C) and the rate of change of applied potential:

$$i_c = C\, dV/dt \qquad (2.17)$$

where i_c is the residual or capacitative current, and dV/dt the scan rate.

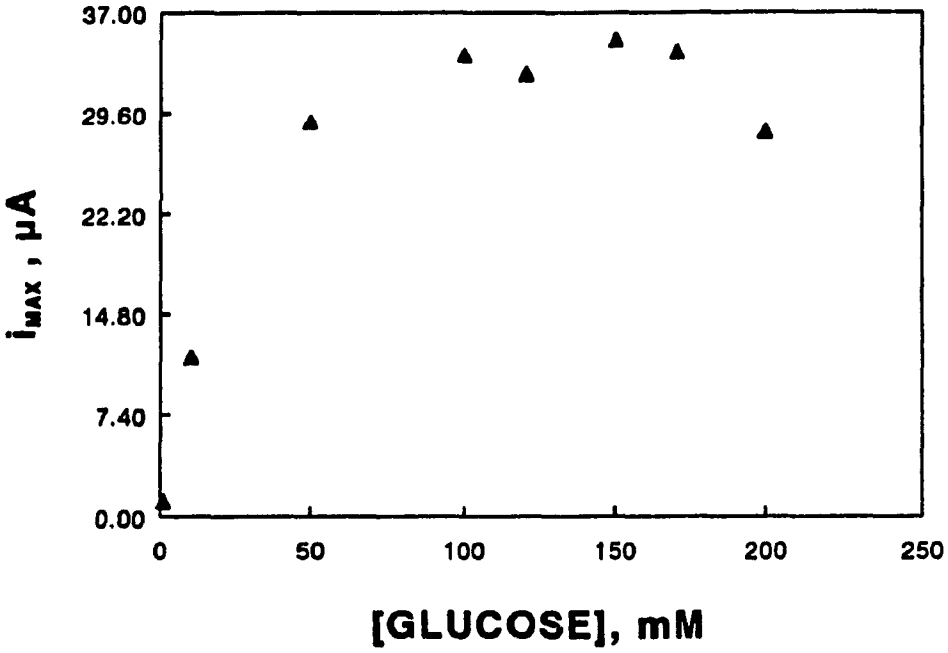

Figure 2.6 Plot of i_{max} vs glucose concentration for 23 µM native GOx using free FCA as mediator at a FCA:GOx ratio of 35:1. The limiting anodic current (i_{max}) was measured at +400 mV vs Ag/AgCl, and the potential was scanned at 2 mV s^{-1} in 0.085 M NaPi buffer, pH 7.2.

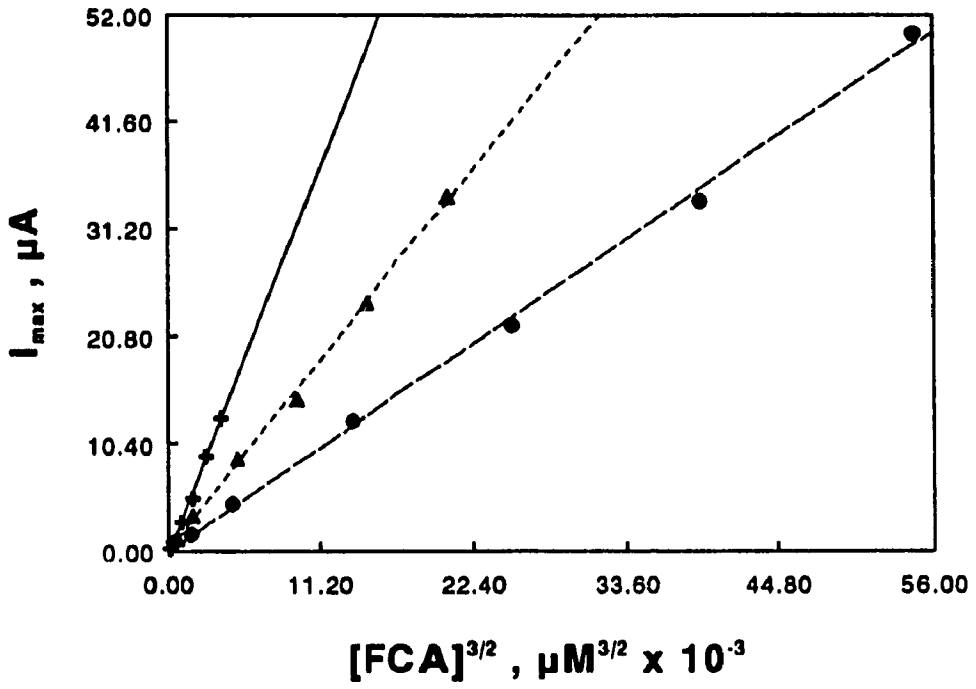

Figure 2.7 Dependence of electrocatalytic current (i_{max}) on $[FCA]^{3/2}$ at three different GOx:FCA ratios: (+) 1:2.5, (▲) 1:7.5, (●) 1:14.4. Triplicate measurements of i_{max} were made at 400 mV for each FCA concentration under anaerobic conditions. The initial GOx concentration was 50 µM in 0.085 M NaPi buffer, pH 7.2, with 100 mM saturating glucose. Samples were diluted using deaerated 100 mM glucose solution in 0.085 M NaPi buffer.

Table 2.3 Calculated k_{12} values from LSV at different FCA:GOx ratios

GOx:FCA Ratios[a]	FCA Concentration Ranges for Dilution Experiments (μM)[b]	Slope ± SD A $M^{-3/2}$	k_{12} ± SD x 10^{-4} M^{-1} s^{-1}
1 : 0.5	25 - 2	8.3 ± 0.8	12.2 ± 2.5
1 : 1	25 - 5	5.7 ± 0.7	11.6 ± 2.5
1 : 2.5	250 - 25	3.3 ± 0.1	9.7 ± 0.6
1 : 5	90 - 9	2.2 ± 0.1	8.6 ± 0.8
1 : 7.5	750 - 75	1.64 ± 0.03	7.2 ± 0.2
1 : 14.4	1440[c] - 143	0.90 ± 0.02	4.1 ± 0.2

[a] GOx concentration based on number of FAD active sites

[b] Three voltammograms were recorded at each concentration

[c] limit of FCA solubility in 0.085 M NaPi buffer solution, pH 7.2

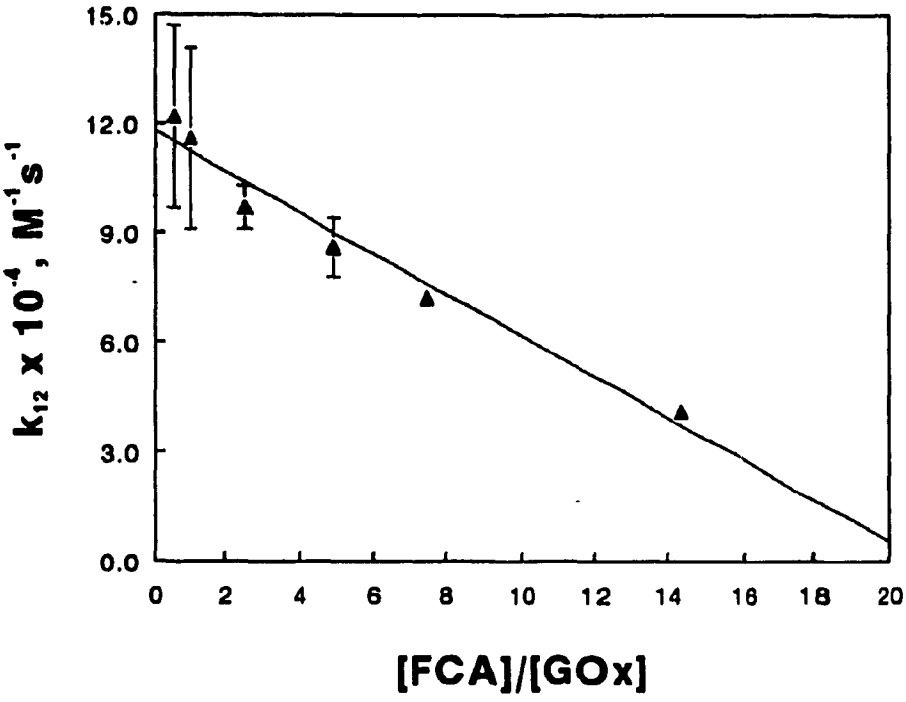

Figure 2.8 k_{12} vs FCA:GOx ratios. The k_{12} values were obtained from the plots of i_{max} vs $[FCA]^{3/2}$ (see Figure 2.7 and Table 2.3). The error bars indicate one standard deviation for each k_{12} value. This plot yields a limiting k_{12} value of $1.2 \pm 0.2 \times 10^5$ M^{-1} s^{-1}.

The second component is the faradaic current that results from the oxidation of FCA present in solution. Measurement of faradaic current to exclude the residual current involves the graphical extrapolation of the current/voltage response from a potential region at which no faradaic current occurs (Figure 2.9B). This extrapolated current is estimated at the measurement potential (+0.400 V), and is subtracted from the total current measured at this potential. This manual procedure is the principal source of uncertainty in measurement of the catalytic current, i_{max}.

Chronoamperometry (CA) is an alternative electrochemical method, which serves to reduce or eliminate the residual current from the measured total current in an equivalent electrochemical system.[35,22] As shown in Figure 2.10A, in this method the potential is *immediately* stepped (in < 1 ms) to a value at which the electroactive species in solution will undergo oxidation (or reduction) at a diffusion-limited rate. In chronoamperometry the potential remains at the stepped value for a set period of time until the current reaches a constant value, after which the potential is returned to its original value. The second potential change is not necessary for the measurement of i_{max}.

Figure 2.10B shows a typical chronoamperogram where the measured current response to the change in potential is plotted against time. Since the electrode surface does not undergo a continuous voltage change, the residual current quickly drops to zero and, after a period of time, only the faradaic current is observed which, for a catalytic system (E_RC_I'), is nearly constant. A comparison (Figure 2.11) of i_{max} vs $[FCA]^{3/2}$ plots as measured by LSV and CA shows that the currents are comparable, provided that the small residual current measured for the appropriate blank solution (Table 2.4) was

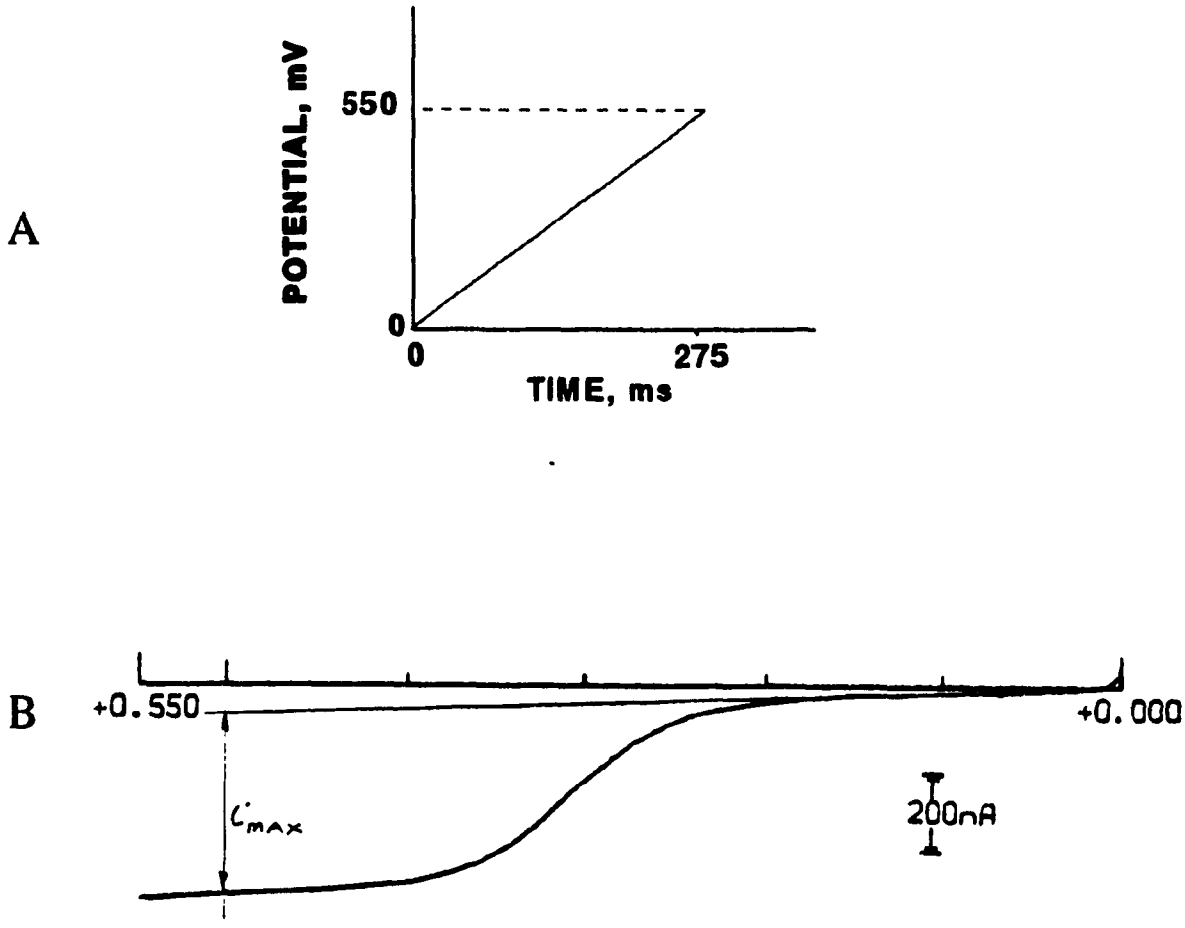

Figure 2.9 Linear sweep voltammetry of 20 μM free FCA and native GOx in 0.085 M NaPi buffer and 100 mM (saturating) glucose under anaerobic conditions. (**A**) Plot of potential scan vs time (2 mV s^{-1}) at a glassy carbon electrode (0.071 cm^2). (**B**) Typical voltammogram showing the graphical extrapolation of residual current and subtraction of this current at 0.400 V vs Ag/AgCl from the observed current to obtain i_{max}.

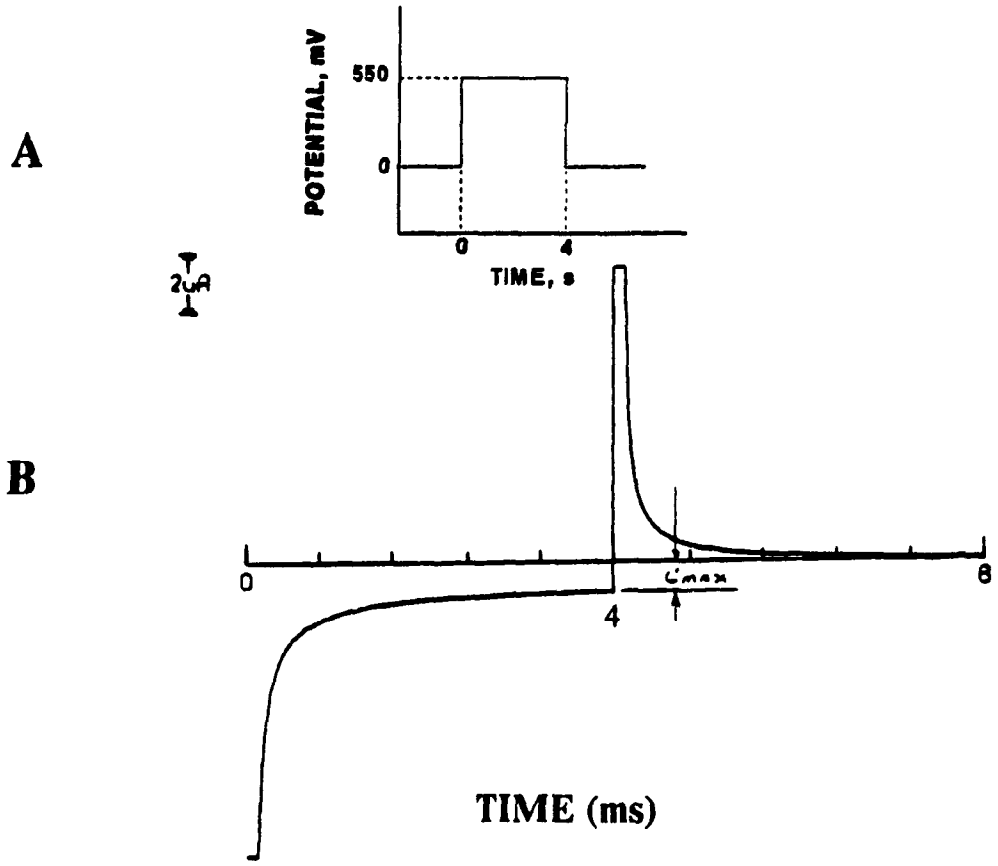

Figure 2.10 Chronoamperometry of 25 μM free FCA and GOx active sites (1:1) in 0.085 M NaPi buffer and 100 mM (saturating) glucose under anaerobic conditions. Chronoamperometry was performed using a glassy carbon electrode (0.071 cm^2). (**A**) Applied potential waveform. (**B**) Typical chronoamperogram showing an initial sharp elevation in current as the potential is stepped to +550 mV and FCA is oxidized, with a subsequent decrease as the residual current approaches zero and the faradaic current subsides to a steady-state level. The limiting current i_{max} is measured in this steady-state region, just before the point at which the potential is returned to its original value.

Table 2.4 Residual Currents in Blank Solutions[a] as Measured by Chronoamperometry

[GOx], μM	t = 4.0 s	t = 8.0 s	t = 10.0 s
Active Sites	i_t[b], μA	i_t, μA	i_t, μA
50	0.333	0.200	0.133
40	0.358	0.167	0.128
30	0.300	0.158	0.125
20	0.400	0.167	0.108
10	0.353	0.15	0.117
5	0.408	0.167	0.108
AVERAGE	0.359 ± 0.04	0.168 ± 0.02	0.120 ± 0.01

[a] Blank solutions containing only GOx (no FCA) in 0.085 M NaPi buffer and 100 mM (saturating) mutarotated glucose.

[b] i_t = average of three measurements at time t.

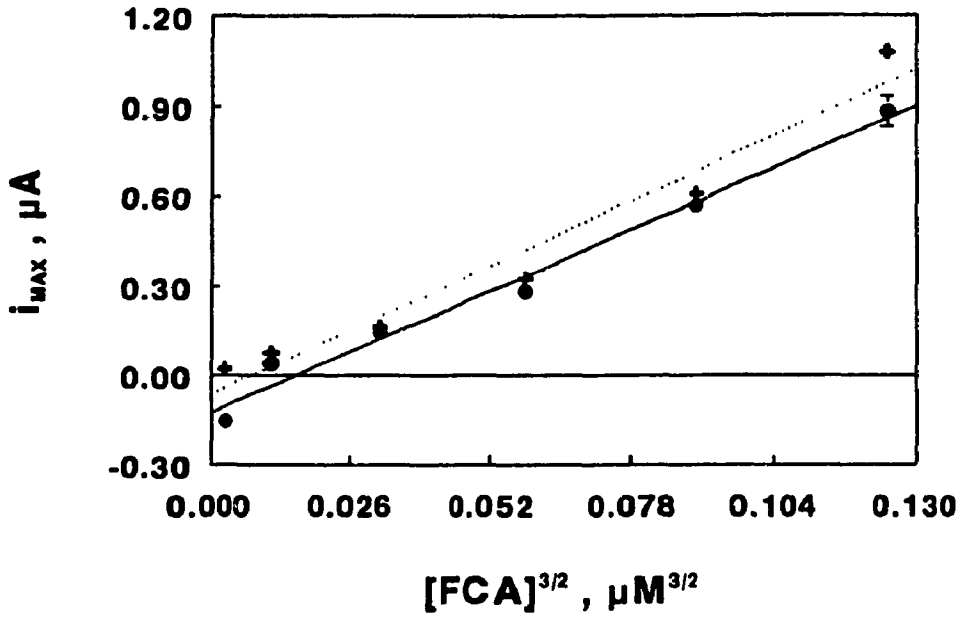

Figure 2.11 Comparison of linear sweep voltammetry (●, solid line) and chronoamperometry (+, dotted line) from dilution experiments in 0.085 M NaPi buffer and saturating glucose (100 mM) under anaerobic conditions. Quadruplicate limiting current (i_{max}) measurements were made for each method at a constant FCA:GOx active sites ratio of 1:1, from 25 to 2 µM GOx. LSV measurements of i_{max} were made at +0.400 V, and corrected for residual current. CA measurements of i_{max} were made at t = 8.0 s following a potential step from 0.000 to +0.550 V vs Ag/AgCl, and corrected for residual current (Table 2.4); Slopes (eqn. 2.16) yielded k_{12} values of 1.05 ± 0.06 x 10^5 M^{-1} s^{-1} and 1.23 ± 0.6 x 10^5 M^{-1} s^{-1} for LSV and CA respectively.

subtracted from the measured limiting current in CA. In order to determine these residual currents, measurements were made at three potential-step time intervals (4.0, 8.0 and 10.0 s) for six blank solutions containing 5 to 50 μM native GOx in 0.085 M NaPi buffer and 100 mM (saturating) glucose. The results, presented in Table 2.4, show that as t increases, the average residual current (i_l) for the blank solutions decreases.

2.3 Discussion

Previous findings have shown that GOx incubated with 3 M urea and subjected to gel filtration retains ~90% activity relative to native GOx and exhibits high FAD absorption.[14] This indicates that FAD is retained within the enzyme, whereas incubation with EDC in the presence of urea, yields a species that has low FAD absorption and retains only ~25% activity.[14] It has thus been shown that EDC in the presence of urea promotes inactivation of the enzyme due to FAD loss. However, with the formation of the NHS ester (Scheme 2.1b) in the absence of urea, EDC appears to have less of an effect. Support for this may be found from the data in the above reference where incubation of GOx in a solution containing 40 mM EDC and 50 mM NHS yielded enzyme having 73% activity and intermediate FAD absorption. In addition, incubation of GOx with FCA, EDC and NHS in the absence of urea yielded, for example, GOx-$(FCA)_{12}$ with 64% activity, whereas GOx-$(FCA)_{13}$ produced from the EDC-urea reaction yielded only 29% activity. It was also shown that, in contrast to the modified species formed by the EDC-urea method, the EDC-NHS procedure yielded a species that retained higher activities and did not lose FCA over time.[14]

The use of urea to partially unfold the enzyme and increase exposure of primary amines to the *o*-acylisourea intermediate (Scheme 2.1a) may allow EDC to deactivate the enzyme. Formation of *o*-acylisourea intermediates with certain carboxylate groups, such as Glu50, which forms a strong hydrogen bond with the ribose moiety of FAD,[14,37] could result in loss of FAD from the enzyme.

The results presented in Table 2.1 indicate that the FCA-derivatization of GOx using the EDC-NHS procedure yielded enzyme with activity values ranging from 58% to 64% of native GOx. These activities are similar to those found in the concurrent study, where activity values ranging from 60 to 69% were observed for GOx modified with FCA, ferrocene dicarboxylic acid (FDA) and ferrocene acetic acid (FAA).[14] In the absence of FCA, EDC-NHS exposure yields GOx with 92% activity, which is similar to the activity on exposure to EDC or urea alone. Table 2.1 also shows that the largest ratio of EDC to NHS yielded a GOx-$(FCA)_n$ derivative with the highest number of FCA (n=12) molecules incorporated into the enzyme and the highest activity (64%). An increase in EDC should mean an increase in the amount of the *o*-acylisourea intermediate formed (Scheme 2.1) which, in the presence of NHS, should cause a corresponding increase in the amount of NHS-ester formed. However, the number, n, of FCA molecules that can be incorporated, under non-denaturing conditions, into GOx using the EDC-NHS procedure seems to reach a limit at n=12[14], although GOx possesses 32 reactive amino groups[36]. Each GOx monomer possesses 15 Lysine residues and one N-terminal primary amino group which could form amide bonds with FCA. Thus, although most Lys residues are on the surface of GOx (Figure 2.12), less than half are reactive towards

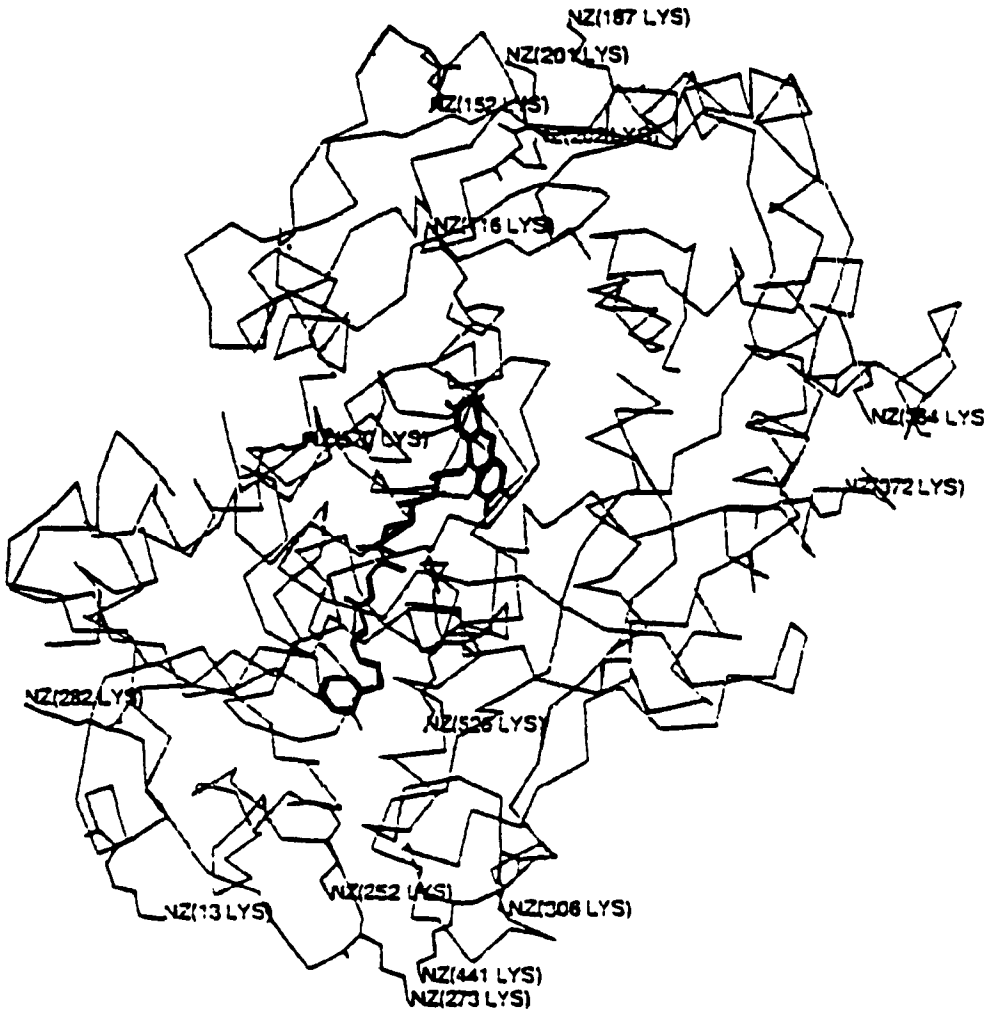

Figure 2.12 Computer graphics display of the C_α backbone of the GOx monomer showing the location of the FAD prosthetic group (bold lines) and lysine residues.[37] This molecular graphics image was produced using the MidasPlus software system from the Computer Graphics Laboratory, University of California, San Francisco[38] (adapted from ref 14).

amide bond formation. Lys accessibility may be hindered by the polysaccharide coat that surrounds the enzyme.[1]

Evidence supporting the covalent derivatization of GOx with FCA comes primarily from fluorescence studies. The peak maximum in the GOx-$(FCA)_{12}$ emission spectrum is at 344 nm rather than 350 nm, as expected for a denatured protein (Figure 2.3) whose Trp residues are exposed to the aqueous solvent. However, the midpoint at half-heightis at ~350 nm, and the blue-shifted peak maximum may be due to incomplete unfolding of GOX-$(FCA)_{12}$ or to possible internal cross-linking between residues during the EDC-NHS reactions (Scheme 2.1). However, the percent fluorescence intensity (Table 2.2) for the GOx control sample incubated with EDC and NHS in the absence of FCA shows that there is no quenching of the unfolded protein and suggests that the action of EDC and NHS alone may not account for the observed asymmetry of the Trp emission peak. The measured FCA-Trp distance of 18 Å for GOx-$(FCA)_{12}$ prepared in this study (Table 2.2) is comparable to measured distances for GOx-$(FCA)_n$ samples that were derivatized using the EDC-urea method in the concurrent study. For example, GOx-$(FCA)_{12}$ and GOx-$(FCA)_{30}$ from the EDC-urea procedure have FCA-Trp distances of 17 Å and 15 Å, respectively.[14]

Figure 2.5A shows the expected independence of the normalized current from GOx-$(FCA)_{12}$ concentration. In contrast, Figure 2.5B shows that the normalized current varies with protein concentration if the modified enzyme has not been sufficiently purified and trace amounts of free FCA are present. It was found that a minimum of three gel filtrations are necessary to remove all traces of free FCA, with the third performed

immediately before the voltammetric dilution experiment. A positive slope of normalized $i_{max}/[GOx\text{-}FCA_n]$ vs $[GOx\text{-}FCA_n]^{1/2}$ was not observed previously for modified enzymes that have been gel-filtered as described.[14] Such plots have only been obtained when free FCA was found to be present, which was observed as voltammetric peaks in the absence of glucose. This underscores the necessity of ensuring that free FCA is thoroughly removed from the enzyme solution.

The measured intramolecular k_{obs} value of 1.6 s^{-1} for $GOx\text{-}FCA_{12}$ (Section 2.2.4, Figure 2.5A) was found to be about ten-fold higher than k_{obs} values found in the literature[14,15] and is probably due to an overestimation of activity loss (75%), since activity was determined after the voltammetric dilution experiment. Assuming 64% activity, as measured for freshly-prepared $GOx\text{-}FCA_{12}$ (Table 2.1), an intramolecular k_{obs} value of 0.24 s^{-1} is obtained, which falls within the k_{obs} range (0.16 to 0.90 s^{-1}) found in the concurrent study.[14] In the reaction schemes developed in eqns 1.1 and 2.10 to 2.13, intramolecular electron-hopping from FC to FC^+ was not considered due to the previous finding[14] that the *number* of FC molecules incorporated into GOx is not critical for efficient electron transfer from the redox center to the surface of an electrode.

In the concurrent study, it was deduced that electron transfer from $FADH_2/FADH^\bullet$ to FCA^+ must be the limiting factor in the overall electrocatalytic rate since the shapes of the LSV waves, in the presence of excess glucose, are similar for $GOx\text{-}(FCA)_{12}$ and native GOx with free FCA. Similar electrocatalytic wave shapes for both systems indicates that there is electrochemical reversibility (eqns. 2.3, 2.10 and 2.12) for FCA at the electrode surface whether it is free or bound to GOx. In terms of glucose biosensor

applications, the intramolecular rates that were obtained in this and the concurrent study are too low to compete with the rate of O_2 conversion to H_2O_2 (eqn. 1.2). An intramolecular electron-transfer rate $\geq 5 \times 10^3$ s^{-1} is required for insensitivity to dissolved O_2 (assuming 240 μM O_2 in air-saturated buffers).[14] Thus, targeting GOx Lys residues with FCA does not lead to an enzyme that is insensitive to oxygen under physiological conditions. The low intramolecular electron-transfer rates in GOx-$(FCA)_{12}$ are not surprising given the large separation between the Lys residues and the FAD center of GOx. The closest distance between the N5 atom of the isoalloxazine ring of FAD (where electron transfer is thought to occur in the active site) and a Lys residue is 23.6 Å (Figure 2.11). Derivatization of two glutamate and eight aspartate residues that were shown to be within 16 Å of the FAD N5 atom by computer graphics analysis should lead to the observation of electron transfer rates that attain the desired value.[14]

For bimolecular electron transfer between GOx and FCA, the limiting value of k_{12} is $1.2 \pm 0.2 \times 10^5$ M^{-1} s^{-1} at [GOx] >> [FCA] from the intercept of Figure 2.8. This value is almost three-fold higher than that found for a GOx:FCA ratio of 1:14.4 (Table 2.3); it is therefore evident that the GOx:FCA ratio does have a significant effect on the observed bimolecular rate constant. A literature[34] value of 2.01×10^5 M^{-1} s^{-1} was obtained by Hill and coworkers and is in good agreement with the bimolecular rate constant obtained in this study. Table 2.3 includes the estimated standard deviations in k_{12} from the uncertainty in the slopes of i_{max} vs $[FCA]^{3/2}$ (Figure 2.7) for the bimolecular reactions of freely-diffusing FCA with native GOx. These SD values increase at lower GOx:FCA ratios, due to increased experimental error in measuring the small electrocatalytic currents

obtained at low FCA concentrations. Nonetheless, good linearity was obtained in the plots of i_{max} vs $[FCA]^{3/2}$ and correlation coefficients at all ratios of FCA:GOx were ≥ 0.98.

Despite the intended use of chronoamperometry (CA) to eliminate the residual current from the observed current, it was still necessary to subtract significant residual currents (Table 2.4) in order to obtain limiting currents comparable with those obtained from LSV. This indicates that the post-excitation time interval, t, was not long enough to allow a sufficient drop in residual current. After the voltage step, time is required for the establishment of steady-state concentration gradients between the bulk solution and the electrode surface.[37] Support for this can be found in the observation (Table 2.4) that as t was increased from 4.0 to 10.0 s, the average residual current decreased by a factor of 3 for the blank solutions. However, at this length of time one would expect that the capacitative component of the residual current would have subsided. The persistent residual current may be due to the oxidation of some amino acid residues of COx at +550 mV vs Ag/AgCl, or to the adsorption of GOx on the electrode surface, which could increase the electrode-solution capacitance. From the above, one can conclude that CA yields comparable results to LSV provided that one takes into account the residual current that persists for CA. For biosensor applications, CA is preferable since i_{max} can be measured directly after only ~10 s, as opposed to LSV which requires up to approximately 275 s at a scan rate of 2 mV s^{-1}.

2.4 References

1. Wilson, R.; Turner, A. P. F. *Biosens. Bioelectron.* **1992**, 7, 165.

2. Kalisz, H. M., Hecht, H. J.; Schomburg, D.; Schmidt, R. D. *Biochim. Biophys. Acta* **1991**, 1080, 138.

3. Degani Y.; Heller A. *J. Phys. Chem.* **1987**, 92, 1285.

4. Bourdillon, C.; Thomas, V.; Thomas, D. *Enzyme Microb. Technol.* **1982**, 4, 175.

5. Bourdillon, C.; Demaille, C.; Moiroux, J.; Savéant, J. M. *J. Am. Chem. Soc.* **1993**, 115, 2-10.

6. Crumbliss, A. L.; Hill, H. A. O.; Page, D. J. *J. Electroanal. Chem.* **1986**, 206, 327.

7. Zakeeruddin S. M.; Fraser, D. M.; Nazeeruddin, M. K.; Grätzel, M. *J. Electroanal. Chem.* **1992**, 337, 253.

8. Bowers, M. L.; Yenser, B. A. *Anal. Chim. Acta* **1991**, 243, 43.

9. Cass, A. E.; Davis, G.; Francis, G. D.; Hill, H. A. O.; Aston, W. J.; Higgins, I. J.; Plotkin, E. V.; Scott, L. D. L.; Turner, A. P. F. *Anal. Chem.* **1984**, 56, 667.

10. *Redox Chemistry and Interfacial Behaviour of Biological Molecules*, Ed. Glenn Dryhurst and Katsumi Niki, Plenum Publishing Corporation, **1988**, pp 151-171.

11. Schuhmann, W.; Ohara, T. J.; Schmidt, H. L.; Heller, A. *J. Am. Chem. Soc.* **1991**, 113, 1394.

12. Heller, A. *Acc. Chem. Res.* **1990**, 23, 128.

13. Bartlett, P. N.; Whitaker, R. G.; Green, M. J.; Frew, J. *J. Chem. Soc., Chem. Commun.* **1987**, 1603.

14. Badia, A.; Carlini, R.; Fernandez, A.; Battaglini, F.; Mikkelsen S. R.; English A. M. *J. Am. Chem. Soc.* **1993**, 115, 7053.

15. Degani, Y.; Heller, A. *J. Am. Chem. Soc.* **1988** 110, 2615.

16. Khorana, H. G. *Chem. Rev.* **1953**, 53, 145.

17. DeLos, F.; DeTar, R. S.; Fulton, F. R. *J. Am. Chem. Soc.* **1966**, 88, 1024.

18. Lundblad, R. L. "Chemical Reagents for Protein Modification", 2nd Ed., CRC Press, Boca Raton, USA, **1991**. pp. 271-272.

19. Staros, J. V.; Wright, R. W.; Swingle, D. M. *Anal. Biochem.* **1986**, 156, 220.

20. Brinkley, M. *Bioconjugate Chem.* **1992**, 3 , 2.

21. Battaglini, F.; Calvo, E. J. *Anal. Chim. Acta* **1992** 258, 151-160.

22. Kissinger, P. T.; Heineman, W. R. (eds.) *Laboratory Techniques in Electroanalytical Chemistry*, **1984**, Marcel Dekker, Inc., New York.

23. *Worthington Enzyme Manual*, Worthington Biochemical Corp., New Jersey, **1972**, p. 19.

24. Keesey, J. *Biochemical Information*, Boehringer Mannheim Biochemicals, Indiananpolis, **1987**, p. 27.

25. Bradford, M. M. *Anal. Biochem.* **1976**, 72, 248.

26. Badia, A.; Thai, N. H. H.; English, A. M.; Mikkelsen, S. R.; Patterson, R. T. *Anal. Chim. Acta* **1992**, 262, 87.

27. Carter, P. *Anal. Biochem.* **1971**, 40, 450.

28. Stookey, L. L. *Anal. Chem.* **1970**, 42, 779.

29. Lakowicz, J. R. *Principles of Fluorescence Spectroscopy*, Plenum Press, New York, **1983**; (a) pp.303-316; (b) pp. 354-363.

30. Campbell, I. D.; Dwek, R. A. *Biological Spectroscopy*, Benjamin Cummings, Menlo Park, CA, **1984**; pp. 113-118.

31. Hill, B. C.; Horowitz, P. M.; Robinson, N. C. *Biochemistry* **1986**, 25, 2287.

32. Stryer, L. *Ann. Rev. Biochem.* **1978**, 47, 819.

33. Weber, G.; Teale, F. W. J. *Discuss. Faraday Soc.* **1959**, 134.

34. Hill, H. A. O.; Sanghera, G. S. *Biosensors: A Practical Approach*, IRL Press, Oxford, **1990**; pp. 19-23.

35. Bard, A. J.; Faulkner, L. R. *Electrochemical Methods*, Wiley, New York, **1980**; pp. 455-461.

36. Wolowacz, S. E.; Yon Hin, B. F. Y.; Lowe, C. R. *Anal. Chem.* **1992**, 64, 1541.

37. Hecht H. J.; Kalisz H. M.; Hendle J.; Schmid R. D.; Schomburg D. *J. Mol. Biol.* **1993**, 229, 153-172.

38. Ferrin, T. E.; Huang C. C.; Jarvis, L. E.; Langridge R. J. *Mol. Graphics* **1988**, 6, 13.

3. DIRECT ELECTROCHEMISTRY OF NATIVE AND DEGLYCOSYLATED GLUCOSE OXIDASE

3.0 Introduction

Direct, unmediated electron-transfer from the redox centers of proteins to the surface of an electrode is considered a desirable characteristic in the application of enzymes and redox proteins to amperometric biosensors. This is due, in part, to the possibilities of dispensing with a conceivably rate-limiting reaction between enzyme and mediator, or mediator and electrode, and the simplification of biosensor construction. In the case of a glucose biosensor, based on glucose oxidase (GOx), facile direct electron transfer between the redox-active FAD centers of GOx and an amperometric electrode could eliminate the competing reaction with oxygen in regenerating the oxidized form of the enzyme (eqn. 1.2):

The use of voltammetric techniques in the study of redox protein electrochemistry is relatively recent because the observed rates of direct (i.e. unmediated) electron transfer between protein redox centers and metal electrodes are too slow to provide useful information.[1,2,3] However, it has been shown[4] that Au or Pt electrode surfaces, devoid of contaminants through the use of aggressive cleaning methods (such as soaking the electrode in aqua regia or heating it in a hydrogen flame) yield an initially strong, quasi-reversible electrode response in the cyclic voltammetry of horse heart cytochrome c (cyt c) that does not persist. The impersistence has been attributed to fouling of the electrode surface by time-dependent, irreversible adsorption and denaturation of protein, the loss

of active surface functional groups on the electrode (in the case of carbon electrodes), or a combination of both.[5a] It has also been shown that lyophilized commercial cyt c, which contains polymeric denatured forms, yields a poor response that deteriorates rapidly.[6] Removal of the denatured cyt c by ion-exchange chromatography yielded a species whose voltammetric response with a bare gold electrode was more durable when tested directly after purification.[5b,2]

Eddowes and Hill have found that quasi-reversible cyclic voltammetry of horse heart cyt c could be obtained at a gold electrode in a cyt c solution containing 4,4'-bipyridyl, an electron-transfer promoter.[7,2] The gold electrode was modified or functionalized[5] to increase electron-transfer rates for direct electrochemistry of cyt c through the reversible adsorption of the electron-transfer promoter to the gold surface. Their postulated multi-step mechanism for electron transfer is shown in Figure 3.1.[2,8] In their scheme, the first step consists of the approach and "docking" of cyt c, through hydrogen bonds between lysine-NH_3^+ groups that surround the exposed heme edge[9] with the heterocyclic N-atoms in the adsorbed 4,4'-bipyridyl monolayer on the gold electrode. It is thus thought that the promoter serves to properly orient the protein for electron transfer. Following this, electron transfer occurs with the subsequent desorption of the product protein from the bipyridyl monolayer. This interaction is seen as analogous to the physiological interaction of cyt c with cytochrome oxidase in mitochondrial respiration.[3]

A drawback in the use of 4,4'-bipyridyl is that this promoter must be present in solution at ~ 10 mM to achieve the desired monolayer coverage on the electrode surface,

since the interaction of the pyridyl nitrogen with gold is weak.[10] In this study and others, attempts at *pre-adsorbing* 4,4'-bipyridyl on a gold electrode by dipping it in a solution of the promoter, with subsequent rinsing of the electrode, have met with rapid desorption of the promoter and consequent loss of reversible electrochemistry.[5] Taniguchi et al.[11] were the first to show that a gold electrode, on which bis(4-pyridyl) disulfide had been pre-adsorbed, gave characteristic quasi-reversible electrochemical behaviour for cyt c. A monolayer of the disulfide reagent was pre-assembled on the gold electrode surface through the strong, irreversible chemisorption of the sulfur moiety to the gold electrode. This electrode modification resulted in persistent electron transfer between cyt c and a gold electrode surface.[5,3]

The difference between a promoter in solution (4,4'-bipyridyl) and a surface-bound promoter (L-cysteine), highlights the dynamic vs static characteristics of promoter-enhanced cyt c electrochemistry. For the bipyridyl, weak adsorption leads to a dynamic equilibrium between adsorbed and free promoter at the gold surface. Over time, and in the presence of cyt c, this led to the net desorption of the promoter from the gold surface, with a consequent loss of the amperometric signal as protein adsorption causes fouling of the surface.[5b] In contrast, thiol/disulfide adsorption gave a stable monolayer of chemisorbed promoter which persisted on the gold surface. This led to the persistence of the amperometric signal in the presence of cyt c.[11,5b,12,3] The ammonium groups on the thiol-containing L-cysteine promoter may serve to release cyt c after electron-transfer with a change in the oxidation state of cyt c. This would mimic the physiological mechanism wherein cyt c reductase preferentially binds cyt(III) c but not cyt(II) c.[13]

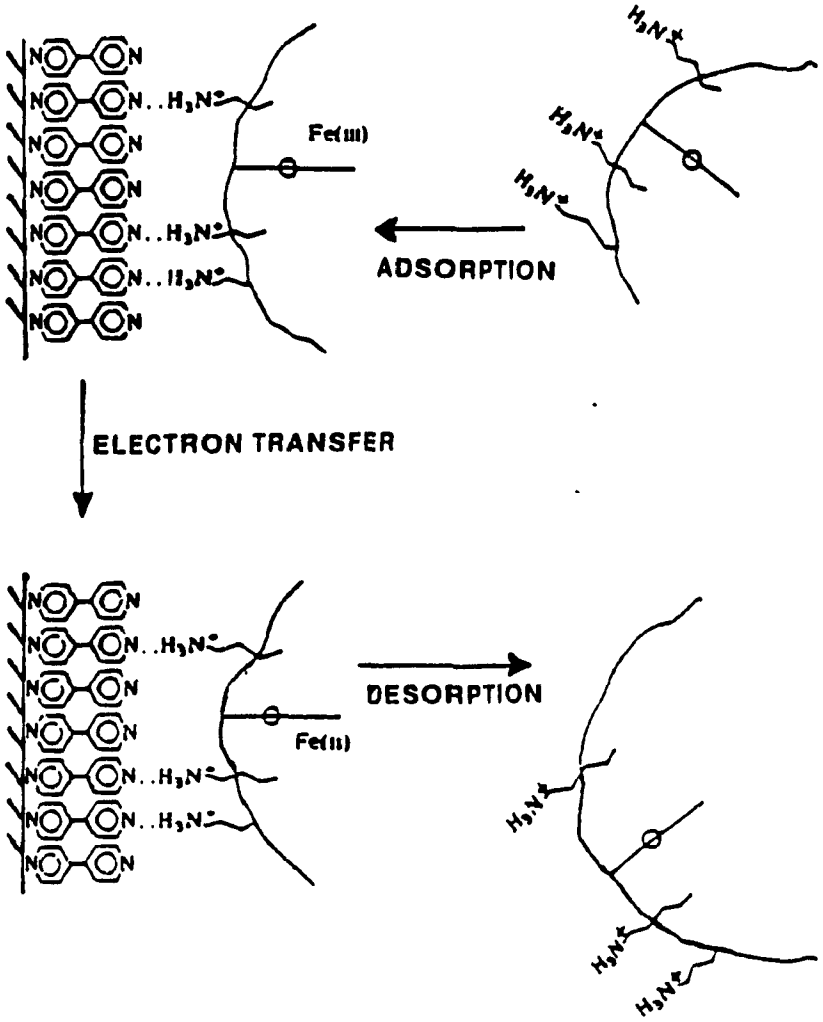

Figure 3.1 Postulated mechanism for electron transfer from cyt c to 4,4'-bipyridyl-modified gold electrode.[2] (Adapted from Figure 4, Armstrong et al.[8])

Further work was done in the study[3,13] of reagents which are electroinactive at the redox potential of cyt c (such as 4,4' bipyridyl) but promote rapid heterogeneous electron transfer at metal electrodes. Such reagents are described as "dual functionality" or "XY" promoters where an "X" group (such as sulfur, phosphorus or nitrogen) has a strong affinity for the metal electrode substrate (such as sulfur with gold) and a "Y" group that can interact with a protein surface. Groups X and Y are usually separated by a rigid linking structure which serves to orient the Y group towards the protein.[13] The large assortment of "Y" groups that are available for these promoters offers a correspondingly wide assortment of surface monolayer characteristics and a large degree of control in the formation of chemically well-defined surfaces for modified electrodes.[13]

Surface charge, hydrophobicity and orientation on the surface of the electrode may all be controlled by selection of the Y group. Such a selection would be a function of the surface charge distribution, hydrophobicity and structural characteristics of the specific redox protein being studied. Thus, the use of promoters could not only increase the rate of electron transfer but also enhance selectivity and diminish or prevent denaturation of the redox protein on the electrode surface.[5b]

In order to achieve greater selectivity and control in the protein-promoter interface, Barker et al. have studied the promoted electron-transfer reactions of four small, well-characterized metalloproteins, including cyt c, using gold electrodes that were modified with cysteine-containing oligopeptides which chemisorb to gold surfaces.[1] Oligopeptides having functional amino acids with negatively-charged residues such as aspartate (Asp) and glutamate (Glu), were shown to promote quasi-reversible behavior for cyt c through

the formation of salt bridges between the Asp and Glu residues on the chemisorbed oligopeptide promoters and the primary amino groups of the lysine residues that surround the heme crevice of cyt c.[14] The rationale for using oligopeptides to enhance electron-transfer rates included matching of the structure of the modified electrode interface to the known structure of the redox protein, introducing flexibility in the chemisorbed oligopeptide to accommodate different protein orientations, and allowing "tunability" through changes in pH and/or ionic strength to enhance selectivity for particular proteins in the presence of others.[1]

In this work, modified gold electrodes were studied for the purpose of promoting direct GOx electrochemistry. The study was limited to simple sulfur-containing promoter reagents (Figure 3.2). These compounds were chosen on the basis of previous work,[13,15] and their charges at pH 7. Methods of electrode modification were tested using the well-characterized and electrochemically well-behaved heme redox protein, cyt c (MW = 12.4 kDa, net charge: +8 at pH 7).[1] The persistence and magnitude of the voltammetric signals obtained for commercial and re-purified commercial cyt c at a clean gold electrode were evaluated and compared with those obtained at gold electrodes modified with 4,4'-bipyridyl and cysteine. This was done in order to verify that purified cyt c has greater electrochemical persistence because it is devoid of non-native species that are found in commercial cyt c. For persistence studies at the modified electrodes, the heterogeneous electron-transfer rate constant, k_s, was evaluated as a function of time.

The use of simple reagents for the promotion of the quasi-reversible direct electrochemistry of GOx was also examined for the deglycosylated form of the enzyme.

GOx is a highly glycosylated glycoprotein possessing 190 mannose and 16 *N*-acetylglucosamine residues.[16] Commercially available α-mannosidase and endo-glycosidase H have been used to remove the carbohydrate moiety from the surface of GOx while retaining most of the activity (~85%).[16] Endoglycosidase H catalyzes the hydrolysis of the *N*-acetylglucosamines in the chitobiose core of high mannose glycoproteins.[17] The other enzyme, α-mannosidase, catalyzes the hydrolysis of α-D-mannoside oligomers to produce D-mannose monomers.[18] In this study, it was hoped that deglycosylation would decrease the distance between the FAD redox centers of GOx and the electrode surface; in addition it was thought that deglycosylation would enhance the interaction of the negatively-charged GOx molecule (-58 at pH 7.0[19], estimated by subtracting the total number of Lys and Arg residues from the total number of Asp and Glu residues) with a positively-charged monolayer formed by aminoethanethiol adsorption onto a gold electrode (Figure 3.2).

Using aminoethanethiol as promoter, direct GOx electrochemistry was also investigated in the presence of low concentrations of urea. It was hoped that partial unfolding of the enzyme in urea would yield a species of GOx that remained active, yet would allow closer interaction between the FAD centers and the modified electrode. The concentrations of urea were chosen on the basis of the fluorescence data in Figure 2.3, which show that GOx is partially unfolded at urea concentrations between ~0.2 to ~5.0 M.

An extension of promoter interactions with GOx was attempted in this study by covalently attaching dopamine, a two-electron mediator, to the carboxylic acid group of

mercaptopropionic acid (Figure 3.2) forming an N-mercaptopropionyl-dopamine mediator (Scheme 3.1) which, in turn, would be chemisorbed to the surface of a gold electrode. The mediator immobilization on a mercaptopropionic acid-modified gold electrode is based on the EDC-NHS procedure (Scheme 2.1), and it was hoped that the electrode-bound electron-transfer mediator would relay electrons from reduced native GOx to the electrode surface.

3.2 Experimental section

3.2.1 Materials. Glucose Oxidase (GOx) from *Aspergillus niger* (E.C. 1.1.3.4), was purchased from Boehringer Mannheim, Grade II, and lot number 12635524-33 was used for all experiments; horseradish peroxidase (HRP, E.C. 1.11.1.7), 10 mg/mL suspension in 3.2 M ammonium sulfate, ~ 250 units/mg, *O*-dianisidine dihydrochloride, 1-ethyl-3-(3-dimethylaminopropyl)carbodiimide hydrochloride (EDC), horse heart cytochrome c (Type VI), α-mannosidase (E.C. 3.2.1.24); 5.3 mg/mL suspension in 3.0 M ammonium sulfate and 0.1 mM zinc acetate, pH 7.5, ~23 units/mg, and flavin adenine dinucleotide (FAD) disodium salt were obtained from Sigma; endoglycosidase H (endo-ß-N-acetylglucosaminid.. e, E.C. 3.2.1.96), was obtained from Genzyme; α-D-glucose, sodium perchlorate, 4,4'-bipyridyl, 2-aminoethanethiol hydrochloride, L-cysteine hydrochloride hydrate, 3-mercaptopropionic acid, DL-α-6,8-dithiooctanoic acid, thiodiglycolic acid, and 3-hydroxytyramine hydrobromide (dopamine) were from Aldrich; N-hydroxysulfosuccinimide (NHS) was from Pierce; Coomassie Brilliant Blue G-250 protein assay dye reagent, and electrophoresis grade urea were obtained from Bio-Rad; dibasic sodium phosphate, dibasic potassium phosphate, and potassium ferricyanide were obtained

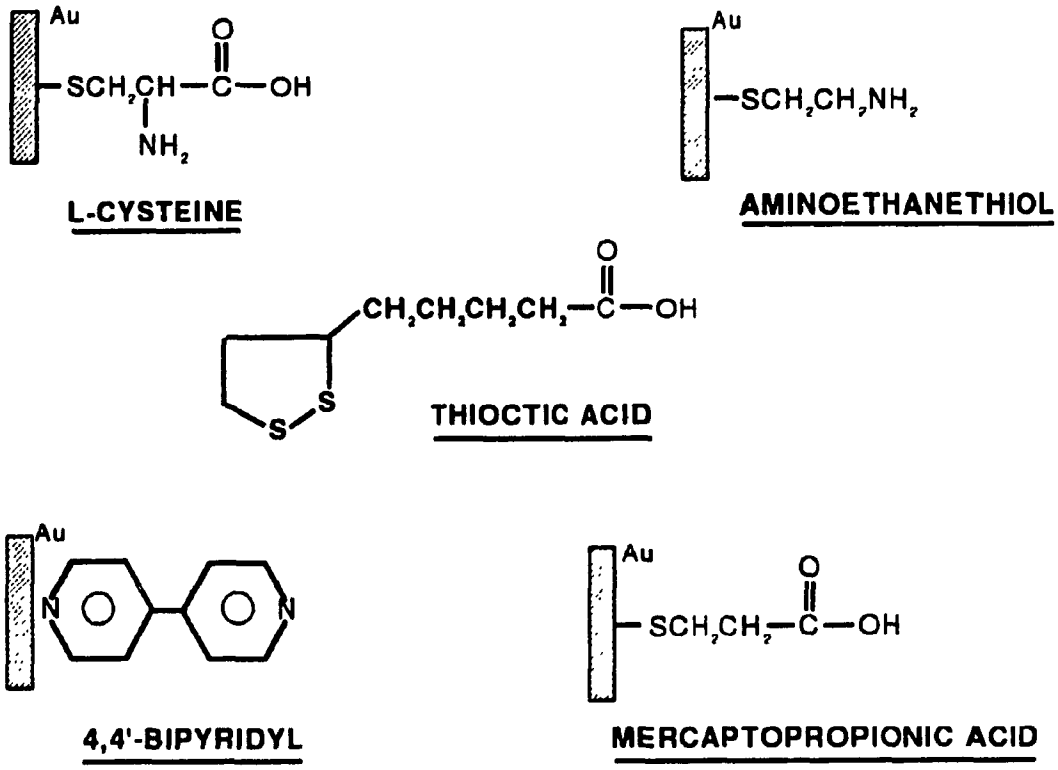

Figure 3.2 Thiol-containing promoters used in the modification of gold electrodes.

from Fisher. All other chemicals were of the best available quality and were used as received.

Non-reagent materials include: Sephadex G-15 (≤ 1,500 MW fractionation range) and G-25 (≤ 2,500 MW fractionation range) gel filtration resins, prepacked HiLoad 16/10 Phenyl Sepharose High Performance FPLC column (16 mm x 10 cm) for hydrophobic interaction chromatography; Q-Sepharose Fast Flow FPLC medium (used in the preparation of a 16-mm x 45-cm column) for anion-exchange chromatography, prepacked Mono S HR 10/10 cation exchange column (10 mm x 10 cm), and CM-Sepharose anion exchange medium (for the preparation of a 1.5- x 60-cm column) (Pharmacia); YM 30 (30,000 MW cutoff) and YM 10 (10,000 MW cutoff) ultrafiltration membranes and stirred ultrafiltration cells (Amicon), Acrodisc syringe filters (1.2 μm-pore) (Gelman Sciences); gold working electrode (geometric area = 0.0201 cm^2) and Ag/AgCl reference electrodes (Bioanalytical Systems); Pt wire (Fisher), and 7.5 % polyacrylamide gel for SDS-PAGE (Bio-Rad). Distilled water that was further purified by passage through a Sybron-Barnstead Nanopure ion-exchange system was used in the preparation of all solutions.

Instrumentation. Absorption spectra were recorded using Varian (Cary 1) and Hewlett-Packard 8451A spectrophotometers. Electrochemical measurements were made using a BAS-100A Electrochemical Analyzer and, when necessary, a BAS PA-1 pre-amplifier (Bioanalytical Systems). Ultra high purity nitrogen was used for purging oxygen from electroanalytical test solutions. FPLC was performed using an LC-500 Plus liquid chromatography controller with P-500 pumps, UV-M Monitor and FRAC-100 fraction collector (Pharmacia). Column chromatography was performed using a Microperspex

peristaltic pump (LKB). SDS-PAGE was done using a Mini-Protean II Dual-Slab Cell system (Bio-Rad).

3.2.2 Methods

3.2.2.1 Gold Electrode Modification with Promoters. Prior to modification, gold electrodes were polished and cleaned according to a literature procedure.[20] Following preliminary polishing in 0.05-μm alumina slurry, the electrodes were cycled electrochemically in 1 M sulfuric acid between -300 and +1550 mV (vs Ag/AgCl) at a scan rate of 100 mV s^{-1} for about 20 cycles, or until the characteristic voltammogram of a bare gold electrode appeared when cycled in a buffer solution. For electrode modification with 4,4'-bipyridyl, 10 mM bipyridyl was added to the protein solution in the electrochemical cell to ensure that there would be monolyer coverage of the gold electrode.[7] The chemisorption of thiol-containing promoters on the gold electrode was done by dipping the electrode, immediately prior to use, in 4 mM aqueous solutions of the thiols for a minimum of 15 min.[11,1] Following this, the electrode was rinsed thoroughly with buffer.

3.2.2.2 Purification of Commercial Cytochrome c. Commercially available lyophilized cyt c preparations contain a variety of deamidated and polymeric forms. Deamidation arises from the hydrolysis of a number of glutamines and/or asparagines to form the corresponding acids.[21] In order to fully oxidize the protein, a few grains of solid $K_3Fe(CN)_6$ were added to 50 mg of cyt c in 1 mL of 100 mM NaPi buffer, pH 7.0. This solution was then applied to a 1.5- x 60-cm CM Sephadex cation-exchange column equilibrated with 100 mM NaPi, at pH 7.0 and 4 °C. Using a flow rate of 30 mL/h

(controlled by peristaltic pump), 10 mL fractions were collected until all visible bands on the column were eluted.

3.2.2.3 Purification of Commercial Glucose Oxidase. Lyophilized GOx contains GOx monomers and various protein and non-protein impurities such as free FAD. Purification was done using gel filtration, followed by hydrophobic interaction FPLC, and finally, by ion-exchange FPLC.[16] Absorbance was monitored at 280 nm for all FPLC applications. Approximately 80 mg of lyophilized GOx was dissolved in ~1 mL of 100 mM NaPi buffer at pH 7.5 and applied to a G-15 Sephadex gel filtration column that was equilibrated in the same buffer. The first intense yellow band that was eluted from the column was concentrated by ultrafiltration (YM 30 membrane) in 10 mM NaPi buffer at pH 7.5 containing 0.85 M ammonium sulfate. The GOx concentrate was then applied to a commercially prepared Phenyl-Sepharose column (1.6 x 10 cm) that was equilibrated in the same buffer/ammonium sulfate solution. GOx was eluted using a 0 to 100% linear gradient of 10 mM NaPi buffer, pH 8.0, from 5.0 to 40.0 mL eluent volume. The GOx-containing fractions were pooled, concentrated and applied to a 1.6- x 45-cm Q-Sepharose ion-exchange column equilibrated with 20 mM NaPi buffer at pH 8.5. GOx was eluted with a linear NaCl gradient (0 to 1 M) in 30.5 mL. GOx activity was measured (see Section 3.2.2.4) after further concentration in 100 mM NaPi buffer at pH 7.0

3.2.2.4 GOx Activity Assay. The activities of purified and deglycosylated GOx were measured using a coupled peroxidase-*o*-dianisidine assay procedure in air-saturated 0.1 M KPi buffer at pH 7.0 and 23 °C, as described in Section 2.1.2.2.

3.2.2.5 GOx Deglycosylation. GOx deglycosylation was done according to the method

of Kalisz et al.[16] with a few modifications. One mg of purified GOx was incubated for 24 h at 37 °C with 6 U of α-mannosidase (E.C. 3.2.1.24) and 20 mU of endoglycosidase H in 30 mM NaPi buffer at pH 5.0. For control purposes, 1 mg of purified GOx was incubated under identical conditions but without the deglycosylating enzymes. In order to remove the carbohydrate residues, the incubate was applied to a G-25 gel-filtration column that was equilibrated in 30 mM NaPi at pH 4.2. The first intense yellow band that eluted was concentrated and applied to a 1.0- x 10-cm Mono S anion-exchange column equilibrated under the same conditions as the G-25 column. The deglycosylated GOx was then eluted using a NaCl gradient of 0 to 0.75 M in 30 mM NaPi at pH 4.2. The samples were concentrated by ultrafiltration in 0.1 M NaPi buffer at pH 7.5. SDS-PAGE was used to assess the molecular weight of the deglysolylated GOx enzyme and was performed by L. D'Astous according to a standard procedure,[16,22] using a 7.5% polyacrylamide gel.

3.2.2.6 Protein Quantitation. Cyt c concentrations were determined spectrophotometrically at 410 nm which is an isosbestic point for the reduced and oxidized forms of cyt c with a molar absorbtivity, of 1.06×10^5 M^{-1} cm^{-1}.[23] GOx concentrations were obtained using the standard Coomassie Blue[24] assay for total protein described in Section 2.1.2.3.

3.2.2.7 Preparation of the N-Mercaptopropionyl-Dopamine Modified Gold Electrode. The procedure used is based on a method for COOH-functionalized electrode modifications.[25] A drop of neat mercaptopropionic acid was placed on a clean gold electrode (see Section 3.2.2.1 for cleaning procedure) and allowed to chemisorb for 30

min. Following this, the electrode was thoroughly rinsed with distilled water. An EDC-NHS solution (1 mg/mL EDC and 2 mg/ml NHS in 20 mM NaPi buffer, pH 7.0) was placed onto the mercaptopropionic acid-modified electrode (Scheme 3.1) and allowed to dry. The electrode was then rinsed with the same buffer immediately prior to the placement of a drop of a 20 mM dopamine in 20 mM NaPi buffer, pH 7.0, and allowed to dry overnight at ambient temperature. The electrode was thoroughly rinsed with the same buffer immediately prior to its use in voltammetric measurements.

3.2.2.8 Voltammetry. A standard three-electrode cell configuration consisting of a gold (0.0201 cm^2) working electrode, Ag/AgCl reference, and Pt auxiliary electrodes was used. A known volume (≥ 200 µL) of protein solution was added to the cell and deoxygenated by a gentle N_2 stream above the solution surface. All electrochemical measurements were performed under a continuous stream of H_2O-saturated N_2, including time-based measurements over several hours. Cyclic voltammograms were recorded for 400 µM (5.0 mg mL^{-1}) solutions of cyt c in 20 mM NaPi buffer (pH 7.0) containing 100 mM $NaClO_4$. The potential was scanned in most cases from -0.155 to +0.245 V (vs Ag/AgCl), at scan rates not exceeding 30 mV s^{-1}. Mutarotated (≥ 24 h at 4 °C) glucose solutions were deoxygenated and transferred by gas-tight syringe to the cell. Cyclic voltammograms were also recorded for 400 µM solutions of GOx in 100 mM NaPi (pH 7.0) at a scan rate of 2 mV s^{-1}, unless otherwise noted. The formal reduction potential, $E^{0'}$, was estimated using the following equation:

$$E^{0'} = E_{p,a} - [(E_{p,a} - E_{p,c})/2] \qquad (3.1)$$

where $E_{p,a}$ is the anodic peak potential and $E_{p,c}$ the cathodic peak potential.

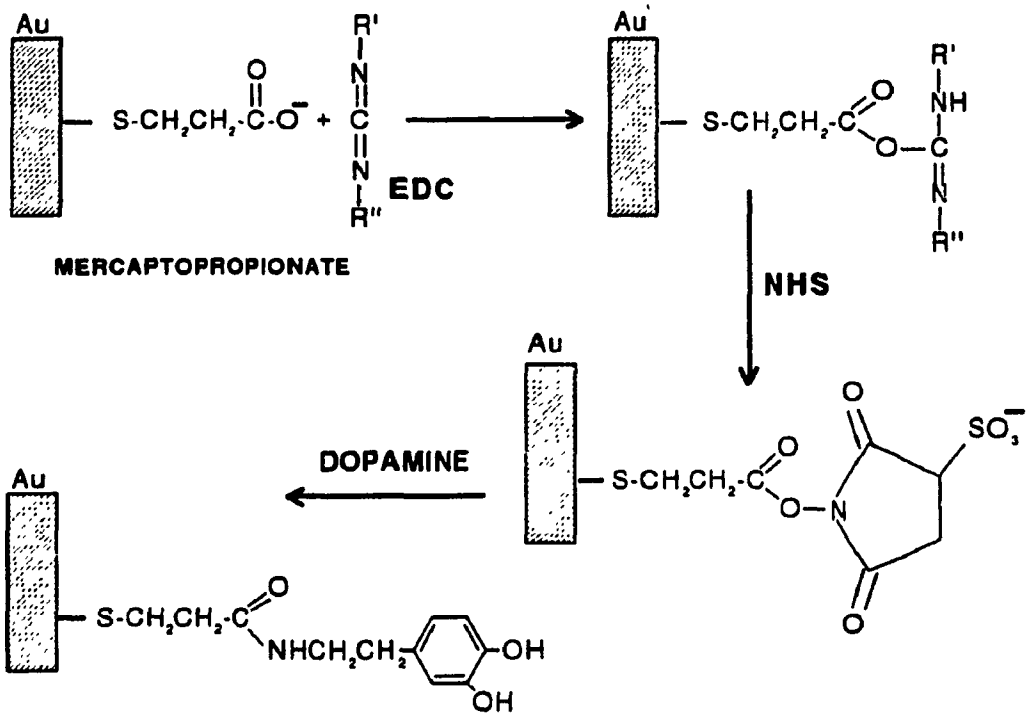

Scheme 3.1 Preparation of N-Mercaptopropionyl-Dopamine modified gold electrode.

3.2.2.9 Voltammetric Determination of the Heterogeneous Electron-ransfer Rate Constant, k_s. The method of Nicholson[26] applies cyclic voltammetry to the evaluation of the heterogeneous electron-transfer rate constant, k_s, for a species that transfers electrons to a planar electrode surface. The peak potential separation in a typical quasi-reversible voltammogram, ΔE_p ($\Delta E_p = E_{p,a} - E_{p,c}$), is related non-analytically to a kinetic parameter, Ψ, and the potential scan rate, ν. If ΔE_p is 59/n mV (where n is the number of electrons transferred per protein), then equilibrium is maintained at the electrode surface, and it is not possible to measure k_s. Estimation of k_s is only possible when the scan rate is increased to a point where the kinetics of electron-transfer become competitive with the rate of potential change at the surface of the electrode; thus ΔE_p is a function of the scan rate for a particular value of k_s. Nicholson's method allows the graphical estimation of k_s from ΔE_p values with the correlation of ΔE_p to k_s at a given scan rate. Figure 3.3 illustrates this correlation with a kinetic parameter, Ψ, and k_s is then calculated from eqn. 3.2:

$$\Psi = (D_O / D_R)^{\alpha/2} k_s [(nF/RT)\pi D_O \nu]^{-1/2} \qquad (3.2)$$

where D_O and D_R are the diffusion coefficients of the oxidized and reduced species, respectively (the ratio D_O/D_R is usually considered as unity), α is the transfer coefficient and is a measure of the symmetry of the free-energy profile of electron-transfer near the transition state[8] (for an ideal, reversible electrode reaction, $\alpha = 0.5$[27]); F is the Faraday

constant (96,487 coulombs mol^{-1}); R is the gas constant (8.31441 J mol^{-1} K^{-1}); ν is the voltammetric scan rate (V s^{-1}) and T the temperature in degrees Kelvin.

3.3 Results

3.3.1 Purification of commercial Cyt c and GOx. Figure 3.4 shows the elution profile of cyt c from a cation exchange (CM-Sephadex) column. Fraction collection was limited to the visible bands on the column which are shown as two sets of fractions whose absorbances were measured at 410 nm. The two overlapping bands that eluted before the large band are probably deamidated forms of cyt c. The native cyt c band (the single large peak in the chromatogram) was very well resolved from the other bands and yielded fractions that were collected from 2.61 to 3.24 L for use in the voltammetric experiments. The native cyt c fractions were pooled and reconcentrated.

Commercial GOx was initially added to a G-15 gel fitration column to remove low molecular weight impurities such as free FAD. The resulting GOx solution was concentrated by ultrafiltration, assayed for total protein and applied to a Phenyl Sepharose hydrophobic interaction chromatography (HIC) column. The elution profile (Figure 3.5) shows a single large peak that elutes at ~18 mL. This intense yellow band was found to contain GOx from its UV-visible absorption spectrum.[28] The other, broader peaks that eluted between 25 and 45 mL were characterized as free FAD upon spectral comparison with commercial FAD. The GOx fractions were pooled, concentrated in 20 mM NaPi (pH 8.5)0 µL and applied to the Q-Sepharose anion-exchange column. spectral comparison with the known spectrum of native GOx, as above. Figure 3.6 shows that in

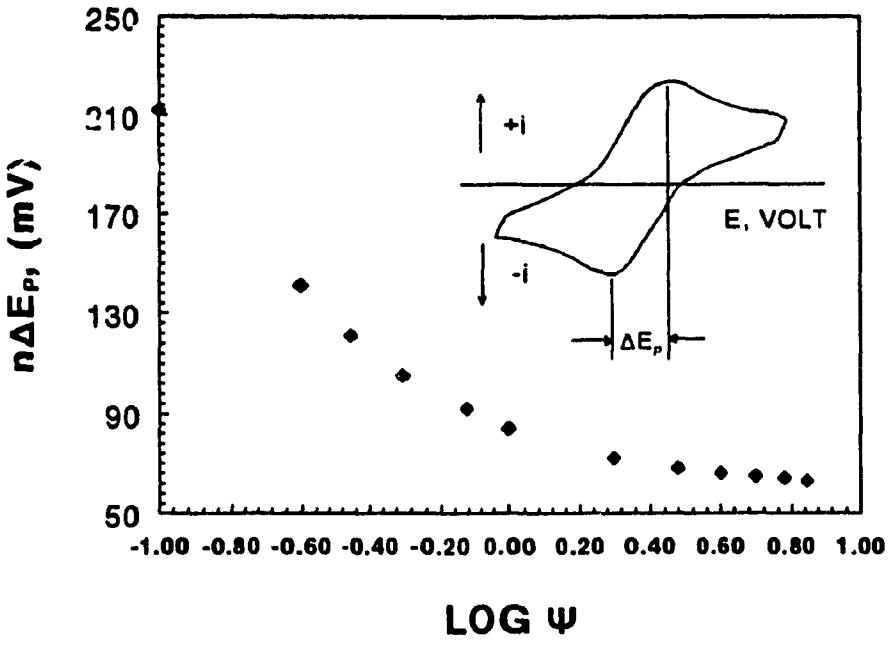

Figure 3.3 Plot of $n\Delta E_p$ vs log Ψ. Inset: Typical symmetrical, quasi-reversible voltammogram showing measurement of ΔE_p where positive and negative currents represent cathodic and anodic processes, respectively, and n is the number of electrons per redox protein that are transferred to the electrode.

the Q-sepharose chromatogram a single large peak is present at ~42 mL. Fractions were pooled and characterized as GOx upon spectral comparison with the known spectrum of native GOx, as above. The components which were eluted after the large peak were not characterized. The recovery of native GOx from the Q-sepharose column was 57%. Activity measurements for commercial and purified GOx yielded 146 U mg^{-1} and 224 U mg^{-1}, respectively, indicating that the purified GOx has a 34% increase in specific activity.

3.3.2 GOx Deglycosylation. Figure 3.7 shows the elution profile of deglycosylated GOx (D-GOx) from the cation-exchange column (Mono S). The first large peak was eluted in the void volume and a second peak is observed at ~15 mL. Fractions containing the first large peak were yellow in appearance and were shown to catalyze the oxidation of glucose through activity measurements. The second peak was not tested for GOx activity since it did not have a yellow colour and it may contain the deglycosylating enzymes, α-mannosidase and endoglycosidase H. In Figure 3.8, a molecular weight calibration curve is shown for the estimation of the molecular weight of D-GOx by SDS-PAGE. The D-GOx sample migrated as a single sharp band to a distance of 35 mm, corresponding to a MW of ~75 kDa. A solution of purified native GOx at the same concentration as D-GOx was also run on this gel and yielded a single sharp band with a migration distance of 33 mm, corresponding to a MW of ~83 kDa. The molecular weight of the D-GOx monomer is therefore ~90% of the native GOx monomer. The activity of D-GOx was found to be 85% that of native GOx which was subjected to incubation at 37 °C in 30 mM NaPi (pH 4.2) without the deglycosylating enzymes, and purified by G-25 gel filtration.

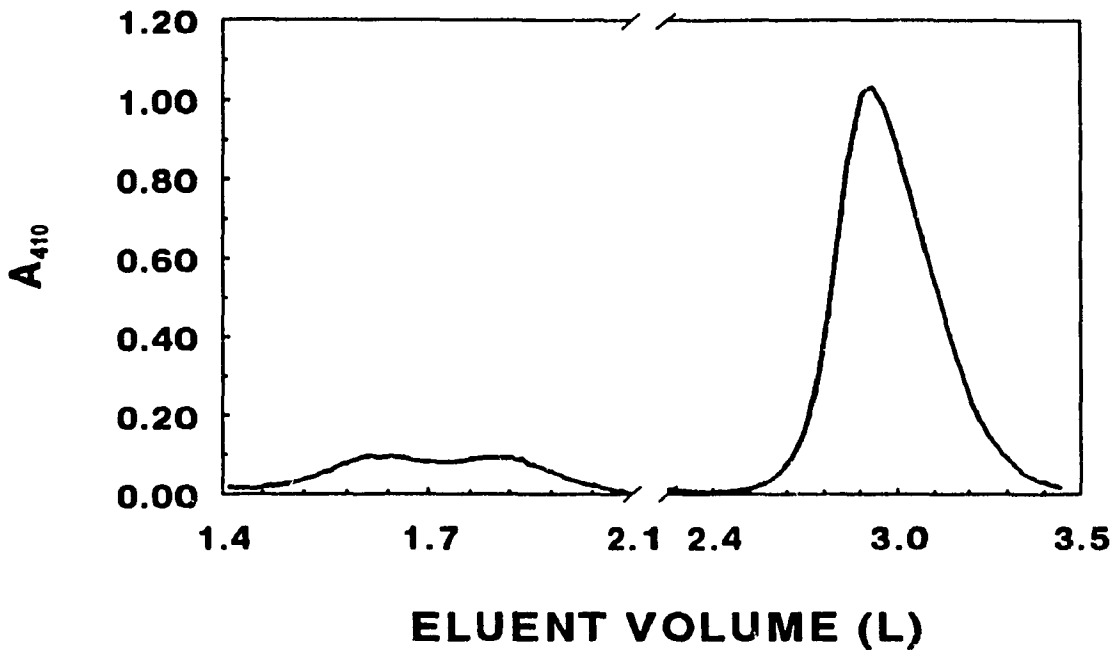

Figure 3.4 Purification of commercial cyt c (50 mg in 1.0 mL equilibration buffer) by cation-exchange (CM-Sephadex) chromatography. Flow rate: 30 mL/h; fraction size: 10 mL. The absorbance of the fractions was read at 410 nm. The sample was loaded onto a 1.5- x 60-cm CM-sephadex column equilibrated with 100 mM NaPi (pH 7.0) at 4 °C, and was eluted with the same buffer. The large peak contains native cyt c.

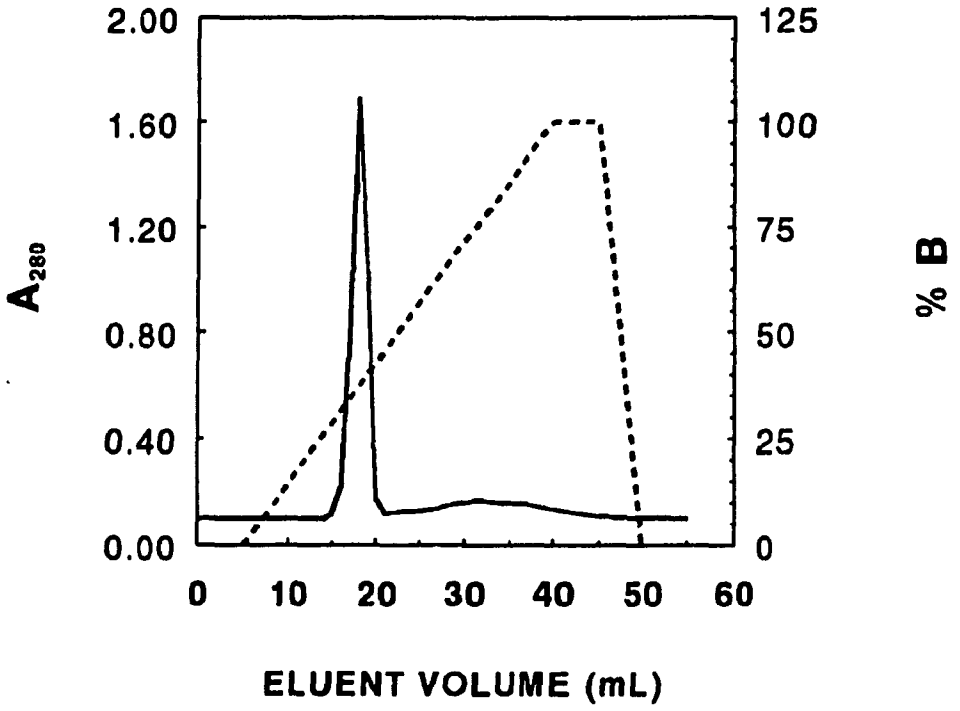

Figure 3.5 Purification of commercial GOx (62 mg in 500 µL of buffer A) by hydrophobic interaction chromatography (Phenyl-Sepharose). Flow rate: 1 mL/min; FPLC Hi-Load 16/10 column (16 mm x 10 cm); eluent: buffer A, 10 mM NaPi and 0.85 M $(NH_4)_2SO_4$, pH 7.5; buffer B, 10 mM NaPi, pH 8.0; linear gradients: 0 to 100% buffer B from 5.0 to 40.0 mL eluent; 0 to 100% A from 45 to 50 mL. Fraction size: 5.0 mL. Absorbance was monitored at 280 nm.

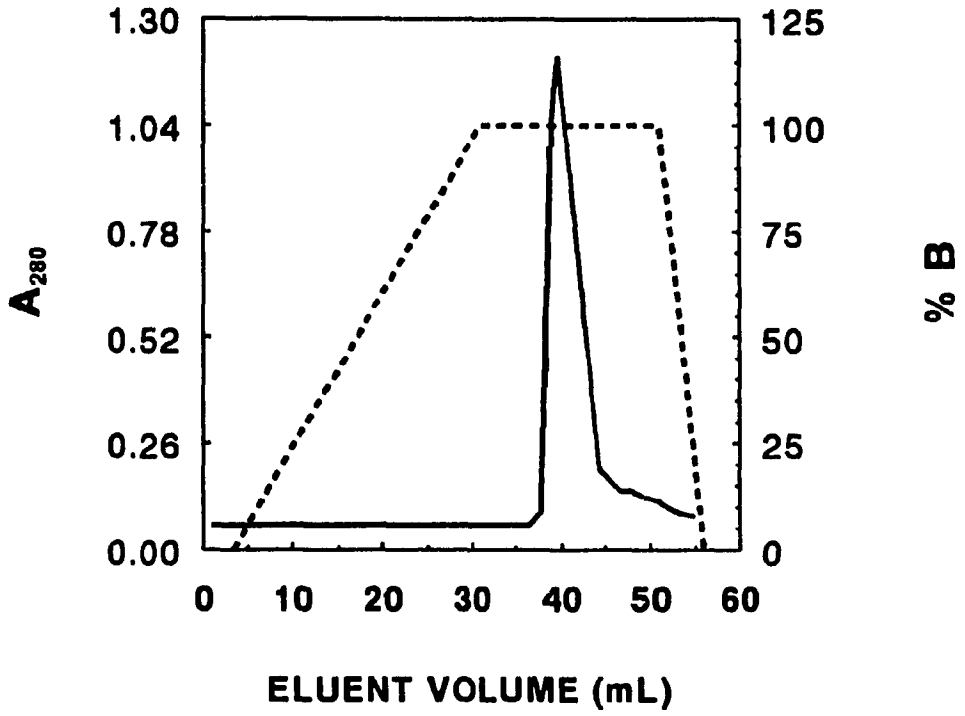

Figure 3.6 Purification of commercial GOx (54 mg in 500 µL buffer A) by anion-exchange chromatography (Q-Sepharose). Flow rate: 1 mL/min; 1.6- x 45-cm Q-Sepharose column; eluent: buffer A, 20 mM NaPi, pH 8.5; buffer B, 20 mM NaPi with 1 M NaCl, pH 8.5; linear gradients: 0% to 100% B (dotted line) from 3.5 mL to 31.0 mL eluent, 0% to 100% A from 50 to 55 mL. Fraction size: 5.0 mL. Absorbance was monitored at 280 nm.

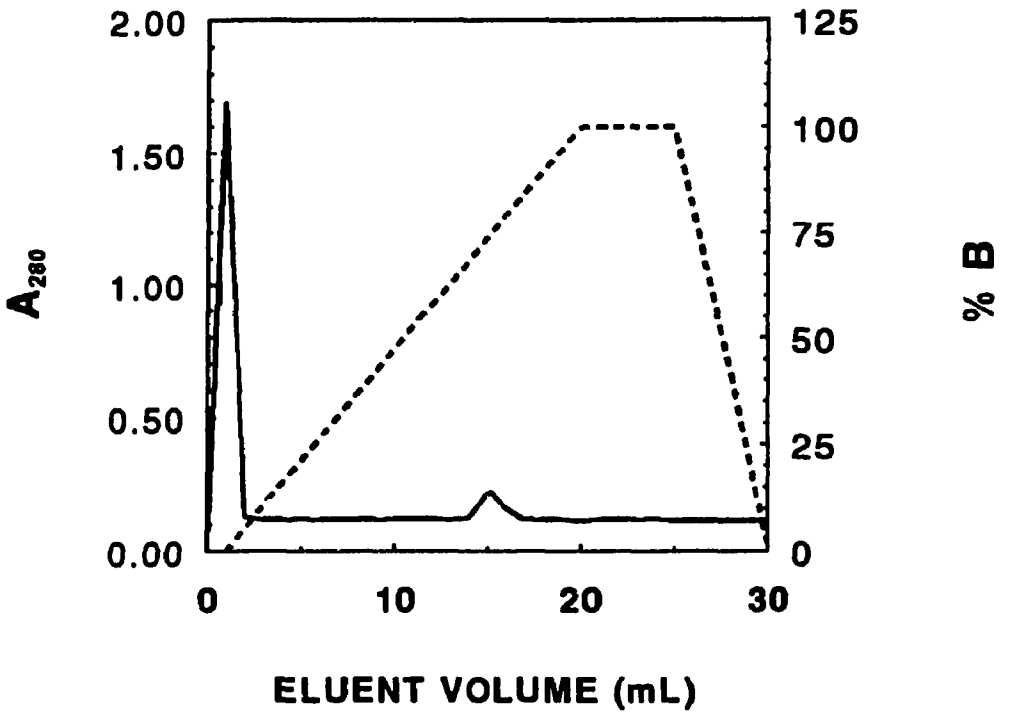

Figure 3.7 Purification of deglycosylated GOx (31 mg in 500 µL buffer A) by cation-exchange (Mono S HR 10/10 column) chromatography. Eluent: solvent A, 30 mM NaPi, pH 4.2; solvent B, 30 mM NaPi with 0.75 M NaCl, pH 4.2; Linear gradients: 0 to 100% B (dotted line) from 1.0 to 20.0 mL; 0 to 100% A from 25 to 30 mL. Flow rate, 1.0 mL/min. Absorbance was monitored at 280 nm.

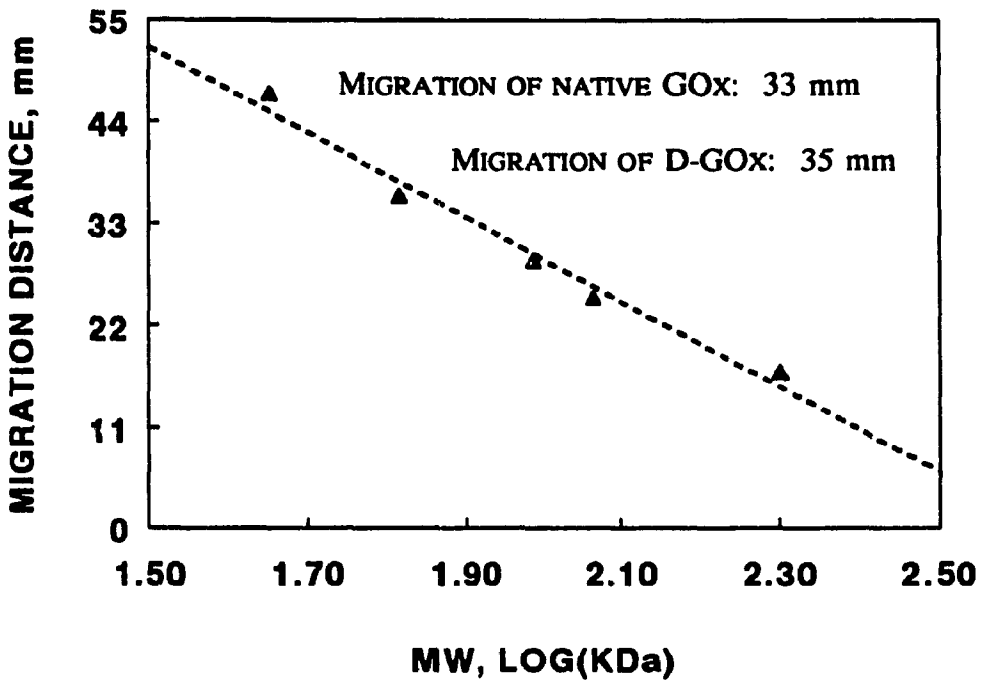

Figure 3.8 SDS-PAGE calibration curve (correlation coefficient = 0.9899) for molecular weight determination of deglycosylated GOx (D-GOx). Solutions of 6.0 mg/mL D-GOx from the cation exchange column, and G-15 gel-filtered native GOx were denatured in SDS reducing buffer and applied (4 µg in 20 µL) to a 7.5% polyacrylamide gel in running buffer (0.025 M tris base, 0.19 M glycine, and 3.5 mM SDS, pH 8.3). A 100 mV gradient was applied to the gel. Molecular weight markers (▲) ranging from 45 to 200 kDa were used. The SDS gel was run by L. D'Astous with molecular markers in one lane, and the D-GOx and native GOx in separate lanes.

3.3.3 Promotion of Cyt c Electrochemistry

3.3.3.1 Comparison of 4,4'-Bipyridyl, L-Cysteine and Mercaptopropionic Acid as Promoters. Figure 3.9 shows the cyclic voltammograms for cyt c obtained with the promoters that yielded significant peaks within the expected potential range. Figure 3.10 illustrates the voltammograms obtained in the presence of thiols that do not act as promoters for cyt c. The fifth cycle in a cyclic voltammogram was chosen for ΔE_p determination since there is a typical pattern of signal stabilization which requires two cycles initially, and a further two cycles to confirm cyclic voltammogram reproducibility.

Comparisons were made between voltammograms from different promoter-modified gold electrodes using the same oxygen-free solution of 400 μM commercial cyt c in 20 mM NaPi, pH 7.0 and 100 mM $NaClO_4$. These are the same conditions used in previous studies by Hill and coworkers except that these workers used purified cyt c.[7] Electrochemically reversible redox couples have peak separations of 59/n mV. For cyt c, n=1,[8] therefore the ΔE_p value for reversible cyt c electrochemistry would be 59 mV. The heterogeneous rate constant, k_s was evaluated only in the presence of those promoters that gave identifiable peaks: 4,4'-bipyridyl, L-cysteine and mercaptopropionic acid. There are regions in the plot of $n\Delta E_p$ vs $\log(\Psi)$ (Figure 3.3) where the determination of k_s is more accurate. For example, in the $n\Delta E_p$ region between ~75 and ~135 mV, uncertainties of $< \pm 5$ mV in ΔE_p yield corresponding uncertainties in k_s of $< \pm 1.01 \times 10^{-4}$ cm s^{-1}. Outside this range, uncertainties increase due to the shape of the curve. Therefore, during voltammetric measurements of quasi-reversible electrode reactions, peak separations were evaluated at scan rates between 5 and 30 mV s^{-1} in order to find ΔE_p

values that fell within the desired range of the working curve.

Table 3.1 summarizes the data for commercial cyt c from triplicate voltammograms that were obtained in the presence of 10 mM 4,4'-bipyridyl at scan rates (ν) ranging from 5 to 30 mV s^{-1}. The expected trend of increasing ΔE_p with ν is seen in these data, while larger uncertainties in ΔE_p result from the broader voltammetric peaks observed at the higher scan rates. The average k_s value obtained from the data in Table 3.1 was found to be $4.6 \pm 0.5 \times 10^{-4}$ cm s^{-1}. This value, for commercial cyt c, is approximately 35-fold less than the literature[2] values of $1.4\text{-}1.9 \times 10^{-2}$ cm s^{-1} obtained with *purified* cyt c under identical conditions.

The k_s values obtained for commercial cyt c using L-cysteine as a promoter on a gold electrode (Table 3.2) were comparable to those observed for the bipyridyl-modified gold electrode (Table 3.1). Cyclic voltammograms were done in triplicate at 200 and 400 μM cyt c to test whether the magnitude of k_s depends on the bulk concentration of cyt c. The average values of k_s are $6.1 \pm 0.2 \times 10^{-4}$ and $7.5 \pm 2 \times 10^{-4}$ cm s^{-1} at 400 and 200 μM cyt c, respectively. Greater variation was observed in the ΔE_p values at a given scan rate for the 200 μM solution, which may be due to noise since the measured peak currents, i_p, are approximately two-fold lower than those measured at 400 μM cyt c.

The reproducibility of electrode modification using L-cysteine as a promoter was investigated (Table 3.3). Triplicate cyclic voltammograms were done at a scan rate of 20 mV s^{-1} for 400 μM commercial cyt c, and the electrode was polished in a 0.05 μm alumina slurry and electrochemically cleaned in 0.1 M sulfuric acid. After cleaning, the electrode was again modified in the usual manner. The results in Table 3.3 reveal no

trend towards increased or decreased ΔE_p values following repeated modification.

The use of mercaptopropionic acid to promote cyt c electrochemistry at a gold electrode was done in the same manner as for L-cysteine at 200 and 400 μM commercial cyt c. The resulting voltammogram peaks appear only at lower scan rates, allowing the determination of k_s for scan rates ranging from 1 to 10 mV s^{-1}. The potential range used for this electrode was widened in order to enhance the peak finding capability of the instrument; therefore, the voltammograms extend from -220 mV to +230 mV, and the results are presented in Table 3.4.

The average values of k_s for the mercaptopropionic acid-modified gold electrode are $6.1 \pm 0.4 \times 10^{-5}$ and $5.1 \pm 0.3 \times 10^{-5}$ cm s^{-1} for the 400 and 200 μM cyt c solutions, respectively. There are fewer ΔE_p values available for the lower cyt c concentration since peaks were not identifiable at scan rates of 10 mV s^{-1} or greater. The k_s values for the mercaptopropionic acid-modified electrode are approximately one order of magnitude lower than those observed for the cysteine-modified electrode.

3.3.3.2 Dependence of k_s on Time at Modified Gold Electrodes. The time-dependence of k_s, determined by the cyclic voltammetry of cyt c, is plotted for commercial and purified cyt c in Figures 3.11 and 3.12, respectively. For commercial cyt c (Figure 3.11), a comparison was made between the responses from L-cysteine- and 4,4'-bipyridine-modified gold electrodes. A clean unmodified gold electrode gave no response. For the bipyridine-modified electrode, the initial k_s value of 3.0×10^{-3} cm s^{-1} is approximately one order of magnitude higher than the initial k_s for the cysteine-modified electrode, however, the bipyridyl rate constant dimishes to zero after about 3 hours.

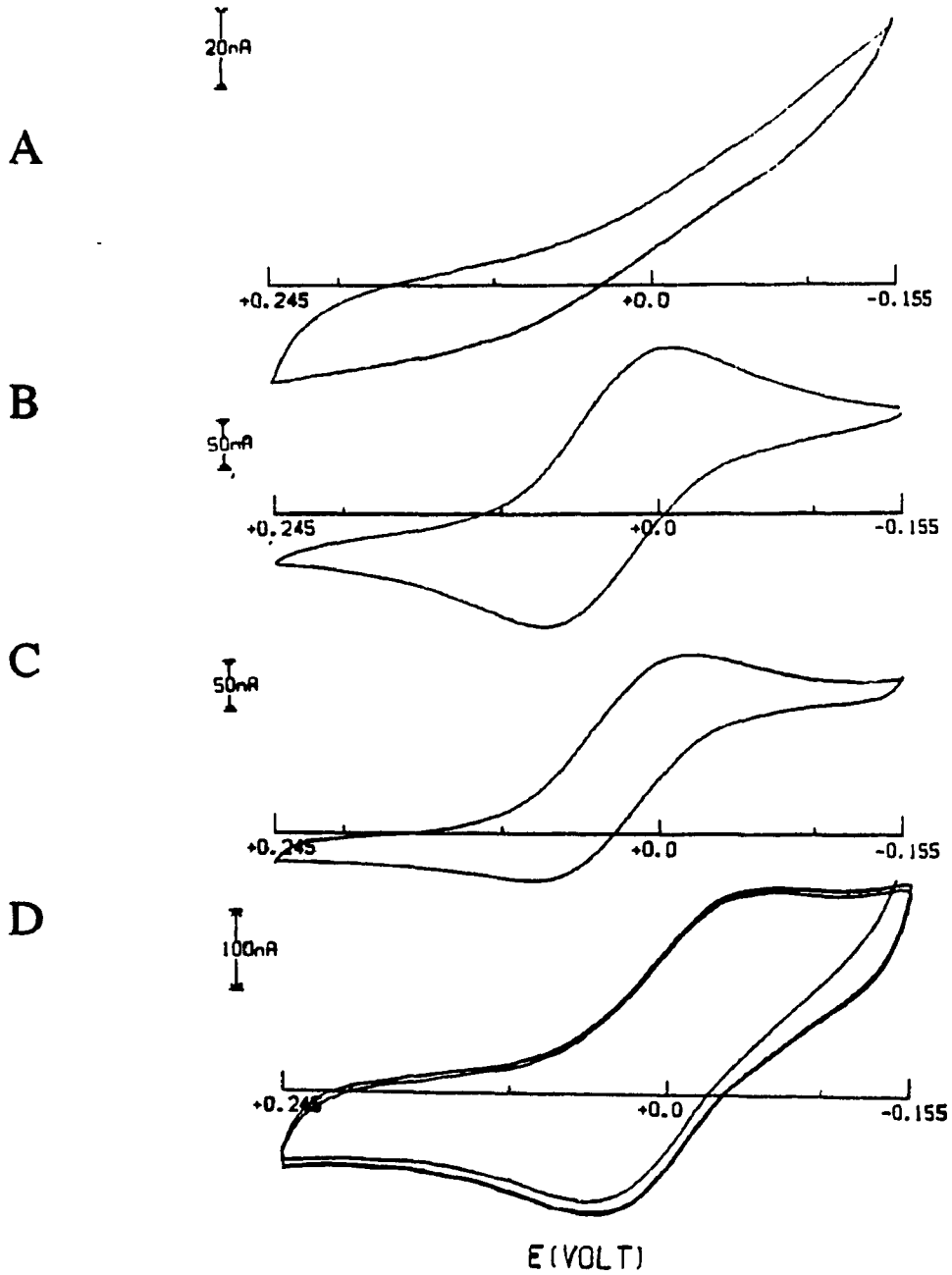

Figure 3.9 Cyclic Voltammetry of cyt c at a gold electrode in absence and presence of promoters. (**A**) unmodified electrode; (**B**) 10 mM 4,4'-bipyridyl; (**C**) L-cysteine-modified electrode; (**D**) mercaptopropionic acid-modified electrode. Voltammograms were obtained from 400 μM commercial cyt c solutions in O_2-free 20 mM NaPi buffer, pH 7.0, with 100 mM $NaClO_4$ at 23 °C. Scan rate: 20 mV s^{-1}. Ag/AgCl reference electrode.

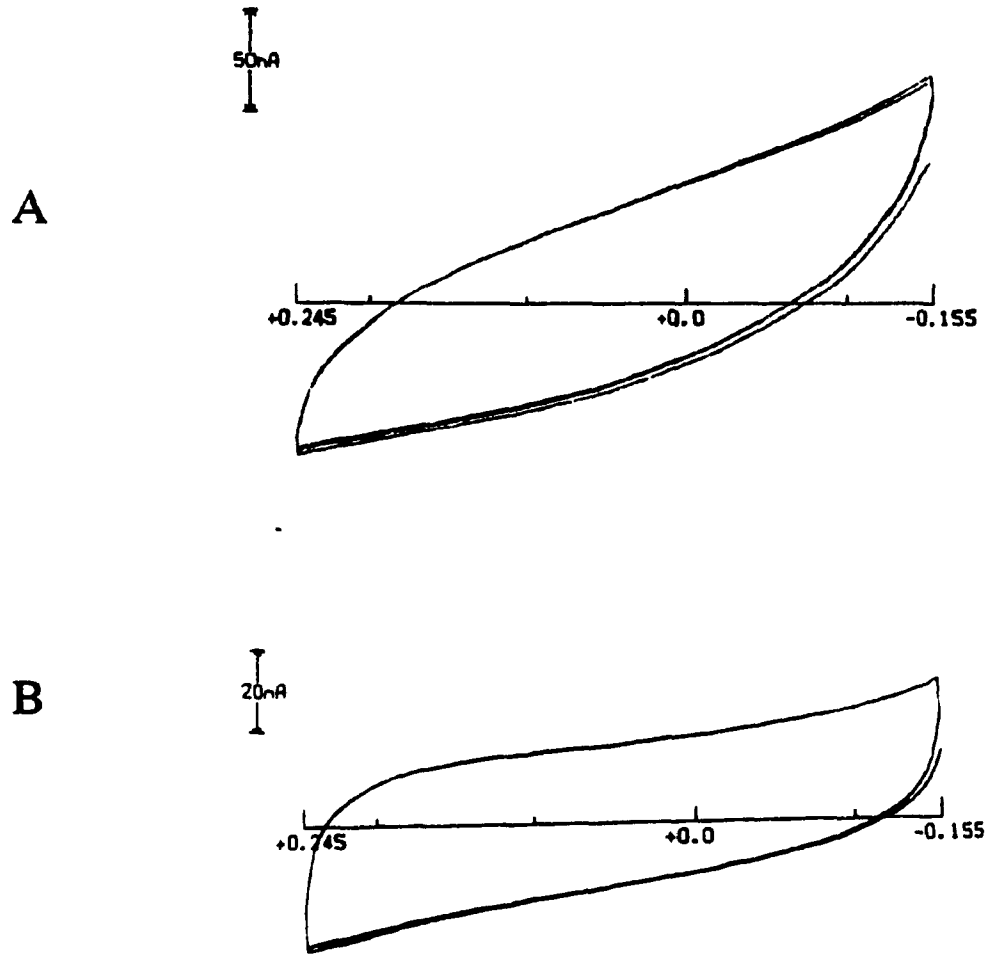

Figure 3.10 Cyclic Voltammetry of cyt c at a gold electrode with nonfunctional promoters. (**A**) thioctic acid-modified electrode; (**B**) aminoethanethiol-modified electrode. Experimental conditions were the same as those given in Figure 3.9.

Table 3.1 Determination of k_s from voltammograms of cyt c at a gold electrode using 4,4'-bipyridyl as a promoter[a]

Scan Rate ($mV\ s^{-1}$)	ΔE_p[b]	$k_s \times 10^4$ ($cm\ s^{-1}$)[c]
5	101 ± 2	4.6
10	112 ± 8	4.9
15	109 ± 8	6.4
20	133 ± 11	4.7
25	164 ± 13	3.4
30	161 ± 15	3.8

[a] Experimental conditions: 400 μM commercial cyt c in O_2-free, 20 mM NaPi buffer, pH 7.0, with 100 mM $NaClO_4$ and 10 mM 4,4'-bipyridine at 23 °C. The electrode was polished in 0.05 μm alumina with subsequent rinsing and sonication after each voltammogram. Scanning range: -0.155 to +0.255 V (vs. Ag/AgCl).

[b] ΔE_p values are the average of triplicate voltammetric runs ± standard deviation.[c]

k_s values calculated using a diffusion coefficient of cyt c: 1.1×10^{-6} from the literature.[2]

Table 3.2 Determination of k_s from voltammograms of cyt c at a gold electrode using L-cysteine as a promoter[a]

Scan Rate ($mV\ s^{-1}$)	[cyt c] μM	ΔE_p[b] (mV)	$k_s \times 10^4$ ($cm\ s^{-1}$)
5	400	82 ± 3	4.0[c]
10	400	82 ± 1	5.9
15	400	84 ± 2	6.3
20	400	89 ± 1	6.2
25	400	92 ± 2	6.1
5	200	83 ± 4	3.8[c]
10	200	85 ± 3	4.9
15	200	80 ± 7	8.2
20	200	85 ± 5	7.2
25	200	83 ± 2	9.7

[a] Experimental conditions: L-cysteine modified Au electrode dipped into O_2-free, 20 mM NaPi buffer (pH 7.0) containing commercial cyt c and 100 mM $NaClO_4$ at 23 °C. Scanning range: -0.155 to +0.255 V (vs. Ag/AgCl).

[b] Average of 3 determinations ± standard deviation.

[c] Excluded from the estimation of k_s (statistical outlier based on Q-test).

Table 3.3 Determination of ΔE_p for 400 μM cyt c at a cysteine-modified gold electrode after cleaning[a]

CLEANING[b] #	ΔE_p[c] (mV)
1	100 ± 5
2	92 ± 1
3	96 ± 1
4	103 ± 2

[a] Experimental conditions are given in footnote to Table 3.2.

[b] Cleaning procedure: initial polishing with a 0.05-μm alumina slurry on a nylon pad followed by electrochemical cycling within a potential range of -305 to 1545 mV (vs Ag/AgCl) in 0.1 M sulfuric acid.

[c] Average ΔE_p values for anodic and cathodic peak separations are from triplicate determinations, ± standard deviation.

Table 3.4 Determination of k_s from voltammograms of cyt c at a gold electrode using mercaptopropionic acid as a promoter.[a]

Scan Rate ($mV\ s^{-1}$)	[cyt.C] μM	ΔE_p[b] (mV)	$k_s \times 10^5$ ($cm\ s^{-1}$)
1	400	137 ± 10	4.4
2	400	140 ± 20	5.9
4	400	161 ± 0	6.2
6	400	170 ± 1	6.7
8	400	180 ± 0	6.8
10	400	194 ± 2	6.4
1	200	138 ± 7	4.3
4	200	179 ± 3	4.9
6	200	183 ± 1	5.7
8	200	200 ± 4	5.3

[a] Experimental conditions: mercaptopropionic acid-modified Au electrode dipped into O_2-free, 20 mM NaPi buffer (pH 7.0) containing commercial cyt c and 100 mM $NaClO_4$ at 23 °C. Scanning range: -0.220 to +0.230 V (vs Ag/AgCl).

[b] Average of 3 determinations ± standard deviation.

In contrast, the cysteine-modified electrode has an initial k_s value of 2.7 x 10^{-4} cm s^{-1}, which rises to 6.8 x 10^{-4} cm s^{-1}, and persists for at least 24 hours.

For purified cyt c (Figure 3.12), a comparison was made between the responses at gold electrodes modified with L-cysteine and 4,4'-bipyridine, and a clean, unmodified electrode. For the bipyridine-modified electrode, the initial k_s value is almost two-fold higher (1.8 x 10^{-3} cm s^{-1}) than the initial k_s value for the cysteine-modified electrode (1.1 x 10^{-3} cm s^{-1}). Extrapolation of the data suggests that k_s values obtained at the bipyridyl-modified electrode decrease to zero after about 20 hours, almost ten times longer than the same electrode with commercial cyt c.

For the cysteine-modified electrode, the average k_s value is 0.92 ± 0.05 x 10^{-3} cm s^{-1} and shows little variability with time compared to k_s obtained for commercial cyt c (Figure 3.11). The unmodified gold electrode yielded an initial k_s value of 0.27 x 10^{-3} cm s^{-1} which decreased to zero in less than 2 hours.

Persistence of k_s over time may depend on the extent of electrode fouling by the protein. This will cause a gradual decrease in the available electrode surface area over time under particular conditions. Since peak currents are directly proportional to area, provided that analyte concentration and diffusion coefficient are fixed, electrode fouling would give rise to a decrease in peak current, with time. Plots of anodic peak current (i_p) vs time for commercial and purified cyt c are presented in Figure 3.13. These values were obtained from the voltammograms used to determine k_s in Figures 3.11 and 3.12. It should be noted that voltammetric peaks can often be detected and measured even when ΔE_p values are too large to be used to estimate k_s. For this reason, i_p values are available

for the 4,4'-bipyridyl-modified electrodes even at 24 hours, with purified cyt c. The only system showing a decrease in i_p with time involved commercial cyt c at a 4,4'-bipyridyl-modified electrode.

The Randles-Sevcik equation[27,22] indicates that peak currents are proportional to the square root of scan rate, for an electrochemically reversible redox couple:

$$i_p = 269\ n^{3/2}\ A\ D^{1/2}\ v^{1/2}\ C^b \quad (A) \qquad (3.3)$$

where n is the number of electrons transferred per redox species, A the electrode area in cm^2, D is the diffusion coefficient of the redox species in $cm^2\ s^{-1}$, v the scan rate, in V s^{-1} and C^b the bulk molar concentration. A plot (Figure 3.14) of the anodic peak currents from the cysteine-modified electrodes vs the square root of scan rate, shows that the current reaches a plateau at scan rates ≥12 mV s^{-1}. This is evidence that the overall electron transfer reaction kinetics are limiting.

3.3.4 Promotion of GOx Electrochemistry

3.3.4.1 Native Glucose Oxidase with Three Promoters. Native GOx solutions were examined at gold electrodes modified by the chemisorption of three different promoters: L-cysteine, mercaptopropionic acid (MPA) and aminoethanethiol (AET). Commercial GOx preparations may contain significant quantities of free FAD, so an initial comparison was made of commercial GOx to G-15 gel-filtered GOx at an L-cysteine-modified electrode.

The cathodic current in the -500 mV region observed for commercial GOx (Figure 3.15A), which is ~5-fold larger than a similar plateau observed for the gel-filtered

solution of GOx (Figure 3.15B), is probably due to free FAD in solution. Upon addition of 100 mM mutarotated glucose to the same gel-filtered GOx solution, neither cathodic nor anodic peaks were observed (Figure 3.15C). In a separate experiment, a gel-filtered 275 μM GOx solution was tested at a cysteine-modified gold electrode before and after overnight storage (4 °C), and the small cathodic current did not change significantly (data not shown). This would suggest that no free FAD was released from GOx during storage.

The direct, unmediated electrochemistry of gel-filtered GOx at gold electrodes was compared for AET, MPA and L-cysteine promoters, and the results are shown in Figure 3.16. Significant peaks are observed only at the AET-modified electrode, where $E^{0'}$ = -0.390 V (vs Ag/AgCl). Despite the addition of 100 mM glucose, no *catalytic* currents were observed for any of the promoters used.

3.3.4.2 Aminoethanethiol-Promoted GOx Electrochemistry. GOx electrochemistry was compared with that for free FAD at an AET-modified gold electrode because redox proteins are known to adsorb and denature on certain electrode surfaces.[8,29] Both $E^{0'}$ and k_s values are expected to be different for free and GOx-bound FAD. Figure 3.17A shows the voltammogram for a 400 μM solution of FAD in 0.1 M NaPi buffer (pH 7.0) with 100 mM glucose. An $E^{0'}$ value of 0.410 V was obtained for free FAD in the presence of 100 mM glucose, and in the absence of glucose (voltammogram not shown) an identical $E^{0'}$ was obtained. GOx subjected to a single gel-filtration, in the presence of 100 mM glucose (Figure 3.17C) showed a redox couple with an $E^{0'}$ value of -0.390 V (vs Ag/AgCl) whereas, singly gel-filtered GOx in the absence of glucose (Figure 3.17B) yielded no peaks.

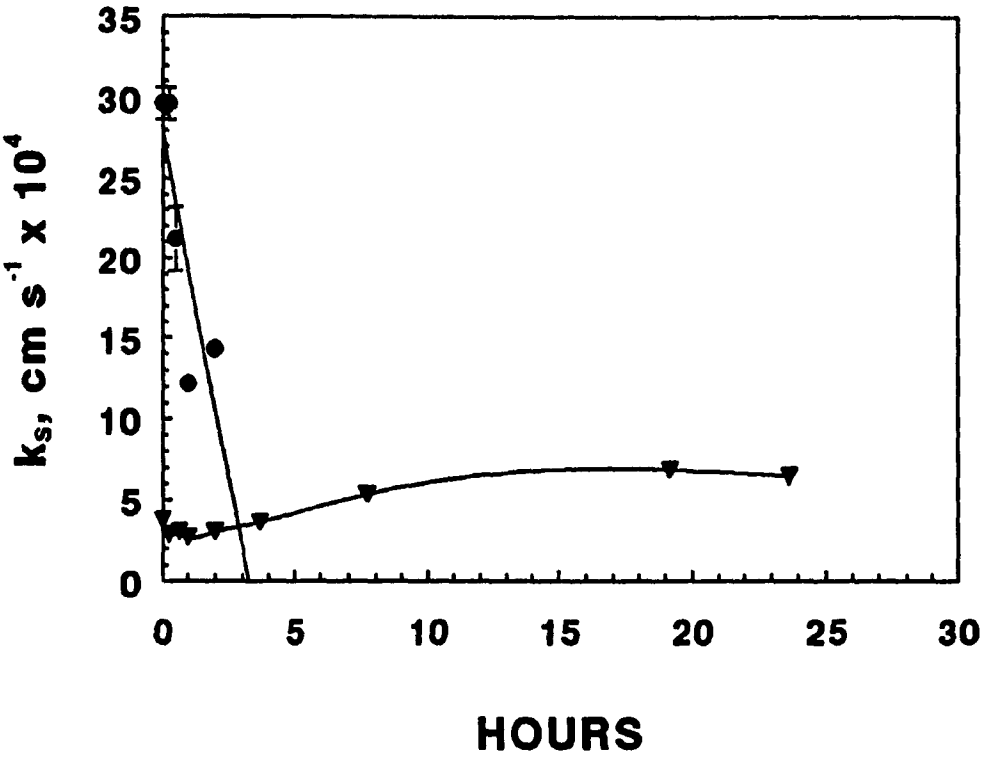

Figure 3.11 Persistence of k_s for commercial cyt c. The electrochemical cell contained 400 µL of 400 µM cyt c in O_2-free 20 mM NaPi buffer (pH 7.0) with 100 mM $NaClO_4$; (●) 10 mM 4,4'-bipyridine added to cell with clean, unmodified gold working electrode; (▾) L-cysteine-modified gold working electrode. All k_s values were obtained from triplicate voltammograms, at a scan rate of 10 mV s^{-1}.

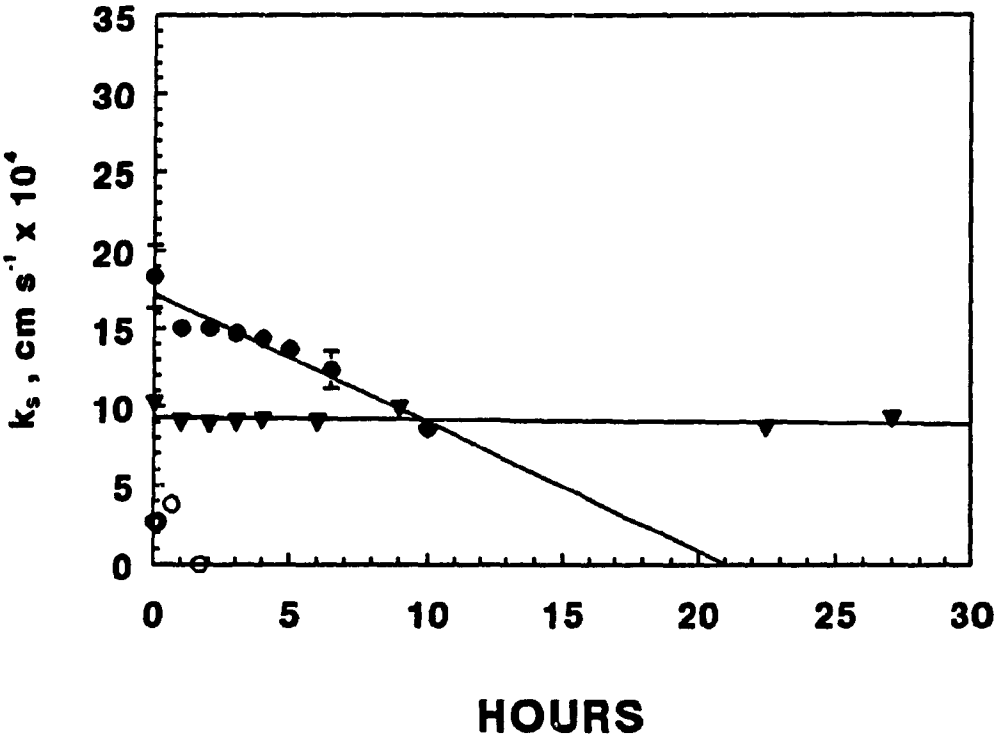

Figure 3.12 Persistence of k_s for purified cyt c. The electrochemical cell contained 400 µL of 400 µM purified cyt c in O_2-free 20 mM NaPi buffer (pH 7.0) with 100 mM $NaClO_4$; (●) 10 mM 4,4'-bipyridine added to cell with clean, unmodified gold working electrode; (▾) L-cysteine-modified gold working electrode; (O) unmodified gold working electrode. k_s values were obtained from triplicate voltammograms, except for the unmodified gold electrode, where only single voltammograms were obtained. The scan rate was 5 mV s^{-1}.

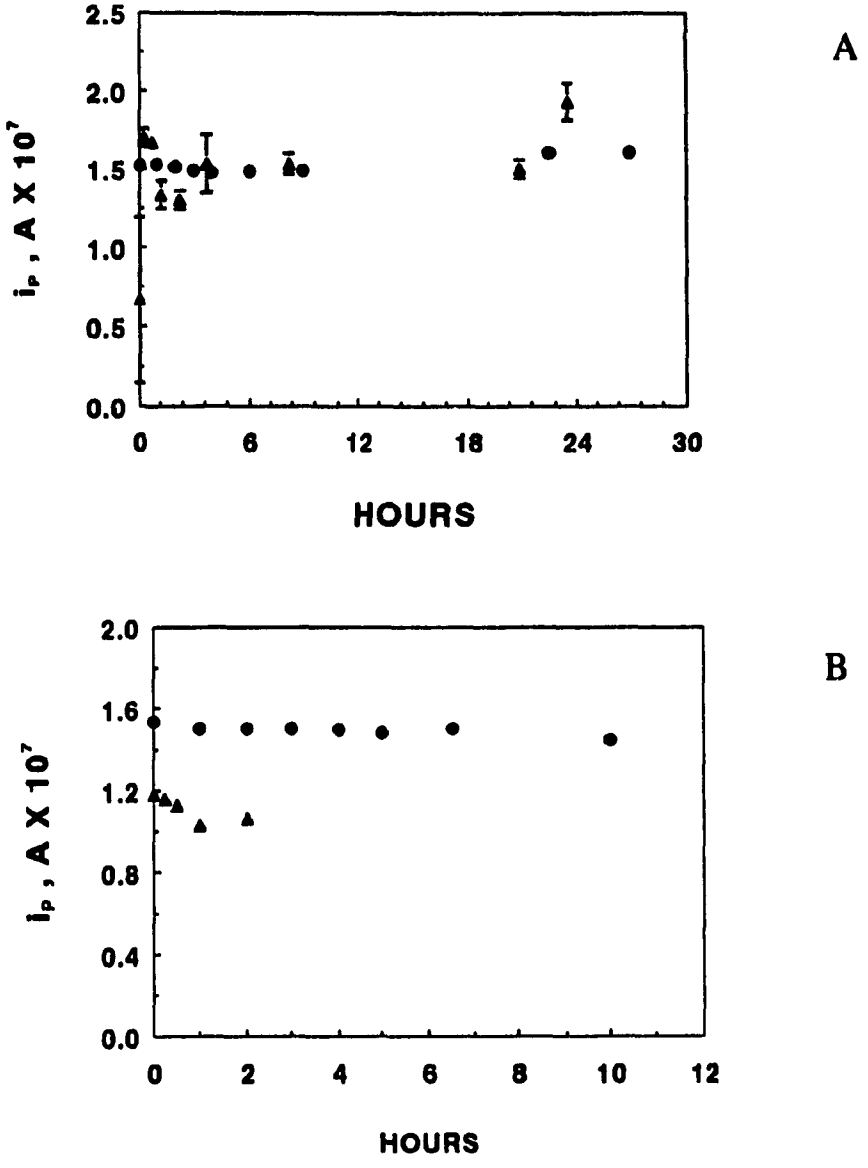

Figure 3.13 Anodic peak current vs time for modified gold electrodes. (**A**) L-cysteine modified gold electrodes; (**B**) 4,4'-bipyridyl modified gold electrodes. (●) 400 μM purified cyt c. (▲) 400 μM commercial cyt c. Experimental conditions as in Figures 3.11 and 3.12.

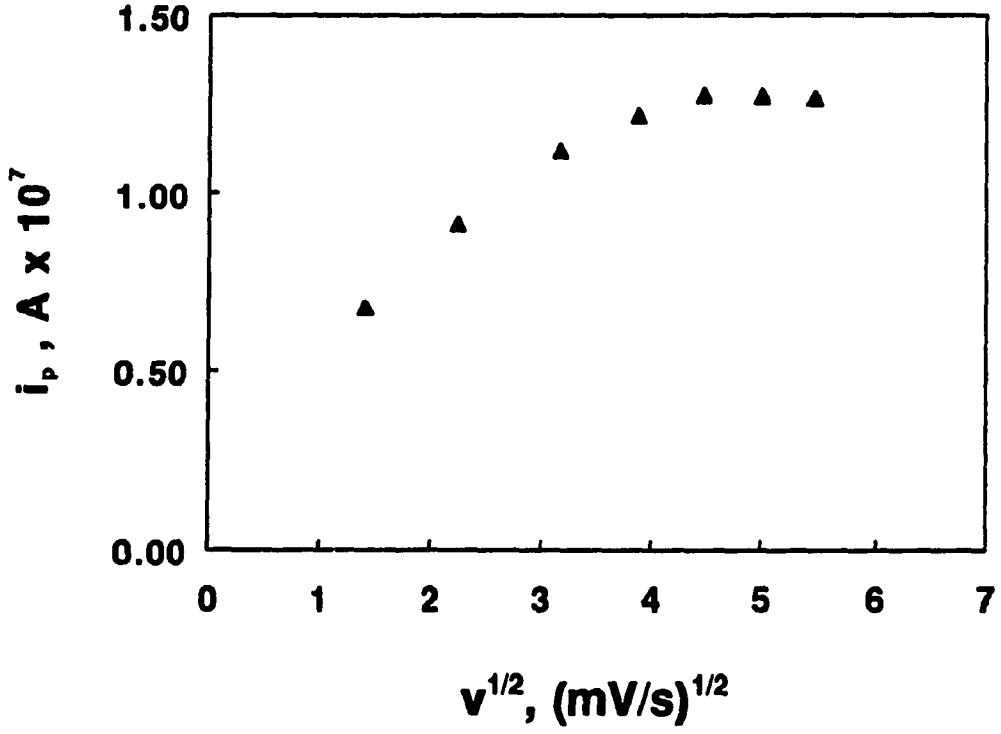

Figure 3.14 Anodic peak current (i_p) vs square root of scan rate ($v^{1/2}$) for an L-cysteine modified gold electrode dipped into O_2-free, 20 mM NaPi buffer (pH 7.0) containing 400 μM commercial cyt c and 100 mM $NaClO_4$ at 23 °C. Scanning range: -0.155 to +0.255 V (vs. Ag/AgCl). Data were obtained from the voltammograms used to determine k_s values in Table 3.2.

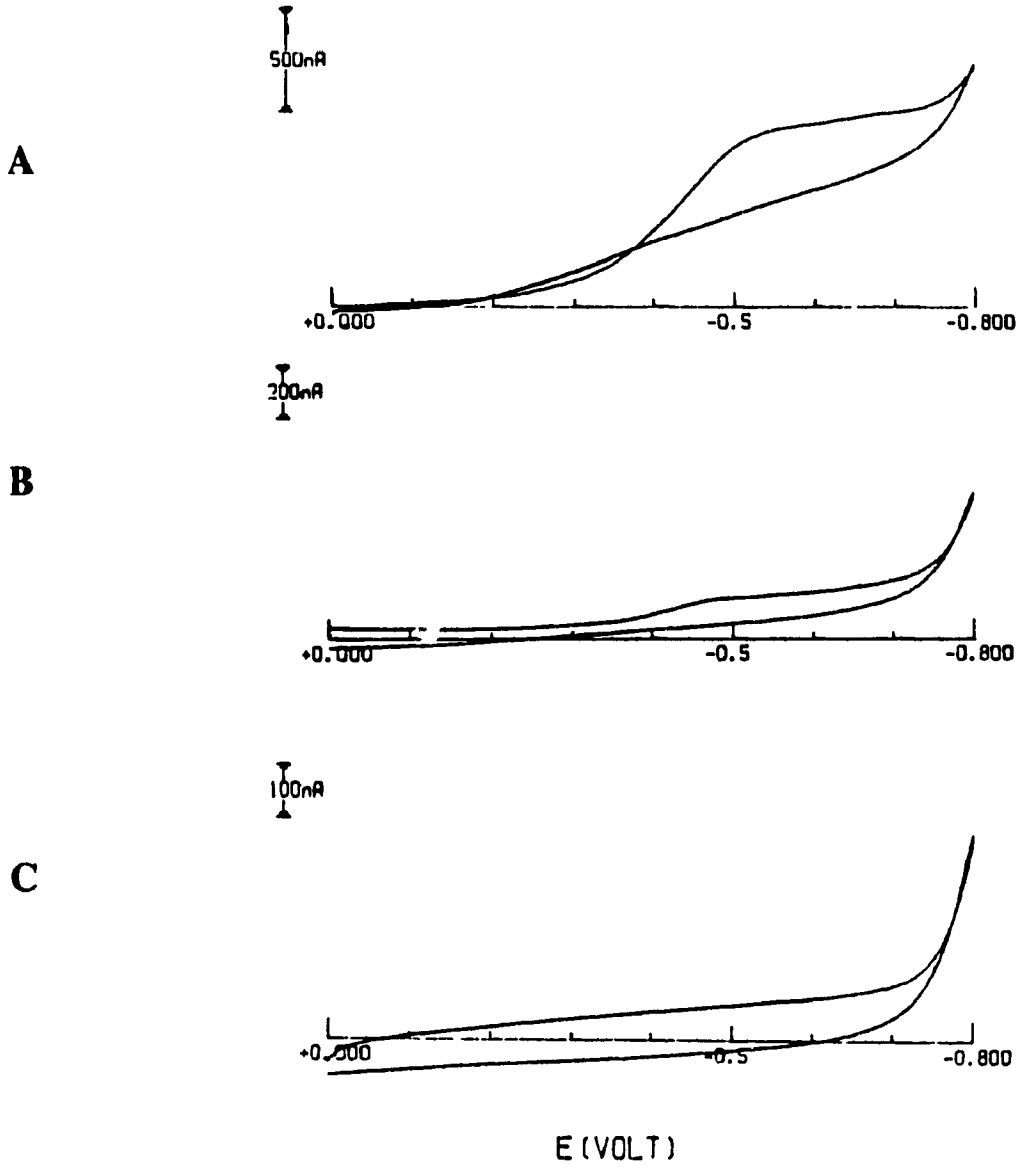

Figure 3.15 Comparison between cyclic voltammograms from L-cysteine-promoted GOx electrochemistry (gel-filtered vs commercial GOx). Voltammograms were from 400 µM GOx solutions in O_2-free 100 mM NaPi buffer at pH 7.00 and 23 °C. (**A**) commercial GOx; (**B**) G-15 gel-filtered GOx; (**C**) gel-filtered GOx with 100 mM glucose added; scan rate: 5 $mV\ s^{-1}$. (Note different current scales).

Figure 3.16 Unmediated cyclic voltammetry of G-15 gel-filtered GOx using promoters on a gold electrode (next page). Promoters: **(A)** aminoethanethiol; **(B)** L-cysteine; **(C)** mercaptopropionic acid; **(D)** clean, unmodified gold electrode. Scan rate: 2 mV s^{-1}. Voltammograms are of 400 μM gel-filtered GOx solutions in O_2-free 100 mM NaPi buffer at pH 7.0 and 23 °C, with 100 mM (saturating) glucose.

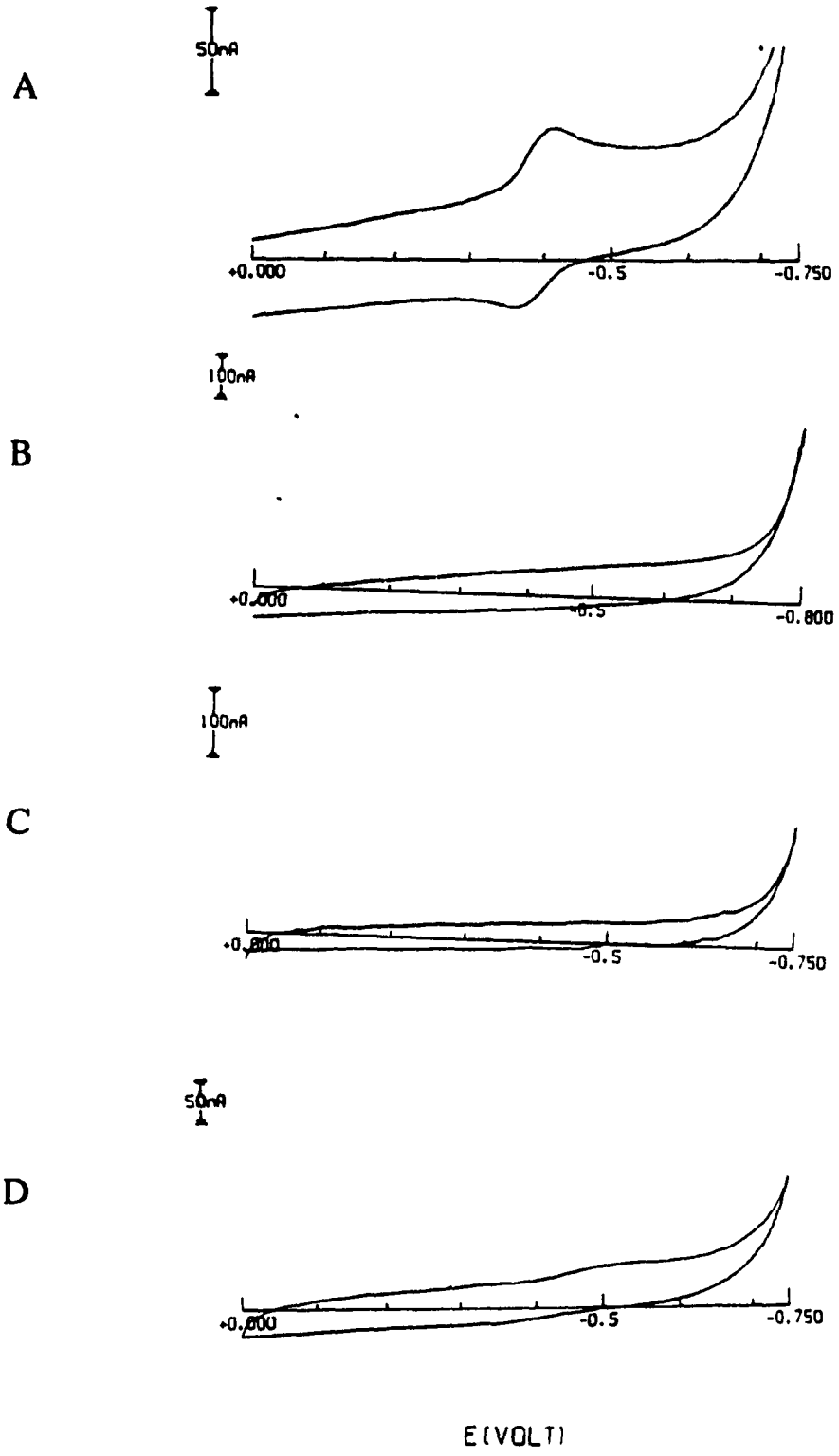
A
50nA
+0.000
-0.5
-0.750
100nA
B
+0.000
-0.5
-0.800
100nA
C
+0.800
-0.5
-0.750
50nA
D
+0.800
-0.5
-0.750
E(VOLT)

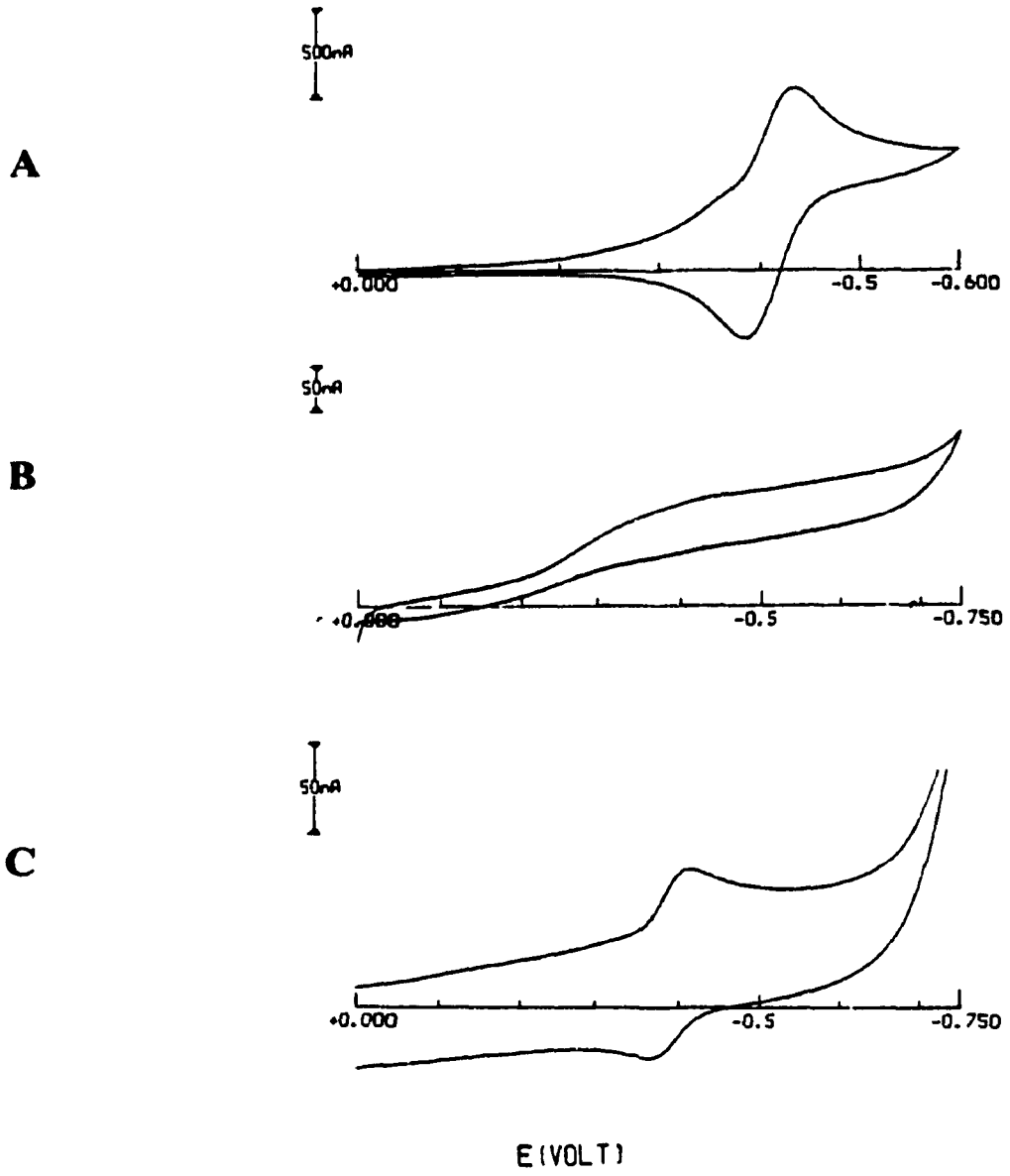

Figure 3.17 Free FAD and GOx electrochemistry at AET-modified gold electrodes. (**A**) free FAD with 100 mM glucose; (**B**) singly gel-filtered GOx; (**C**) same as (**B**) but with 100 mM glucose. Scan rate: 2 mV s^{-1}. Voltammograms were from 400 µM solutions in O_2-free 100 mM NaPi buffer at pH 7.0 and 23 °C. Note differences in voltage and current scales.

Figure 3.18 Doubly gel-filtered GOx electrochemistry at AET-modified gold electrode (next page). (**A**) AET-modified electrode with 100 mM glucose only; (**B**) AET-modified electrode with 400 µM GOx and no glucose; (**C**) AET-modified electrode with 400 µM GOx and 100 mM glucose; (**D**) Cleaned, unmodified electrode; (**E**) AET-modified electrode with 400 µM FAD in 100 mM glucose (shown for comparison). Cyclic voltammograms were of 400 µM, twice gel-filtered GOx solutions in O_2-free 100 mM NaPi buffer at pH 7.0 and 23 °C. Scan rate: 2 mV s^{-1}.

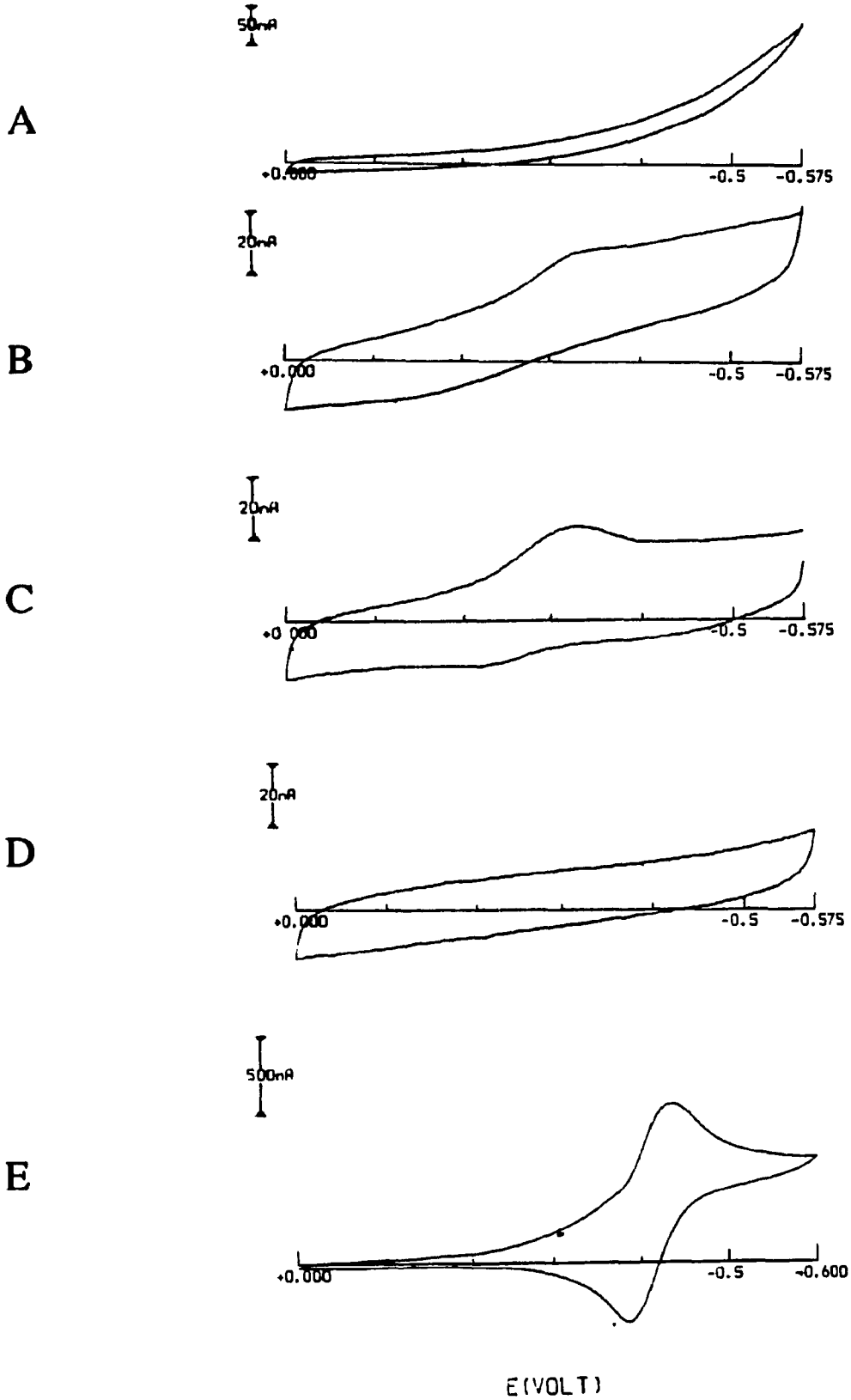
A
50nA
+0.000
-0.5
-0.575
B
20nA
+0.000
-0.5
-0.575
C
20nA
+0 000
-0.5
-0.575
D
20nA
+0.000
-0.5
-0.575
E
500nA
+0.000
-0.5
-0.600
E(VOLT)

AET-promoted electrochemistry was repeated for GOx samples that had been subjected to two successive G-15 gel-filtrations. The results, shown in Figure 3.18C, yield an $E^{0'}$ value of -0.274 V (vs Ag/AgCl) which is significantly more positive than values obtained with GOx samples that had been subjected to only one gel-filtration step. This strongly suggests that in the latter GOx solutions, free FAD is present.

3.3.4.3 Glucose Oxidase in Urea Solutions. GOx was incubated overnight in urea in order to investigate the effect of partial unfolding on AET-promoted voltammetry. In experiments with the AET-modified electrode, a single prominent redox couple appeared with GOx in the presence of 0 to 0.8 M urea and 100 mM glucose. The average formal potential of this redox couple, $E^{0'}$, was -0.408 V (vs Ag/AgCl), and the average $E^{0'}$ value for GOx in 2.0 and 4.0 M urea was comparable at -0.425 V. For free FAD alone, the $E^{0'}$ value in 0.4 M urea at an AET-modified gold electrode under identical conditions, was found to be -0.410 V (vs Ag/AgCl) with a ΔE_p value of 50 mV which, in turn, yielded a k_s value of 1.2×10^{-3} cm s^{-1} (eqn. 3.4). These experiments were performed on GOx prior to the finding that 2 gel filtrations were required to remove free FAD (Section 3.3.4.2), therefore free FAD was present even before denaturation took place withou urea (Figure 3.17C). However, the addition of urea markedly increased the prominence of the free FAD peaks, as discussed below.

Figure 3.19 shows voltammograms of singly gel-filtered GOx in 0.4 M urea in the absence and presence of 100 mM glucose (curves B and C, respectively). From these, it can be seen that the redox couple of free FAD (Section 3.3.4.2) appears upon the addition of glucose. A comparison voltammogram of GOx at a clean, unmodified gold

electrode (Figure 3.19A) in the same solution with glucose shows no identifiable peaks despite the possible presence of free FAD.

Figure 3.20 shows voltammograms obtained at AET-modified electrodes for singly gel-filtered GOx in the presence of 0.4, 0.6 and 0.8 M urea. The modification of this electrode with AET was different in that the cleaned, polished electrode was dipped overnight in AET solution, then polished again and quickly remodified in AET. A pre-amplifier was used to diminish signal noise during the experiment because currents were found to be very low (~ 10^{-8} A). All voltammograms show the -410 mV redox couple for free FAD, and its intensity also increases with urea concentration. At higher urea concentrations, a *second* redox couple appears with a formal potential of -205 mV (vs Ag/AgCl). This $E^{0'}$ value is close to that found for twice gel-filtered GOx (-0.250 V vs Ag/AgCl) using the AET-modified gold electrode (Figure 3.18), and suggests that this couple may be due to GOx-bound FAD.

Specific activities were obtained for urea-treated GOx samples that were already purified as in Section 3.2.2.3, using hydrophobic interaction and anion-exchange chromatography. Two urea-treated samples were prepared: 0.2 M and 0.6 M urea with 300 μM purified GOx in 100 mM NaPi buffer at pH 7.0. Activities of 113 U mg^{-1} and 93 U mg^{-1} were obtained for GOx in 0.2 and 0.6 M urea, respectively, corresponding to 106% and 88% of purified native GOx activity (106 U mg^{-1}). These results indicate that a significant amount of activity was retained for GOx samples at these concentrations of urea.

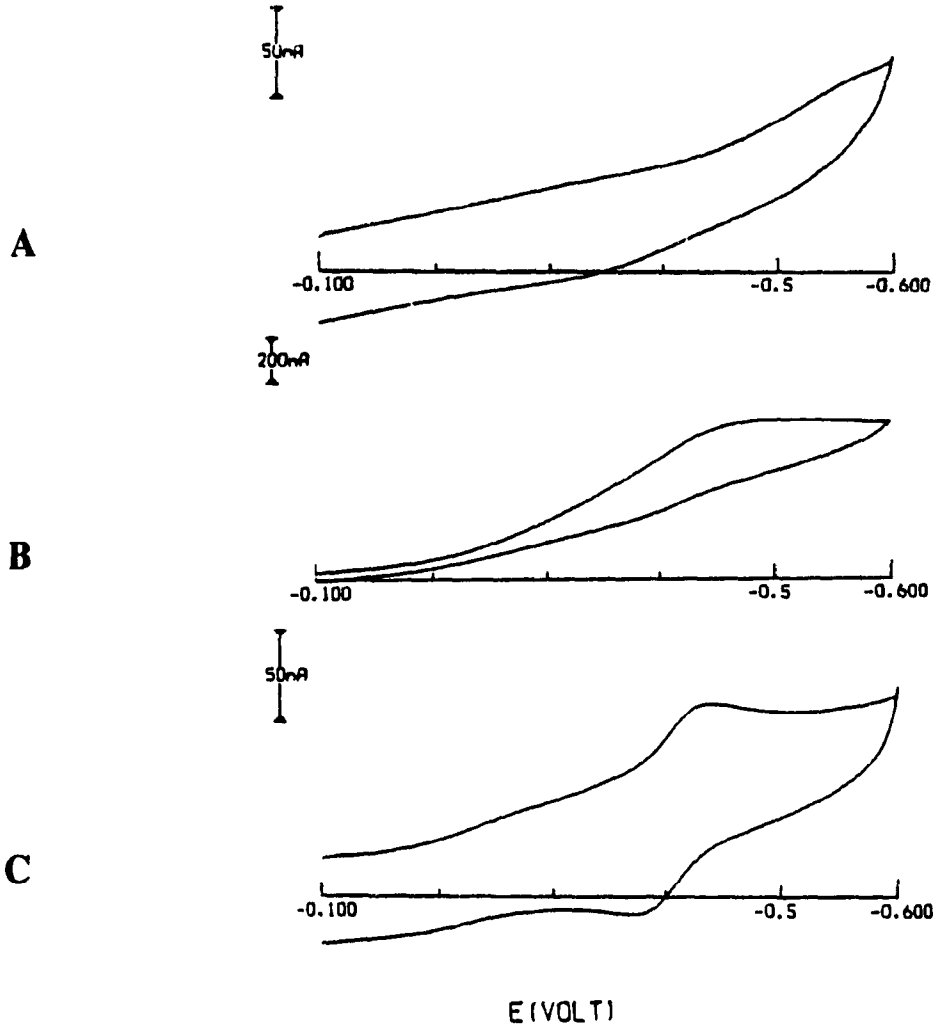

Figure 3.19 Cyclic voltammograms of 0.4 M urea-treated GOx using at gold electrodes. Voltammograms were from 400 µM singly gel-filtered, GOx solutions in O_2-free 100 mM NaPi buffer (pH 7.0) with 0.4 M urea at 23 °C at (**A**) a clean, unmodified electrode with 100 mM glucose; (**B**) an AET-modified gold electrode without glucose, and (**C**) same as (B) with 100 mM glucose present. GOx was incubated in 0.4 M urea overnight prior to obtaining the voltammograms. Scan rate: 5 mV s^{-1}.

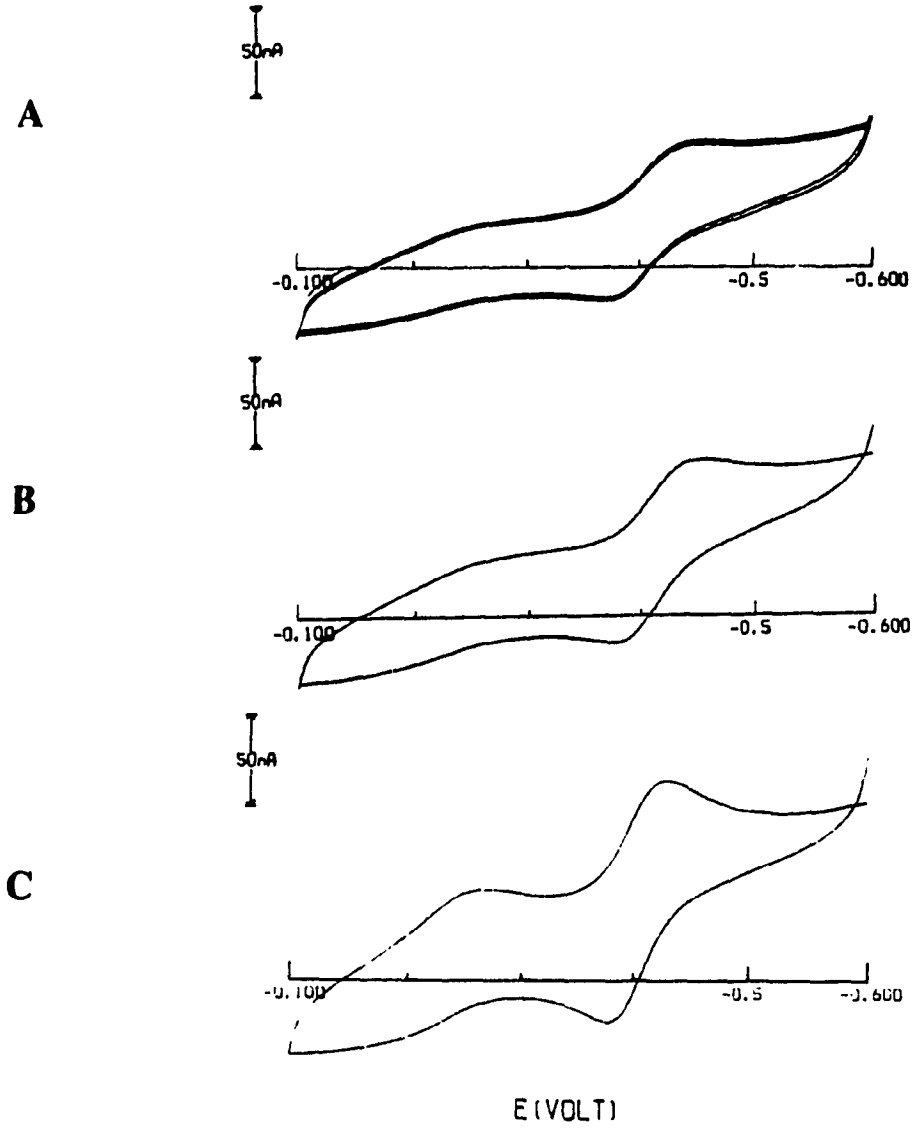

Figure 3.20 Appearance of a second redox couple in the GOx voltammograms with increasing urea concentration in the presence of 100 mM glucose. (**A**) 0.4 M urea; (**B**) 0.6 M urea, and (C) 0.8 M urea. Experimental conditions given in Figure 3.19. Gold electrode was pre-modified with AET (Section 3.3.4.3) and a pre-amplifier was used for measurement of current.

3.3.4.4 Deglycosylated GOx Voltammetry. No voltammetric peaks or catalytic currents were observed over the potential range 0.0 to -0.650 V (vs Ag/AgCl) at an AET-modified electrode for either the D-GOx or the native GOx controls at 40 μM (data not shown). Only 40 μM D-GOx was available after deglycosylation.

3.3.4.5 Gold Electrode Modified With N-Mercaptopropionyl-Dopamine. Dopamine was immobilized on the surface of a mercaptopropionic acid-modified gold electrode using EDC and NHS to form an amide bond between the chemisorbed carboxylic acid and the primary amino group of dopamine. Figure 3.21A shows the voltammogram obtained at the resulting electrode in 20 mM NaPi buffer (pH 7.0) containing 100 mM glucose. Anodic and cathodic peaks are present, and the formal potential of about +0.18 V vs Ag/AgCl corresponds to a value of +0.17 V vs Ag/AgCl obtained in 0.1 M Pi (pH 7.0) for free dopamine in solution.[30]

Figure 3.21B shows voltammograms obtained at the dopamine-modified electrode for solutions of GOx in the absence and presence of 100 mM glucose. A catalytic wave can be seen when glucose is present, and this wave appears at potentials positive of the dopamine oxidation peak.

3.4 Discussion

Quasi-reversible voltammograms were obtained for cyt c using the three promoters L-cysteine, mercaptopropionic acid and 4,4'-bipyridyl. A summary of the estimated k_s values for commercial and purified cyt c, together with the literature values are presented in Table 3.5.

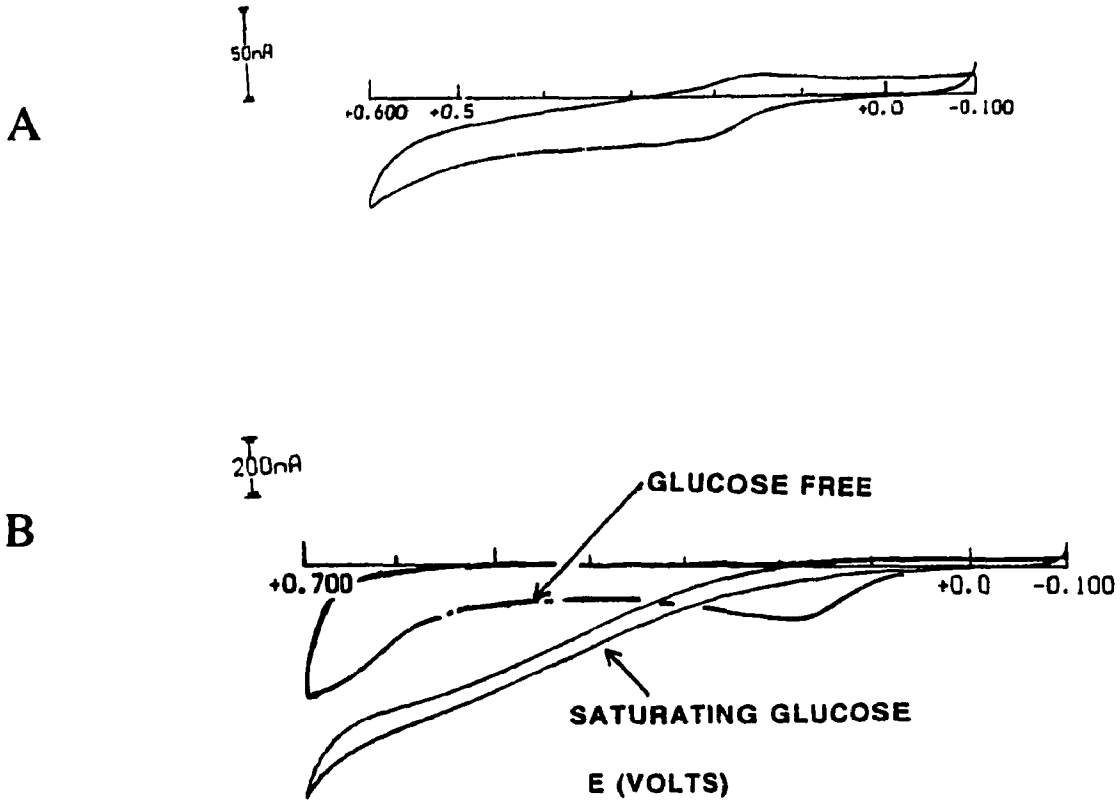

Figure 3.21 Voltammograms of GOx at N-Mercaptopropionyl-Dopamine modified gold electrode. (**A**) voltammogram of modified electrode in buffer and 100 mM glucose showing dopamine peaks. (**B**) voltammogram of 300 μM commercial GOx with and without 100 mM glucose. Experimental conditions: O_2-free 20 mM NaPi buffer (pH 7.0) at 23 °C. Scan rate: 2 mV s^{-1}. Note differences in current and voltage scales.

Table 3.5 Average k_s values for cyt c at modified gold electrodes

Promoter	commercial cyt c 10^3 k_s (cm s^{-1})	purified cyt c 10^3 k_s (cm s^{-1})	Literature[13,12,15] values 10^3 k_s (cm s^{-1})
L-cysteine	0.75 ± 0.1	0.92 ± 0.05	3.2 - 4.0[a]
	(0.61 ± 0.01)[b]		
4,4'-bipyridyl	0.46 ± 0.05	1.8	14 - 19[a]
Mercaptopro-pionic acid	0.061 ± 0.004	---	0.4[c]
	(0.051 ± 0.003)[b]		

[a] k_s values are of 400 µM purified cyt c solutions under identical conditions as those specified in Tables 3.1, 3.2 and 3.4.

[b] k_s values for 200 µM solutions of commercial cyt c.

[c] Result from "pre-activated" (see Discussion) gold electrode under identical conditions.[13]

These results show that L-cysteine-modified electrodes gave the highest heterogeneous electron-transfer rate constants, k_s, for both 400 and 200 μM solutions of commercial cyt c. A slightly lower k_s value was obtained at a 4,4'-bipyridyl modified electrode, and mercaptopropionic acid-modification gave k_s values about one order of magnitude less than the other two, again for both 400 and 200 μM commercial cyt c. It should be noted that approximately one order of magnitude difference also exists between the literature values of k_s for mercaptopropionic acid and L-cysteine.

Purification of cyt c yielded increases in k_s of 18% and 74% for the L-cysteine- and 4,4'-bipyridyl-modified electrodes, respectively. Literature values of k_s for purified cyt c, using the cysteine-modified electrode[15,12] were found to be about five and four times higher than the commercial and purified cyt c results, respectively. As stated in the results section, the literature[2] value of k_s using 4,4'-bipyridyl is roughly 35 times higher than the results obtained here with the same promoter. For the mercaptopropionic acid promoter, the literature k_s value is six times the one found here. These discrepancies in k_s may reflect differences in cyt c purification. As shown, purification yields k_s values that are closer to the literature results. In addition, pre-activation[13] may account for part of the discrepancy in k_s for mercaptopropionic acid-modification. This method involves pretreatment of a gold electrode with 4,4'-dithiodipyridine, followed by polishing and subsequent modification with the desired promoter. Significant improvement in performance was observed for a number of promoter compounds, including mercaptopropionic acid, following pre-activation.[13] In this study, pre-activation with AET (Section 3.3.4.3) was found to enhance the appearance of a second redox couple for urea-

denatured GOx.

Differences in k_s values have been interpreted as a reflection of the fundamental differences in promoter mechanism.[5] For example, if the bipyridyl co-adsorbs with cyt c (see below), then it does not act as an electron channel or conductor transferring electrons from cyt c to the electrode surface, whereas cysteine can only act as such a conduit for electrons since it forms a monolayer which restricts direct access to the electrode surface.[15]

At pH 7.0, L-cysteine is zwitterionic, mercaptopropionic acid exists as the anion, and 4,4'-bipyridyl is neutral.[31] All species, however, are capable of forming hydrogen bonds with positively-charged side chains of Lys residues surrounding the heme crevice. It is interesting to note that the two most effective promoters, L-cysteine and 4,4'-bipyridyl have N groups which can interact with cyt c. Mercaptopropionic acid has no N and yields a k_s value one order of magnitude lower than those obtained with the other two promoters. It was previously shown[15] that a N-acetylcysteine-modified gold electrode gave a voltammetric peak separation of 105 mV on the initial scan, and a faradaic current which decreased to zero with continued cycling. In contrast, modification of the electrode with cysteine ethyl ester yielded a slightly higher ΔE_p value than for cysteine, but the signal was persistent. These findings indicate that the $-NH_3^+$ rather than the $-COO^-$ on cysteine is important for reversible, diffusion-controlled cyt c electrochemistry. Perhaps at pH 7.0 the amino groups serve to attenuate interaction of carboxylate groups with the Lys residues surrounding the heme crevice of cyt c, thereby facilitating desorption of the protein from the electrode surface.

The finding that a 200 μM solution of cyt c yields peak currents (i_p) about two-fold less than those obtained from a 400 μM cyt c solution closely follows the Randles-Sevcik equation (eqn. 3.3), which predicts that i_p is directly proportional to concentration. Calculation of i_p according to eqn. 3.3, using the reported[32] diffusion coefficient for cyt c of 1.1 x 10^{-6} cm^2 s^{-1}, and a scan rate of 5 mV s^{-1}, yields i_p values of 7.7 x 10^{-8} and 1.5 x 10^{-7} A for 200 μM and 400 μM cyt c solutions, respectively, whereas the experimental data yielded 4.7 x 10^{-8} and 1.2 x 10^{-7} A, respectively. However, despite this drop in peak current at the low concentration, the k_s values for both concentrations are comparable. This is expected since ΔE_p values, and hence k_s, values are independent of bulk concentration and electrode surface area. Nevertheless, the slight drop in k_s observed at 200 μM commercial cyt c for both the cysteine- and mercaptopropionic acid-modified electrodes (Table 3.5) may be due to the peak broadening (not shown) that occurs at low currents, which makes peak identification more uncertain.

From the time-dependence experiments using commercial cyt c, it was shown that the voltammetric signal deteriorated rapidly when using bipyridyl as a promoter (Figure 3.11). The initial k_s value however, was 3.0 ± 0.2 x 10^{-3} cm s^{-1} which is one order of magnitude higher than the initial k_s value for the cysteine-modified electrode. For purified cyt c, however, the initial k_s value for the bipyridyl-modified electrode diminished to 1.8 ± 0.4 x 10^{-3} cm s^{-1}, which is only two-fold higher than the initial k_s value from the cysteine-modified electrode which yields a stable voltammogram (Figure 3.12). The higher initial rates of electron-transfer for commercial, lyophilized cyt c, which is known to contain deamidated and polymeric forms,[21] may in fact be due to the

reaction, at the same redox potential, of some or all of these impurities at the modified electrode surface. However, deterioration of the signal occurs more rapidly for commercial cyt c than for the purified protein. Deterioration of the voltammetric signal may be due to the adsorption of non-native cyt c on the electrode surface and the displacement of the bipyridyl promoter. Cysteine, which adsorbs strongly to the gold electrode surface, prevents electrode fouling and yields stable voltammograms.

Another explanation for the consistently lower k_s values that are observed at cysteine-modified electrodes, in comparison with the bipyridyl, lies in the incomplete chemisorption of cysteine to the gold electrode surface. From the voltammograms illustrated in Figures 3.9B and C for bipyridyl- and cysteine-modified electrodes, respectively, it can be seen that peak broadening occurs in the cysteine-promoted voltammogram, whereas the bipyridyl-promoted voltammogram exhibits sharper peaks. Peak broadening, in turn makes peak finding less certain, therefore, ΔE_p values would tend to increase, thus lowering k_s. This broadening may be due to protein denaturation occurring at the electrode surface in those regions that were not chemisorbed to cysteine. Another explanation may be due to the distancing between the electrode surface and cyt c that is a consequence of the formation of a stable cysteine monolayer. Electron transfer rates are known to be sensitive to the distance between electron donor and acceptor.[33] Furthermore, it has been hypothesized[8] that the bipyridyl promoter may in fact stabilize the native conformation of *directly adsorbed* cyt c, thereby diminishing the distance between cyt c and the electrode. Evidence for this comes from IR-reflectance studies which show that 4,4'-bipyridyl and cyt c co-adsorb at the gold surface[34] allowing direct

contact between stabilized protein and electrode. If this is true, then the bipyridyl is unable to stabilize the denatured cyt c species and the signal deteriorates more rapidly due to electrode fouling. Support for this can be found from the use of bipyridyl with purified cyt c, which yields strikingly more persistent electrochemical signals than were found for commercial cyt c.

The i_p values shown in Figure 3.13 (A and B) for the bipyridyl- and cysteine-modified electrodes do not change significantly over time. Acccording to the Randles-Sevcik equation (eqn. 3.3), at a constant scan rate the peak current, i_p, could change as a result of a change in either the area, A, the diffusion coefficient, D, or the bulk concentration of the protein, C^b. D could change as a result of protein aggregation, but the stability of the cysteine-modified electrode response in 400 μM cyt c over >24 hours (Figures 3.11 and 3.12) eliminates this possibility. Furthermore, a reduction in the bulk concentration, C^b, of cyt c is also discounted since this should also lead to reduction of i_p at the cysteine-modified electrode.

Significant electrode fouling also does not occur with time as this would reduce electrode area and hence i_p. Therefore, the observed time-dependent decay of k_s with the bipyridyl promoter cannot be correlated to electrode fouling. It may be that conformational changes occur in cyt c at the electrode surface without causing electrode fouling. Such conformational changes may hinder the protein desorption step (Figure 3.1) over time, which would diminish electron-transfer rates.

In contrast with the bipyridyl, the cysteine-modified gold electrode gave a persistent signal which could have lasted indefinitely beyond the duration of the

experiment for both commercial and purified forms of cyt c. Figure 3.14 confirms that cyt c adsoption is not occurring at the electrode surface since a plot of i_p vs $V^{1/2}$ for electrode-adsorbed species is concave upward.[27] In contrast, the observed levelling off of i_p with scan rate indicates that one or more of the electron-transfer steps (Figure 3.1) are rate limiting. Signal persistence for the cysteine-modified electrode is probably due to the stronger gold-sulfur bond which resists displacement by cyt c.

Time-dependence studies of direct cyt c electron transfer with an unmodified polished glassy carbon electrode have been reported by Dong et al.[35] In this study it was found that commercial horse heart cyt c gave a steadily declining electrochemical signal that lasted for approximately 12 hours. Subsequent polishing led to the regeneration of the electrode surface and a return to normal k_s values ranging from 1.9 x 10^{-2} cm s^{-1} to 2.4 x 10^{-3} cm s^{-1}. This study also showed that repetitive cycling and increasing ionic strength cause a decline in the electrochemical signal. The glassy carbon surface is therefore less prone to fouling than the bipyridyl-modified gold electrode, but it is not as effective as the cysteine monolayer at preventing electrode fouling.

The purification of GOx yielded a 34% increase in specific activity which is in good agreement with the 38% increase after purification reported by Kalisz et al.[16] Activity measurements after deglycosylation are also in good agreement with those of Kalisz and coworkers who reported an 11% decrease in activity, which was assumed to be the result of exposure to the deglycosylating conditions rather than the effect of deglycosylation itself. The molecular weight of 75 kDa for the D-GOx monomer obtained by SDS-page is higher than the expected value of 61 kDa obtained from SDS-

page of deglycosylated GOx and the 61.15 kDa estimated by Kalisz from amino acid analysis.[16] However, the MW of 83 kDa for native GOx is comparable to the value of 80 kDa found by Kalisz, indicating, that under our conditions, the deglycosylation is only partially complete.

Of the three thiols tested, mercaptopropionic acid (MPA), L-cysteine and aminoethanethiol (AET), only AET-modified gold electrodes yielded quasi-reversible faradaic currents in the presence of GOx (Figure 3.18C). It is noteworthy that the zwitterionic cysteine monolayer promoted cyt c electrochemistry, but did not promote direct GOx electrochemistry. Since cyt c has a charge of + 8, while GOx has a charge of -58 at pH 7,[9,19] it is possible that the magnitude of the charge, or its distribution on the surface of GOx, prevents orientation of GOx for electron transfer.

The formal potential ($E^{0'}$) obtained for singly-gel-filtered GOx at an AET-modified gold electrode (Figure 3.17C) was -0.395 V vs Ag/AgCl. This value is very close to that obtained with free FAD (-0.410 V, vs Ag/AgCl), and suggests the presence of free FAD in commercial GOx preparations, or the dissociation of FAD from GOx as a result of interaction with the AET monolayer.[36] Assuming that the peaks in Figure 3.17C are due to free FAD, the k_s value evaluated using the FAD diffusion coefficient[37] of 3.8 x 10^{-6} cm^2 s^{-1} was 1.24 x 10^{-3} cm s^{-1}.

Direct electrochemistry of GOx is expected to proceed with an $E^{0'}$ value that is more positive than that of free FAD. At pH 7.0, the two-electron two-proton reduction of FAD to $FADH_2$ has $E^{0'}$ = -0.420 (vs Ag/AgCl),[38] while differential pulse voltammetry (DPV) at a dropping mercury electrode yielded $E^{0'}$ = -0.295 V vs Ag/AgCl for GOx at

pH 7.0 in 0.1 M phosphate buffer.[39] A difference of about 120 mV is therefore expected between free and GOx-bound FAD at pH 7.0.

Direct electrochemistry of GOx-bound FAD is observed for GOx that has been subjected to two consecutive gel filtration steps (Figure 3.18B and C). The $E^{0'}$ value of the redox couple apparent in these voltammograms is -0.250 V vs Ag/AgCl, which compares favourably with the value of -0.295 V vs Ag/AgCl reported by Scheller et al.[39] in their DPV study. In the presence of glucose, no large catalytic current was observed, but the shape of the voltammogram was slightly different (Figure 3.18C). The magnitude of this change is not great enough for sensing applications and denaturation of GOx at the electrode surface is suspected.

For GOx in 0.4 - 0.8 M urea, quasi-reversible peaks were obtained at AET-modified gold electrodes, both at the free FAD $E^{0'}$(-0.410 V vs Ag/AgCl), and at the GOx-bound FAD $E^{0'}$ (-0.205 V). Activity (Section 3.3.4.3) and fluorescence measurements (Figure 2.3) indicated that most FAD remains bound to GOx with urea concentrations up to 3 M; for example, in 0.6 M urea the enzyme has 88% of the activity of native GOx. The GOx peak currents at $E^{0'}$~ -0.205 V vs Ag/AgCl clearly increase with urea concentration (Figure 3.20), suggesting that partial unfolding of GOx in 0.4 - 0.8 M urea facilitates direct GOx-bound FAD electrochemistry. The shift in the FAD $E^{0'}$ value occurs only in denatured GOx. This suggests that the earlier $E^{0'}$ measurements of GOx-bound FAD at a mercury electrode (referenced above) and the redox couple found in the AET-modified electrode experiments with native GOx (Figure 3.18) were also from partially denatured GOx. This may help to explain the absence of a catalytic current, as

described above, for the voltammograms in Figure 3.18.

A shift in $E^{0'}$ on protein denaturation in urea was also found in a study by Pilard et al. using cyt c.[40] This study used a 4,4'-bipyridyl-modified gold electrode, and as the urea concentration was increased, a second redox couple appeared in the cyclic voltammograms at $E^{0'}$ = 0.05 V vs NHE, in addition to the native cyt c peak at $E^{0'}$ = 0.255 V vs NHE. The $E^{0'}$ of the native protein decreased steadily with increasing urea, and was replaced by the $E^{0'}$ = 0.05 V redox couple at 4 M urea.

Due to low yields of deglycosylated GOx (D-GOx), peaks at the AET-modified gold electrode were not observed. A thin-layer cell that can operate with smaller quantities of redox species[27] would have been useful for these experiments; alternatively, greater quantities (up to 400 μM) of D-GOx could be produced to obtain data comparable with those obtained for native GOx.

A catalytic current was observed for the N-mercaptopropionyl-dopamine electrode (Figure 3.21B). This indicates that an immobilized mediator covalently attached to a flexible promoter which is chemisorbed to a gold electrode is able to shuttle electrons from the $FADH_2$ center of native GOx to the electrode surface. Extension of this to the construction of a glucose biosensor requires that a catalytic current proportional to the glucose concentration be observed. Greater quantities of immobilized dopamine may be adsorbed onto the gold electrode if the thiol-dopamine-derivative was prepared and purified prior to adsorption. Furthermore, the use of deglycosylated GOx (D-GOx) with this electrode could be attempted, since the transfer of electrons to the dopamine moiety from D-GOx-bound $FADH_2$ may be more facile than to native GOx-($FADH_2$).

3.5 References

1. Barker, P. D.; Di Gleria, K.; Hill, H. A. O.; Lowe, V. J. *Eur. J. Biochem.* **1990**, 190, 171-175.

2. Eddowes, M. J.; Hill, H. A. O.; Uosaki, K., *Bioelectrochem. Bioenerg.*, **1980**, 7, 527-537.

3. Frew, J. E.; Hill, H. A. O. *Eur. J. Biochem.* **1988**, 172(2), 261-269.

4. Bowden, E. F.; Hawkridge, F. M.; Blount, H. N. **1984**, *J. Electroanal. Chem.*, 161, 355.

5. Fraser A. Armstrong, "Probing Metalloproteins by Voltammetry", *Struct. Bonding 72*, Springer-Verlag Berlin Heidelberg **1990**, (a) pp 137-148, (b) pp 151-154.

6. Reed, D. E.; Hawkridge, F.M. *Anal. Chem.* **1987**, 59, 2334.

7. Eddowes, M. J.; Hill, H. A. O., **1977**, *J. Chem. Soc. Chem. Commun.* 771.

8. Armstrong, F. A.; Hill, H. A. O.; Walton, N. J. *Quart. Rev. Biophys.* **1985**, 18, pp 279-286.

9. Koppenol, W. H.; Margoliash, E. *J. Biol. Chem.* **1981**, 257, 4426-4437.

10. Wilde, C. P.; Ding, T. *J. Electroanal. Chem.*, **1992**, JEC01932.

11. Taniguchi, I.; Toyosawa, K.; Yamaguchi, H.; Yasukouchi, K. *J. Chem. Soc. Chem. Commun.* **1982**, 1032.

12. Santucci, R.; Brunori, M. *Bioelectrochem. Bioenergetics* **1991**, 29, 177-184.

13. Allen, P. M.; Hill, H. A. O.; Walton, N. J. *J. Electroanal. Chem.*, **1984**, 178, 69-86.

14. Adman, E. T. **1985**, in *Metalloproteins*, (Harrison, P. M., ed.) vol. 1, MacMillan, London.

15. Di Gleria, K.; Hill, H. A. O.; Lowe, V. J.; Page, D. J. *J. Electroanal. Chem.* **1986**, 213, 333-338.

16. Kalisz, H. M.; Hecht, H. J.; Schomburg, D.; Schmid, R. D. *Biochim. Biophys. Acta*, **1991**, 1080, 138-142.

17. Tarentino, A. L.; Maley, F. *J. Biol. Chem*, **1974**, 249, 811.

18. Li, Y. T. *J. Biol. Chem* **1967**, 242, 5474.

19. Frederick, K. R.; Tung, J.; Emerick, R. S.; Masiarz, F. R.; Chamberlain, S. H.; Vasavada, A.; Rosenberg, S. *J. Biol. Chem.* **1990**, 265, 3793-3802.

20. Dalton, D.; Hill, H. A. O.; Nakayama, H. *J. Electroanal. Chem.* **1991**, 297, 309-314.

21. Brautigan, D. L.; Ferguson-Miller, S.; Margoliash, E. *Methods Enzymol.* **1978**, 53, 128.

22. Laemmli, U. K. *Nature* **1970**, 227, 680.

23. Babul, J.; Stellwagen, E. *Biochemistry* **1972**, 11, 1195.

24. Bradford, M. M. *Anal. Biochem.* **1976**, 72, 248.

25. Millan, K.; Mikkelsen, S. R. *Anal. Chem.* **1993**, 65, 2317-2323.

26. Nicholson, R. S. *Anal. Chem.* **1965**, 37, 1351-1355.

27. Bard, A. J. & Faulkner, L. R. **1980**, *Electrochemical Methods, Fundamentals and Applications.* New York: Wiley.

28. Swoboda, B. E. P.; Massey, V. *J. Biol. Chem.* **1965**, 240, 2209-2215.

29. Szucs, A.; Hichman, G. D.; Bockris, J. O. M. *J. Electrochem. Soc.* **1989**, 136, 3700-3748.

30. Battaglini, F.; Koutroumanis, M.;English, A. M.; Mikkelsen, S. R. *Bioconjugate Chem.*, **1994**, (in press).

31. Xie, Y.; Dong, S., *Bioelectrochem. Bioenerg.*, **1992**, 29, 71.

32. Albery, W. J; Eddowes, M. J.; Hill, H. A. O.; Hillman, A. R., *J. Am. Chem. Soc.* **1981**, 103, 3094-3910.

33. Marcus, R. A.; Sutin N. *Biochim. Biophys Acta* **1985**, 811, 265.

34. Niwa, K.; Furukawa, M.; Niki, K. *J. Electroanal. Chem.* **1988**, 245, 141.

35. Dong, S.; Quijin, C. *Bioelectrochem. Bioenerg.* **1992**, 29, 237-245.

36. Szucs, A.; Hichman, G. D.; Bockris, J. O. M. *J. Electrochem. Soc.* **1989**, 136, 3700-3748.

37. Verhagen, M. F. J. M.; Hagen, W. R. *J. Electroanal. Chem.*, **1992**, 334, 339-350.

38. Handbook of Biochemistry and Molecular Biology, Physical and Chemical Data, 3rd ed.; CRC press; Cleveland, OH, **1976**; Vol. 1, p.127.

39. Scheller, F.; Strnad, G.; Neumann, B.; Kuhn, M.; Ostroswski, W. *Bioelectrochem. Bioenerg.*, **1979**, 117.

40. Pilard, R.; Haladjian, J.; Bianco, P.; Serre, P.A.; Brabec, V. *Biophys. Chem.* **1983**, 17, 131-137.

4.0 SUMMARY AND SUGGESTIONS FOR FURTHER WORK

GOx was covalently modified with FCA using EDC and NHS to promote selective coupling to surface lysines. By this method, GOx became electroactive at a glassy carbon electrode and transferred electrons to the electrode without a mediator. The k_{obs} value for intramolecular electron transfer was found to be 1.6 s^{-1} for GOx-$(FCA)_{12}$. This value is not sufficient to compete with the rate of O_2 oxidation, therefore the use of ferrocene-modified GOx at Lys residues in a biosensor is limited to anaerobic conditions or in whole blood glucose measurement devices (*in vitro*) where the concentration of O_2 is less than 1 μM.

A value for the bimolecular rate constant k_{12}, for FCA-mediated electrochemistry, extrapolated to very low FCA:GOx ratios, yielded a limiting k_{12} value of $1.2 \pm 0.2 \times 10^5$ $M^{-1}s^{-1}$. Mediation of electron transfer by increasing the FCA:GOx ratio invalidates the assumption that the reduced GOx concentration is equal to the total concentration of GOx and therefore the measurement of k_{12} is underestimated.

Linear sweep (LSV) and chronoamperometric (CA) voltammetries yielded comparable bimolecular rate constants in the range 1.0 - 1.3 x 10^5 M^{-1} s^{-1}. Therefore CA can be used for the detection of glucose with FCA mediation and is preferable due to its short scanning duration.

Direct cyt c electrochemistry was promoted by the use of L-cysteine and mercaptopropionic acid, which are thiol-containing electrochemical promoters. It was found that L-cysteine was better able to provide a persistent electrochemical signal. This

was reflected in a voltammetric signal that persisted beyond 27 hours for purified and commercial cyt c at the cysteine-modified electrode, compared to ~22 hours for purified cyt c and <4 hours for commercial cyt c at a bipyridyl-modified electrode. From this, it can be concluded that the cysteine promoter, which forms a chemisorbed monolayer at a gold electrode surface, persists because it is better able to resist protein adsorption and denaturation at a modified gold electrode than 4,4'-bipyridyl over time.

Direct GOx electrochemistry was promoted using aminoethanethiol provided that the GOx was gel-filtered twice. Using this promoter, the formal redox potential, $E^{0'}$, for GOx-bound FAD was -0.250 V vs Ag/AgCl. Therefore, removal of free FAD allows the appearance of the GOx-bound redox couple in AET-promoted electrochemistry.

In the presence of 0.4 - 0.8 M urea two redox couples appeared with $E^{0'}$ = -0.410 V and $E^{0'}$ = -0.250 V (vs Ag/AgCl). Both redox couples were found to increase with urea concentration. In 0.6 M urea in O_2-free 100 mM NaPi buffer (pH 7.0), GOx retained 88% of its activity. Thus, partial urea denaturation facilitates both free and GOx-bound FAD electrochemistry while retaining a significant amount of activity.

For both cyt c and GOx, the overall charge and its distribution on the surface of the proteins is an important factor in the selection of a promoter. Projected hydrogen bond formation between specific Y groups on the promoters (-COO^- and/or -NH_3^+) and charged residues on the protein were found to be important factors in the direct electrochemistry of redox proteins. The N-mercaptopropionyl-dopamine-modified electrode, yielded a catalytic current for native GOx in the presence of saturating glucose, indicating that an immobilized mediator can shuttle electrons from the buried $FADH_2$

redox center of native GOx to the electrode surface.

Further work needs to be done to determine the glucose concentration range in which the N-mercaptopropionyl-dopamine electrode gives a linear response at GOx concentrations comparable to those used in Section 2.0 (2 - 50 μM). From this, the K_m value for this electrode could be determined. It was recently found in this laboratory by L. D'Astous that glucose attenuated the signal for a cyt c solution whose electrochemistry is promoted by cysteine. Investigation of the effects of glucose on thiol modifiers and the above dopamine electrode should be done to determine whether displacement of the promoter occurs in the presence of glucose.

Spectroscopic characterization of the urea-treated GOx samples could help determine the amount of GOx-bound FAD, since the extinction coefficient of free FAD is lower than GOx-bound FAD.[28]

Future work might involve a thorough characterization of the modified gold electrode surfaces that were used in this study. Recently developed techniques such as scanning electrochemical microscopy[1] can be used to provide surface topographies that may be useful in determining the extent and configuration of electrode coverage with thiol promoters that chemisorb onto gold. Other positive Y-group electrochemical promoters could be tried with the various forms of GOx that were investigated here in order to find a better promoter for GOx electrochemistry. Additionally, ionic strengths and pH could be varied with AET as a promoter in order to investigate the effects that these parameters

---

[1] Meral, A.; Bard, A. J.; Horrocks, B. R.; Richards, T. C.; Treichel, D. A. *Analyst*, **1994**, 119, 719-726.

have on direct GOx electrochemistry.

Thiol-containing oligopeptides and derivatized antibodies could also be used as electrochemical promoters, since these may be structurally modified to accommodate the structure, charge distributions, and dynamics of a redox protein such as GOx, thereby enhancing electron transfer through closer and/or more efficient contact with the enzyme.